TAMPEREEN TEKNILLINEN YLIOPISTO
TAMPERE UNIVERSITY OF TECHNOLOGY

DUC NGUYEN THANH

LTE INDOOR MIMO PERFORMANCE AND ANTENNA CONFIGURATION

MASTER OF SCIENCE THESIS

Subject approved by the department council
on January 9th 2013.
Supervisors: Dr. Tech Tero Isotalo
Dr. Tech Jarno Niemelä

PREFACE

This Master of Science thesis has been written for the completion of my M.Sc degree in Information Technology in Tampere University of Technology. The thesis works, measurements and writing process, have been conducted in the Department of Electronics and Communications Engineering at Tampere University of Technology. I have been working on my Master thesis project from August 2012 to November 2013. While undertaking this project I have had much encouragement from many people, I would like to express my sincere gratitude.

First, I would like to thank my supervisors Tero Isotalo and Jarno Niemelä for recommending the work and for all advices and guidance, they provided during the whole duration of the thesis. Their advices help to not only complete the thesis successfully, but also give me valuable experiences that surely help me for future.

Second, I am thankful Nokia Siemens Networks for providing LTE radio network equipment, Anite Finland for providing field measurement software, and Nokia Test Network for providing LTE network infrastructure.

Last but not the least, I would like to thank my girlfriend ThanhMai for all the continuous supports and love and encouragement that I have got.

I would like to dedicate the thesis to my whole family, my brother and my parents. Without their support and encouragement, I ‘m not able to be where I am today.

Tampere, November 2013
Duc Nguyen Thanh

CONTENTS

ABSTRACT

TAMPERE UNIVERSITY OF TECHNOLOGY
Degree Programme Information Technology
DUC, NGUYEN THANH: LTE Indoor MIMO Performance and Antenna Configuration
Master of Science Thesis, 77 pages, 2 appendix pages
November 2013
Major subject: Communication Engineering
Supervisors: Dr. Tech Tero Isotalo, Dr. Tech Jarno Niemelä
Keywords: LTE, MIMO, antenna, indoor network, space diversity, polarization diversity, field measurements.

Long-term evolution (LTE) and multiple input multiple output (MIMO) have earned reputations to be a cutting–edge technology, which can boost significantly wireless communication performances. However, many aspects influence on LTE MIMO efficiency; those include propagation environments and antenna configurations.

The goal of the thesis is to study performances of LTE MIMO on downlink in indoor. MIMO gains over transmit diversity and single antenna are the objective. Additionally, the study compares MIMO indoor performances with different antenna configurations at LTE base station and UE, including space diversity and polarization diversity.

Some results obtained in this thesis follow the expectations what have been studied in literature and previous practical studies but some differences are also pointed out.

Medium access control throughput (MAC TP) and some system parameters in LTE network that are linked with TP are analysed; those parameters are CQI, MCS as well as MIMO utilization. Effects of indoor propagation, such as LoS, NLoS, good and bad signal levels on SNR strength and MIMO utilization are clarified.

In overall, MIMO outperforms transmit diversity (TxDiv) and single antenna in LTE indoor. The overall MIMO MAC TP gains are about nearly 40.0% over TxDiv and more than 20.0% over single stream. LoS environment boost SNR strength. Hence, up to 35.0% TP gain over single antenna is achieved. However, LoS signals make the channel become correlated due to lack of multipaths, causing that MIMO is not fully utilized. The gain of MIMO over single antenna is reduced at no LoS environments, particularly only around 17.0% and 21.0% MAC TP gains are recorded at NLoS channels with good signal levels and weak signal strength, relatively.

The overall TP gain the UE experiences by using TxDiv over single antenna is roughly more than 20.0%, but LoS environment limits TxDiv performance. Hence, at LoS channel, TxDiv performance is reduced by around 2.0% compared to single stream. The worse the channel, the better TxDiv performs. The highest gain is at cell edge environment when TxDiv improves throughput more than 40.0% over single antenna.

Clearly, antenna configuration impacts network performance. Large horizontal separation (7λ) between antenna elements outperforms small separation (0.5λ) in terms of SNR, MIMO utilization and MAC TP. The MAC TPs of large separation by using omni-directional and directional antennas are almost similar, around 27.0 Mbps. Space diversity with omni-directional antennas provides roughly 14.0% MAC TP improvement while only approximately 4.5% TP gain can be achieved with directional antennas. Vertical–horizontal polarization pair deployed at LTE base station is found to provide better performance over vertical–vertical polarization and X–pol pairs. Signals also appear to be more correlated with vertical-horizontal polarization pair since MIMO utilization gets better values, MIMO utilization gains are around 18.0% over vertical-vertical polarization pair and 6.0% over X-pol pair, resulting in around 31.7% and 17.0% MAC TP gains over the two latter, relatively. The results also point out that changing polarizations at UE do not give clear MAC TP and MIMO utilization improvements.

From the radio network planning point of view, the results obtained in this thesis can be considered as guidelines for indoor network planning and optimization for network operators. It is important to conclude that based on the measurements made in this thesis, space diversity (7λ) with omni-directional antennas and vertical-horizontal polarization pairs appear to give optimal indoor performance.

However, it should be taken into consideration that all results presented in this thesis are highly dependable on the chosen antennas, LTE network systems, devices and indoor environment where the measurements are carried out. Hence, the results may vary with the factors mentioned.

LIST OF ABBREVIATIONS

1G	First Generation
2G	Second Generation
3G	Third Generation
3GPP	Third Generation Partnership Project
ADSL	Asymmetric Digital Subscriber Line
AMPS	Analogue Mobile Phone System
ARQ	Automatic Repeat reQuest
AuC	Authentication Center
BER	Bit Error Rate
BLER	Block Error Rate
BSC	Base Station Controller
BTS	Base Transceiver Station
CDF	Cumulative Distribution Function
CL-SM	Closed-Loop Spatial Multiplexing
CMC	Connection Mobility Control
CN	Core Network
CP	Cyclic Prefix
CQI	Chanel Quality Indicator
CRC	Cyclic Redundancy Check
DAB	Digital Audio Broadband
DAS	Distributed Antenna System
DFT	Discrete Fourier Transform
DHCP	Dynamic Host Configuration Protocol
DL-SCH	Downlink Shared CHannel
DRA	Dynamic Resource Allocation
DVB	Digital Video Broadband
eNodeB	E-UTRAN NodeB
EPC	Evolved Packet Core
EPS Bearer	Evolved Packet System Bearer
ETSI	European Telecommunication Standard Institute
E-UTRAN	Evolved-UMTS Terrestrial Radio Access Network
FDD	Frequency Division Duplex
FEC	Forward Error Correction
FFT	Fast Fourier Transform
FIR	Finite Impulse Response
FSTD	Frequency Switched Transmit Diversity
GI	Guard Interval
GPRS	General Packet Radio Service
GSM	Global System for Mobile Communication

HARQ	Hybrid Automatic Repeat reQuest
HSPA	High Speed Packet Access
HSS	Home Subscriber Server
ICI	Inter-Carrier Interference
IDFT	Inverse Discrete Fourier Transform
IEEE	Institute of Electrical and Electronics Engineers
IFFT	Inverse Fast Fourier Transform
IP	Internet Protocol
ISI	Inter Symbol Interference
J-TACS	Japanese Total Access Communication System
LoS	Line of Sight
LS	Least Square
LTE	Long Term Evolution
MAC	Medium Access Control
MAC TP	Medium Access Control Throughput
MCS	Modulation and Coding Scheme
MIMO	Multiple Input Multiple Output
MISO	Multiple Input Single Output
MME	Mobility Management Entity
MMSE	Minimum Mean Square Error
NMT	Nordic Mobile Telephone
NLoS	No Line of Sight
OFDM	Orthogonal Frequency Division Multiplexing
OL-SM	Open-Loop Spatial Multiplexing
PAPR	Peak-to-Average Power Ratio
PCCC	Parallel-Concatenated Convolutional Code
PCFICH	Physical Control Format Indicator CHannel
PCRF	Physical Control Charging Rules Function
PDN	Packet Data Network
P-GW	Packet Data Network Gateway
PHICH	Physical Hybrid ARQ Indicator CHannel
PMI	Pre-coding Matrix Indicator
PSS	Primary Synchronization Signal
PUCCH	Physical Uplink Control CHannel
PUSCH	Physical Uplink Shared CHannel
QAM	Quadrature Amplitude Modulation
QoS	Quality of Service
QPSK	Quadrature Phase Shift Keying
RAC	Radio Admission Control
RAN	Radio Access Network
RB	Resource Block
RBC	Radio Bear Control

RE	Resource Element
RI	Ranking Indicator
RNC	Radio Network Controller
RNP	Radio Network Planning
RRM	Radio Resource Management
RS	Reference Signal
RSRP	Reference Signal Received Power
SAE	System Architecture Evolution
SC-FDMA	Single Carrier-Frequency Division Multiple Access
SFBC	Space Frequency Block Code
S-GQ	Serving Gateway
SIMO	Single Input Multiple Output
SINR	Signal-to-Interference plus Noise Ratio
SNR	Signal to Noise Ratio
SISO	Single Input Single Output
SMS	Short Message Service
SON	Self-Organizing Network
SSS	Secondary Synchronization Signal
STBC	Space Time Block Code
TB	Transport Block
TDD	Time Division Duplex
TDMA	Time Division Multiple Access
TM	Transmission Mode
TTI	Transmission Time Interval
TxDiv	Transmit Diversity
UE	User Equipment
USCH	Uplink-Shared CHannel
UMTS	Universal Mobile Telecommunication System
UP	User Plane
VSWR	Voltage Standing Wave Ratio
WCDMA	Wideband Code Division Multiple Access
WiMax	Worldwide Interoperability for Microwave Access
WLAN	Wireless Local Area Network

LIST OF SYMBOLS

Δ^{DL}	Downlink Overhead
Δf_c	Coherent Bandwidth
Δg	Guard Interval
Δf	Subcarrier Space
a_f	Floor Attenuation
a_w	Wall Attenuation
$C_{MAC}{}^{DL}$	MAC Downlink Capacity
$C_{MAC_{2\times 2MIMO}^{DL}}$	MAC Downlink Capacity with 2x2MIMO
f_c	Centre Frequency
L	Path Loss
L_F	Free Space Loss
n	Path Loss Exponent
n_1	Refractive Index of Medium 1
n_2	Refractive Index of Medium 2
N_A	Number of Antenna Ports
n_f	Number of Floors
N_l	Number of Data Streams
n_w	Number of Walls
$N_t \times N_r$	Transmitter Antennas and Receiver Antennas Matrix
N_{RB}^{DL}	Number of Downlink Resource Block
r	Distance
$R_{PEAK_{2\times 2MIMO}^{DL}}$	Downlink Physical Peak Data Rate With $2 \times 2\mathrm{MIMO}$
$R_{PEAK_{2\times 2MIMO}^{UL}}$	Uplink Physical Peak Data Rate With $2 \times 2\mathrm{MIMO}$
T_u	OFDM Symbol Duration
T_{CP}	Cyclic Prefix
X-pol	Cross-polarization
τ	Delay Spread
λ	Wavelength of the signal
$\Vert$	Half-wavelength Separation
$\vert \quad \vert$	Seven-wavelength Separation
$\vert-$	Vertical-Horizontal Polarization Pair
Γ	Cross–Polar Ratio
Ø	Angular Spread
$Ø_i$	Angle of Incident Wave
$Ø_r$	Angle of Reflected Wave
$Ø_t$	Angle of Refracted Wave

1. INTRODUCTION

The mobile communication network has a long history and has been tremendously developed since the cellular system was firstly initialized by Bell Laboratories, opening the way for mobile service coming out to market in June 1946 in US [1]. This was then followed by analogue 'First Generation' (1G) system in the 1980s. The First Generation comprised a number of incompatible systems worldwide such as Japanese Total Access Communication System (J–TACS), used in Japan and Hong Kong in 1979, Nordic Mobile Telephone (NMT), used in parts of Europe, 1981–1985 and Analogue Mobile Phone System (AMPS), used in US, 1983 and it was analogue–based technology [1].

The 'Second Generation' (2G) mobile network started in the early 1990s and was based on digital technology and made global roaming possible. The 2G network was mainly designed to carry voice traffic. European Telecommunication Standard Institute (ETSI) standardized Global System for Mobile Communication (GSM) in Europe, while USA and Japan developed their own standard Code Division Multiple Access (CDMA). The 2G GSM was built on the base of Time Division Multiple Access (TDMA) and Frequency Division Multiple Access (FDMA) techniques. The second–generation digital mobile communication opened the opportunities for network operators to provide data services. The primary data services offered in 2G were short message service (SMS) and circuit–switched data services enabling e–mail and other data applications [2].

Since the demands for higher data services were increased, there needed an evolution of 2G networks, leading to the introduction of packet–switched General Packet Radio Service (GPRS) in second half of 1990s. However, the data rates were still limited and inspired the introduction of 'Third Generation' (3G) networks. Universal Mobile Telecommunication System (UMTS), which was standardized by 3rd Generation Partnership Project (3GPP), is the most widely deployed 3G networks. The use of packet switching rather than circuit switching for data transmission is the main technical difference that distinguishes 3G from 2G. Then, an evolution in 3G network occurred, offering a significant improvement in data rates. This evolved 3G is called High Speed Packet Access (HSPA), also referred to 3.5G mobile networks. The latest mobile cellular networks, 'Fourth Generation' (4G) Long–Term Evolution (LTE), was introduced firstly in 2004, giving a solid promise to provide very much higher data rate than ever before. LTE eliminates circuit switching, uses completely packet switching on the base of IP–connectivity.

There are evolutions in radio interface and system architecture in LTE networks since it is designed on the IP–connectivity base. Orthogonal Frequency Division Multiple

1. INTRODUCTION

Access (OFDMA) has been adopted as downlink access scheme and Single Carrier–Frequency Division Multiple Access (SC–FDMA) is used for uplink multiple access. MIMO is a very promising technique that boosts remarkably system capacity. The MIMO concept is based on the existence of multiple separated radio channels between transmit and receive antenna arrays in the scattering propagation environment. Theoretically, the capacity is linearly proportional with the number of antennas in MIMO configuration. However, many aspects have influenced MIMO efficiency; those include propagation environments, antenna configurations, etc.

Radio network planning (RNP) is a very important process and must be done before the practical network deployment starts. The planning process starts by defining the requirements of a network for a certain planning area, and then deciding the optimum network configurations to reach the needs for quality of service (QoS), capacity, and coverage. Various new services, different adaptive network operation modes, dynamic properties of radio interface of LTE standardizations generate new challenges in RNP, optimization and QoS management [3]. Propagation in indoor environments is excepted to be more complicated than propagation in outdoor environments and therefore have impacts on LTE RNP.

This thesis focuses on LTE MIMO transmission and antenna configurations in indoor environments. The purpose is to provide basic understanding of LTE performance with MIMO modes and different antenna configuration that impact on MIMO performance. Some system performance and configuration thresholds due to indoor propagation and antenna configuration influences are studied based on measurements.

The first goal of the thesis is to study performances of LTE MIMO system on downlink with variations of indoor channel conditions. MIMO gains over transmit diversity and single antenna, are also the objective. The second goal is to find an optimum antenna configuration at E–UTRAN NodeB (eNodeB) and User Equipment (UE) for a particular indoor environment. Antenna configuration is related to space diversity and polarization diversity.

The thesis is organized as follows: Chapter 1 introduces the thesis, and LTE standardization is introduced in Chapter 2. Chapter 3 focuses on providing knowledge on LTE transmission modes and multiple antenna techniques used in those transmission modes. In Chapter 4, some fundamental electromagnetic wave transmission mechanism and indoor propagation models are studied. Chapter 5 introduces indoor radio network planning. Chapter 6 and Chapter 7 describe measurement set–up and measurement results, respectively. The thesis is concluded in Chapter 8.

2. LTE STANDARDIZATION

Since demands for mobile network data rate and requirements for better QoS have remarkably risen over recent years, evolutions on mobile network to meet the demands therefore happened. As a result, by the fall of 2004, a workshop on 3GPP LTE was organized by Technical Specification Group (TSG) Radio Access Network (RAN). The workshop was the starting mark of the development of LTE radio interface. The discussion defined targets and requirements of next generation of mobile network. Evolutions on radio access as well as system architecture were needed. The result of LTE workshop is that a 3GPP TSG Work Group was created in December 2004. Then six months later in June 2005, a very first 3GPP technical report was approved. The most important requirements of the document were about evolutions on higher peak data rate, lower round trip time. Additionally, the flexibility of spectrum and maximum commonality between Frequency Division Duplex (FDD) and Time Division Duplex (TDD) were also noticed [2]. This chapter focuses on the System Architecture Evolution (SAE) architecture and specifications in LTE.

2.1. LTE Network Architecture

LTE has principally been aimed at packet–switched services, in contrast with previous cellular networks such as GSM and UMTS that were modelled mainly for circuit–switched services. LTE networks establish Internet Protocol (IP) connectivity between an UE and a Packet Data Network (PDN). The IP connectivity helps end users to take advantage of real time applications and prevents any disruption to end users' applications while moving [1].

An Evolved–UMTS Terrestrial Radio Access Network (E–UTRAN) replaced for UTRAN was one of the main evolutions designed for LTE and there is no centralized control in between E–UTRAN and Core Network (CN). IP–based packets are directly routed between an UE and an Evolved Packet Core (EPC) by bearing on an Evolved Packet System Bearer (EPS Bearer) with a defined QoS degree, depending on types of required applications. Figure 2.1 presents an overall picture of EPS architecture, in which E–UTRAN and EPC are the key elements. In this subchapter, key elements and main functions of E–UTRAN and EPC are introduced.

2.1.1. Core Network

One of the biggest evolutions designed for LTE is toward to the design of CN, which is called EPC in SAE system. As mentioned previously, there are no IP–connectivity nodes in between an UE and CN. The IP–based packets are transferred bi–directionally between two domains; UE and CN. An EPC has main logical elements as follows [1]:

- PDN Gateway (P–GW).
- Serving Gateway (S–GW).
- Mobility Management Entity (MME).

In addition to those logical nodes, the EPC has some other logical nodes and functions; Home Subscriber Server (HSS) and Policy Control Charging Rules Function (PCRF) are two of them. There are differently functional interfaces shown in Figure 2.1 to inter–connect those logical nodes within the EPC. The details of logical nodes are as follows:

HSS is a database server where user–related and subscriber–related information are stored. Moreover, HSS provides knowledge for location management and call setup [1]. The subscribers' profile contained in HSS records the information about the services that are appropriate to the user, including information of PDN connection permissions, and permission on whether that user is allowed to roam to a certain visited network. Moreover, Identities of P–GWs, which are in use, are available on HSS database. The HSS also provides a permanent key for user authentication to identify the right users, for access authorization to verify whether that user is suited for the services [4]. The permanent key, which is also needed for encryption and decryption users' data, is stored in the Authentication Centre (AuC), a part of the HSS. For location management, the HSS interacts with MMEs through S6a interface. The HSS should be able to know identities of MMEs that UEs are allowed to move to. The HSS will release the connection with a previous MME and update a new MME which is current MME serving for UE. The HSS database server is maintained centrally in the home operator's premises.

As depicted in Figure 2.1, there is an element called System Architecture Evolution Gate Way (SAE GW). This element is a combination of two gateways: S–GW and P–GW. SAE GW deals with User Plane (UP) in EPC. The interface S5/S8 connects the two gateways to transport IP–based packets from UEs to external networks.

S–GW: The principal function of a S–GW is UP tunnel management (for mobility management) and IP packet switching. The S–GW is logically located in EPC and maintained centrally at operators' premises. For packet switching, the S–GW is an anchor of a CN that forwards all IP packets it received from radio–side, eNodeB, to EPC–side, P–GW, and vice versa on UP. General Packet Radio Service Tunnelling Protocol–User Plane (GTP–U), the highest layer operated at S–GW, performs tunnelling to the IP–based packets and mapping to S1–U interface to E–UTRAN or S5/S8 interface to P–GW. For mobility management, while a UE performs handover among eNodeBs, the MME commands the S–GW to modify the tunnelling. Furthermore, the mobility of an UE between S–GWs, the MME also reallocates S–GWs accordingly, by updating a new S–GW tunnelling and clearing the previous S–GW tunnelling [4].

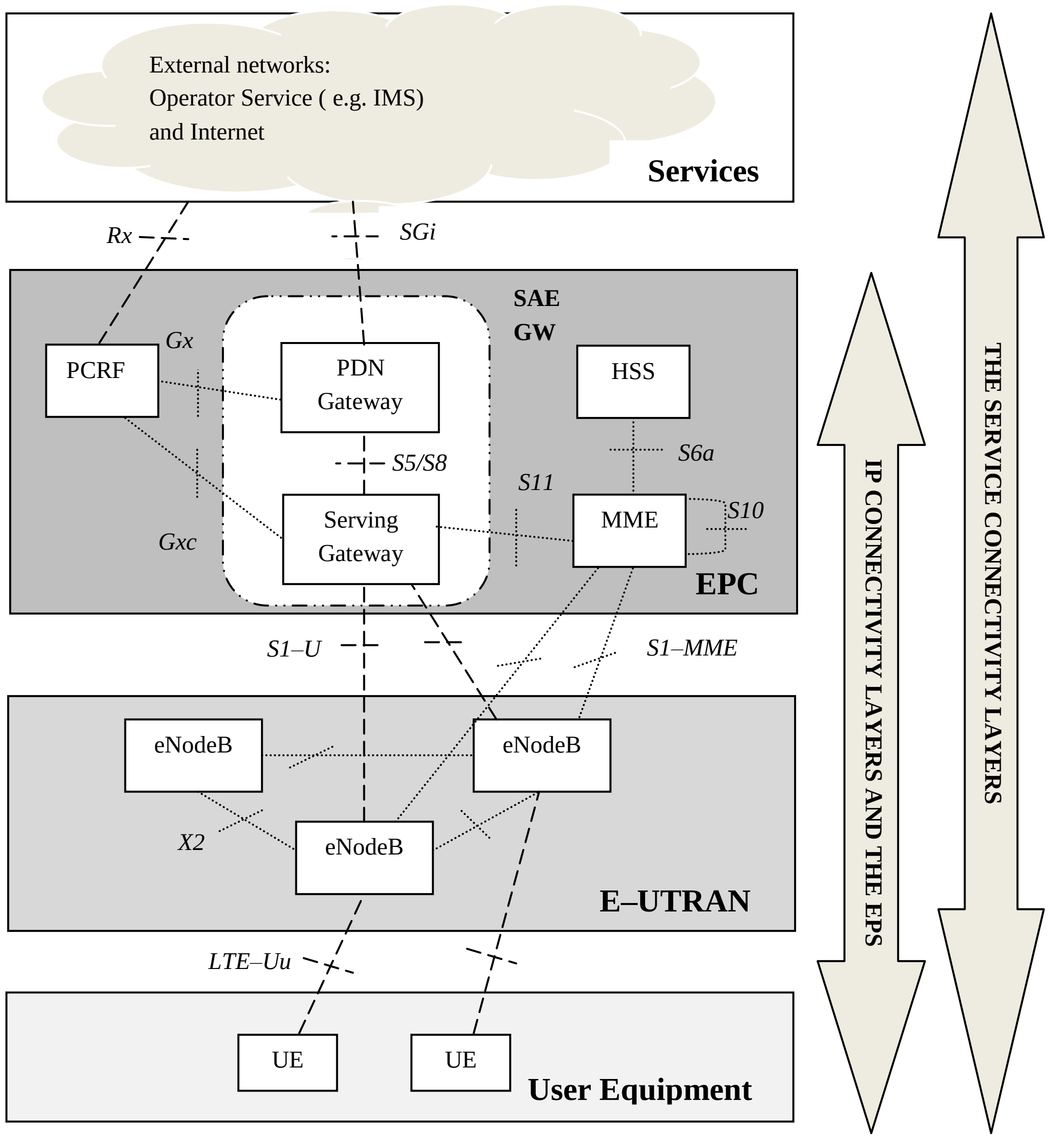

Figure 2.1: The LTE system architecture [4].

P–GW: The P–GW is an anchor router between a EPC and external IP networks. These external networks are also called data packet networks that are why P–GW often has another abbreviation as PDN–GW. The P–GW is the highest mobility level anchor of the system, as illustrated in Figure 2.3, which shows UP protocol stack and involved elements. It acts as an IP attachment for UEs. An UE is allocated an IP address if it wants to communicate with PDN networks such as the Internet. The P–GW employs Dynamic Host Configuration Protocol (DHCP) for IP–address distribution to UEs when they request a PDN connection.

MME: Unlike S–GW and P–GW, MME operates only in Control Plane (CP) and is responsible for mobility management, authentication and security, and managing subscription profile and service connectivity [4].

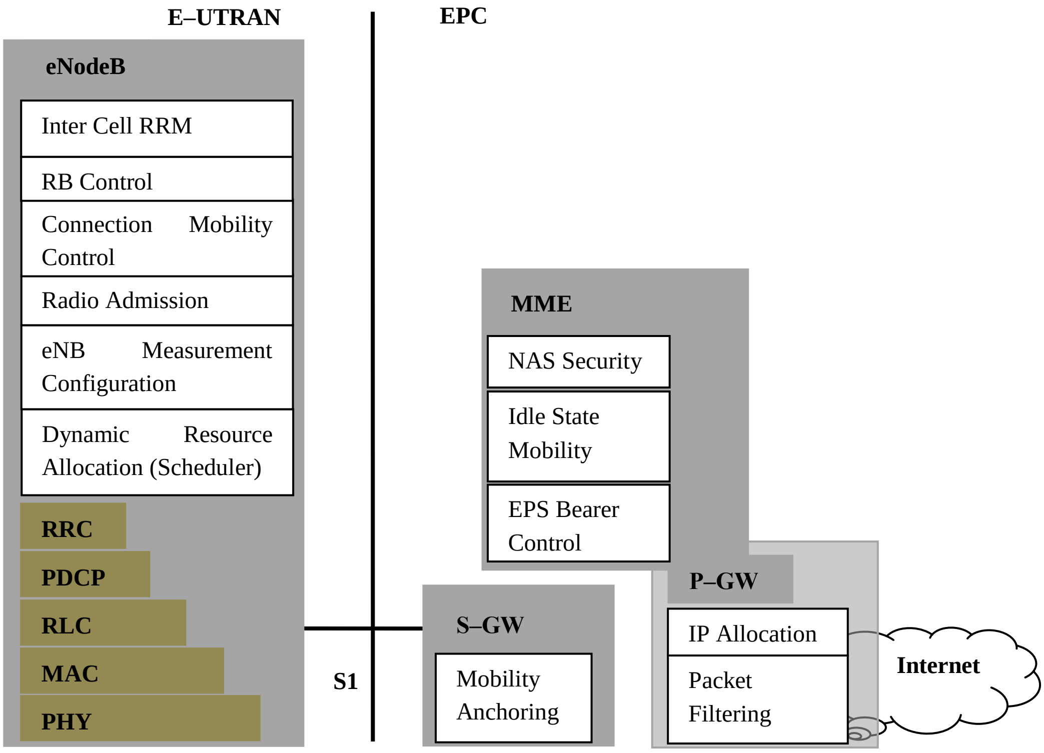

Figure 2.2: Split functionalities between E–UTRAN and EPC [4].

Figure 2.2 shows the functional split of E–UTRAN and EPC of EPS architecture, giving the overall illustrational functions managed by a CN and an E–UTRAN. In the next subchapter, the functionalities of the E–UTRAN will be discussed in details.

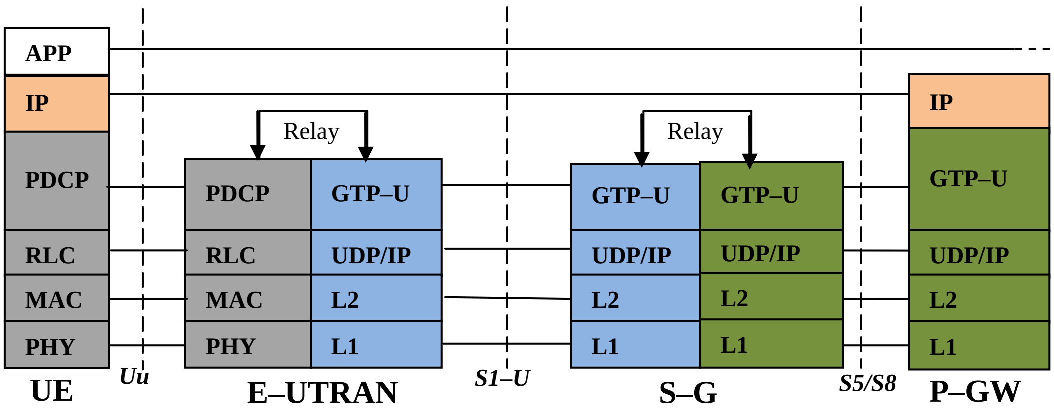

Figure 2.3: User plane protocol stack [4].

2.1.2. E–UTRAN NodeB

The LTE radio access network typically is the network of Evolved–UTRANs, which is co–called eNodeB, an evolutional Base Transceiver Station (BTS) of Wideband Code Division Multiple Access (WCDMA) NodeB. It is important noting that in LTE there is no a centralize node existed in between a radio BTS and a CN anymore as it used to be; such as a 2G GSM Base Station Controller (BSC) or a 3G WCDMA Radio Network Controller (RNC). The primary purpose of removing an intelligent controller is to speed up a procedure of connection establishments and lessen handovers' time. This evolution is essential since the connection set–up time for real time applications is very important for an end–user, for example online game applications. The time decrease for a handoff also is needed for real time services since an user would tend to terminate the call if he would wait too long for a handover.

An eNodeB is communicated to EPC CNs by means of S1 interface and it connects to its neighbouring eNodeBs by means of X2 interface. A new advanced feature has been introduced for LTE, Self–Organizing Network (SON). SON means the network is able to reconfigure and reorganise by itself. The interface Uu connects an UE with its eNodeB. Since centralized nodes are removed, therefore an eNodeB is given more functionalities than those given to NodeB. Below are some fundamental functionalities provided by an eNodeB as depicted in Figure 2.2.

An eNodeB basically functions as a layer 2 bridge connecting an UE to EPC. The eNodeB is like a transitory station between radio–connectivity side toward the UE and IP–based connectivity side toward the EPC, relaying the reformatted data between the two domains. In order to do so, the eNodeB performs ciphering and deciphering of the data suitable for each type of connectivity. The eNodeB also performs IP hearer attachment and detachment, which helps to identify the ordering packets and avoid sending repeatedly a packet. Packet segmentation is also a function of an eNodeB, which means the size of packets is modified suitably with the various types of interfaces.

The eNodeB has many important functions in CP. The eNodeB is also responsible for Radio Resource Management (RRM) function, which ensures efficient utilization of the radio resource. LTE RRM is basically different kinds of algorithms to control system radio resource such as power control, load control, resource blocks, mobility, etc. The objective of RRM is to control intelligently the limited radio resource of the system while QoS and fairness criteria of an individual bearer have to be satisfied and the overall used resources has to be minimized. Some of the aspects of RRM are listed below as shown in Figure 2.2:

- Radio Admission Control (RAC), which bases on algorithms to determine whether a UE is allowed to access the network.
- Radio Bear Control (RBC), which assists an eNodeB to determine what kind of bearer, is used to carry a specific packet. The criteria base on types of data, priorities, QoS, etc.

- Connection Mobility Control (CMC): An eNodeB measures and analyses strength level of signals toward UE and performs measurements by itself to make a handover decision among cells.
- Dynamic Resource Allocation (DRA). An eNodeB distributes the resource blocks to users dynamically, depending on users' requests and QoS the decision is made.
- Load Balancing.
- Inter–cell interference co–ordination.

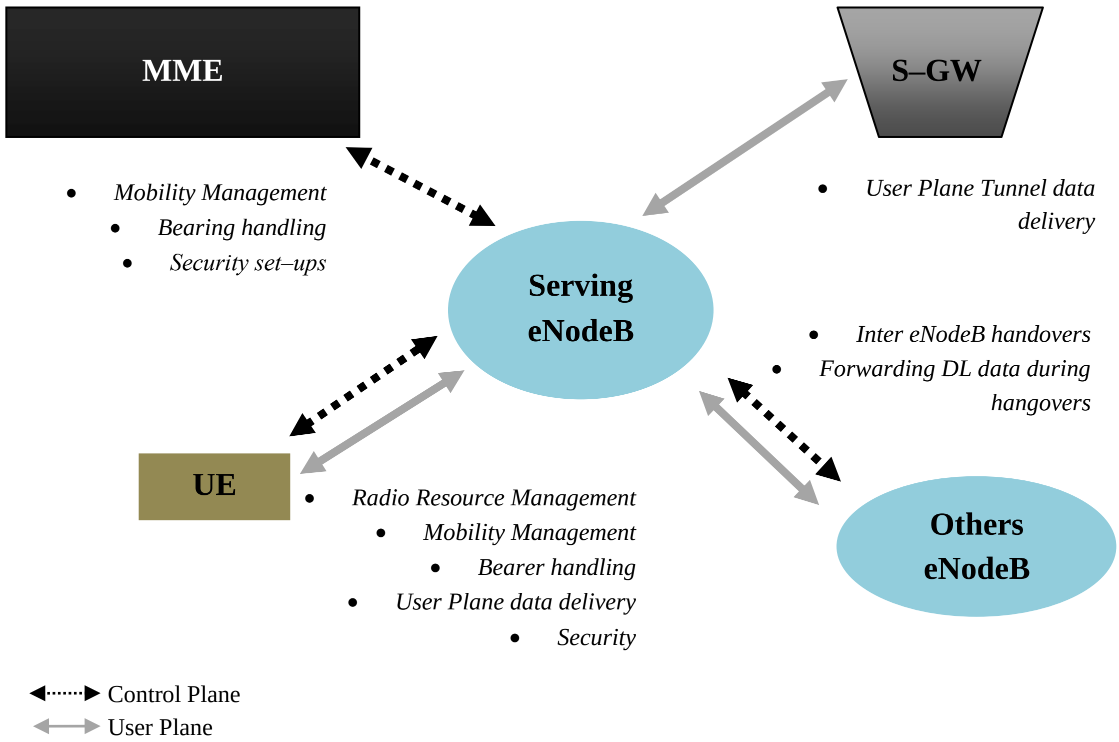

Figure 2.4: Interactions of a serving eNodeB with others logical nodes and functionalities [4].

2.2. LTE Multiple Access Techniques

Choices of proper multiple access schemes and modulations would boost higher data rate. There appears an evolution in multiple access techniques in LTE physical layer. The Orthogonal Frequency Division Multiplexing (OFDM) has been designed as the multiple access scheme for 3GPP LTE downlink while Single Carrier–Frequency Division Multiple Access (SC–FDMA) is being adopted as the uplink transmission pattern. Those multiple access techniques will be illustrated in basic manner in this subchapter.

2.2.1. OFDM in LTE Downlink Transmission

The multi–carrier modulation has been adopted as a modulation scheme in physical layers to achieve higher data rate, it was first introduced in 1960s. Transmission by means of multicarrier means data is modulated by hundreds of narrowband subcarriers instead of only one wideband carrier. The available channel is divided into many parallel sub–channels called multi–carriers. The idea of channel division is that subcarriers are non–frequency–selective or frequency–flat, and therefore effects of signal fading in wireless communication are mitigated.

OFDM is a special case of multicarrier techniques. Multi–carriers are designed in such a way that they are orthogonally overlapping. Hence, OFDM is highly spectral effective since there is no need of guard band separated carriers, which is very attractive in implementation. However, it is worth to note that the use of OFDM cannot benefit against time–variant channels without channel coding. In LTE, combinations between OFDM, channel coding and Hybrid Automatic Repeat reQuest (HARQ) are needed to overcome deep fading, which supposes to happen in each individual carrier [1].

The first cellular communication system designed on the base of OFDM was proposed in [5], paving the way for OFDM to LTE downlink. Additionally, OFDM is widely used in either wireless communication systems like: Institute of Electrical and Electronics Engineers (IEEE) 802.11a, g, n, Wireless LANs (WLANs), IEEE 802.16d, e, Worldwide Interoperability for Microwave Access (WiMAX), Digital Video Broadband (DVB), Digital Audio Broadband (DAB), or wire–line systems such as: Asymmetric Digital Subscriber Line (ADSL), Power Line Communication (PLC) [6].

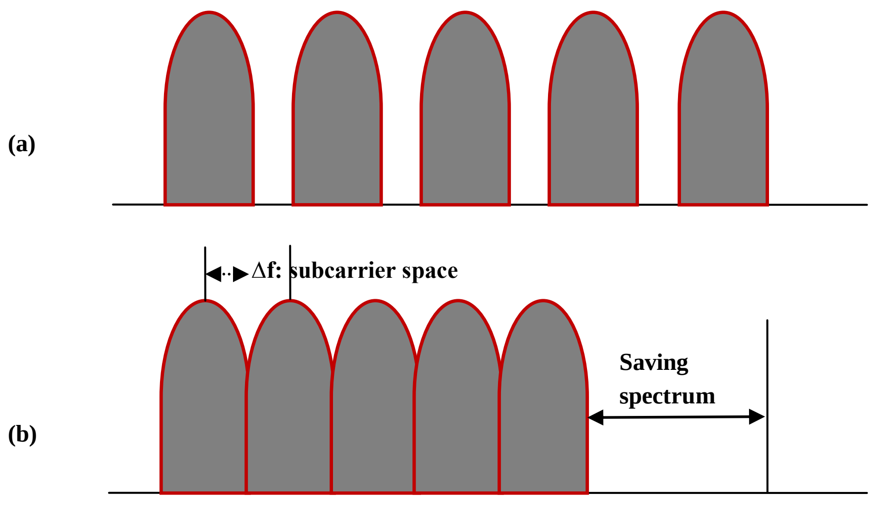

Figure 2.5: (a) The classical multicarrier systems spectrum. (b) The OFDM system spectrum.

Subcarrier space $\Delta f = {}^{1}/_{T_u}$ as shown in Figure 2.5, which is one of the basic OFDM system parameters, is the frequency separation between subcarriers, where T_u is the per–subcarrier modulation symbol duration. And thus the subcarrier space is equal to per–subcarrier modulation rate $1/T_u$. The symbol duration T_u is chosen in a way that it is not too long to lose the symbol rate but not too short for the system to work effectively.

One of the main advantages of OFDM system is its robustness against multipath components in wireless communication, which leads to fast fading and Inter Symbol Interference (ISI). Fading and ISI cause Bit Error Rate (BER) at receivers to be high and system performance to be low, they are therefore very critical issues in wireless system. On one hand, Cyclic Prefix (CP), $T_{CP,}$ or Guard Interval (GI), Δg, is introduced to each useful OFDM symbol interval to avoid ISI problem. GI must be chosen to be longer than or at least equal to expected delay spread τ, $(\Delta g \geq \tau)$, so that multipath components of previous symbols cannot interfere with the next symbol. In an OFDM system, CP addition is done by copying a part of the useful symbol at the end and attaching it to the beginning. On the other hand, GI ensures orthogonality between subcarriers by keeping the OFDM symbol periodic over the extended symbol duration and therefore avoiding Inter–carrier Interference (ICI). However, a disadvantage of CP attachment is that the CP makes waste of spectrum and therefore lowers the system performance effectiveness. [7] and [8] give the evaluation performances between OFDM system models with CP attachment and CP removal. The efficiency loss in dB can be given [8]:

$$\text{Efficiency loss} = -10\log_{10}\left(\frac{\Delta g}{\Delta g + \text{Tu}}\right) \qquad (2\text{–}1)$$

An OFDM system can have from hundreds to thousands subcarriers, frequency space is range from a few kHz to several hundred kHz. Whenever subcarrier is chosen, the number of subcarrier to use depends on the available bandwidth of a system. In LTE, the subcarrier space is 15 kHz in Release 8. LTE spectrum is flexible, which means the number of subcarriers is also varied dependent on bandwidth flexibility. For example, in case of 10 MHz bandwidth, the system has around 600 subcarriers, while 20 MHz spectrum allocation makes use of approximately 1200 subcarriers. Other example towards to the choice of CP in LTE; LTE specifies both normal and extended CP lengths. The normal CP, which CP is equal to 4.69 μs, is intended for most of the scenarios. While the extended CP, which CP is equal to 16.67 μs, is intended for scenarios with long delay spread.

The practical implementation of an OFDM system is based on Discrete Fourier Transform (DFT) and Inverse Discrete Fourier Transform (IDFT) operations, which equivalently transfer signals between time and frequency domains. Length of FFT, should be an integer number, is power of two. For LTE system, the size of FFT operation varies correspondingly to bandwidth flexibility. For instance, the FFT size of 1.25 MHz system is 128 while the length of FFT is 512 with 5 MHz spectrum. A system, which uses 20 MHz spectrum for transmission, uses 2048 points for FFT size [2]. Transmitters employ an Inverse Fast Fourier Transform (IFFT) block to generate a signal in time domain representative from its frequency domain representative and a Fast Fourier Transform (FFT) block at receivers do inverse execution as depicted in Figure 2.6. Data symbol stream at transmitters is first serial–to–parallel converted into N streams, each is representing for a subcarrier in frequency domain, and thus each stream is modulated and demodulated independently with other subcarriers. The IFFT is followed by CP addition. After IFFT operation, the signal now is in time domain representative and sent to RF module for transmission. The receiver executes FFT to recover original data but before that, an OFDM receiver is able to perform timing synchronization and frequency synchronization. Synchronization helps to receive the correctly expected frames. Timing synchronization is basically obtained by using correlation calculation with a known samples, as for example in LTE, the reference symbols, guard interval. Frequency synchronization estimates frequency offset between transmitters and receivers.

OFDM has proved as a good choice for LTE downlink since it provides many advantages. However, a few disadvantages must be solved for this technique to become a success. High Peak–to–Average Power Ratio (PAPR) appears to be one of those serious drawbacks. PAPR is defined as the ratio of the peak power to the average power of the transmit signal. An OFDM signal is basically a sum of many complex random variables, each of them can be considered as a complex modulated signal at different frequencies. Therefore, it may exhibit a very high instantaneous signal peak with respect to the average signal level. [6] proves that in case of N subcarriers, the voltage PAPR is proportional to $\sqrt{N}$ and there are some solutions for this issue are also mentioned in [6].

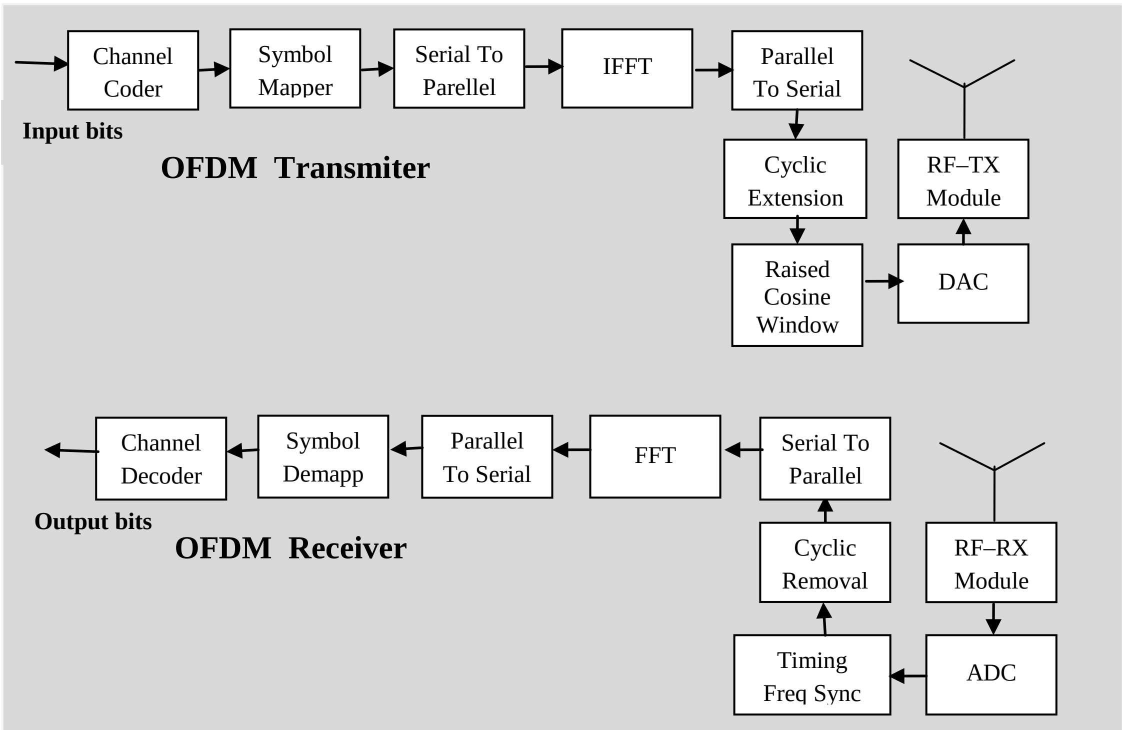

Figure 2.6: OFDM system transceiver block diagram [6].

2.2.2. SC–FDMA in LTE Uplink Transmission

As discussed previously, OFDM technology, which is adopted as a downlink LTE, has some disadvantages in implementation, in which high PAPR of the transmitted signal is a very critical issue. Such undesirable high powers imply a reduced power–amplifier efficiency and higher power–amplifier cost. Even though, there are some solutions introduced to come up with this matter, those methods still have limitations in terms of to what extent the powers can be diminished. This is especially crucial in LTE uplink transmission due to the very importance of low power consumption and cost for UEs. SC–FDMA is a choice for the LTE uplink access scheme.

LTE uplink transceivers' structure are typically similar to that in LTE downlink, only differences are presents of an additional DFT block at uplink transmitters and IDFT at uplink receivers placed right before FFT block and IFFT block, respectively, as drawn in Figure 2.8. Hence, SC–FDMA can be seen as OFDM system with an additional DFT–mapper. After data bits are mapped into modulation symbols, the transmitter groups those modulation symbols into a block of N symbols. Those blocks of N symbols in time domain are fed into a N–point DFT to be transformed into frequency domain. Frequency domain samples are then mapped to a subset of M subcarriers where M is typical greater than N and is the multiple of 12. Zeros are then padded among the output samples. Then similarly to what happens in OFDM system, an M–point IFFT converts these frequency–representative samples to time–representative samples, which are followed by adding CPs. In OFDM, each symbol is directly mapped to an individual subcarrier for a OFDM symbol duration in time domain. In contrast, in SC–FDMA multiple subcarriers carrier each data symbol because the mapping is performed with symbols' frequency domain samples to subcarriers. Therefore, it can be considered as a single carrier since a subset of subcarriers carries a symbol at a time. Figure 2.7 shows the principle on how OFDM and SC–FDMA differ.

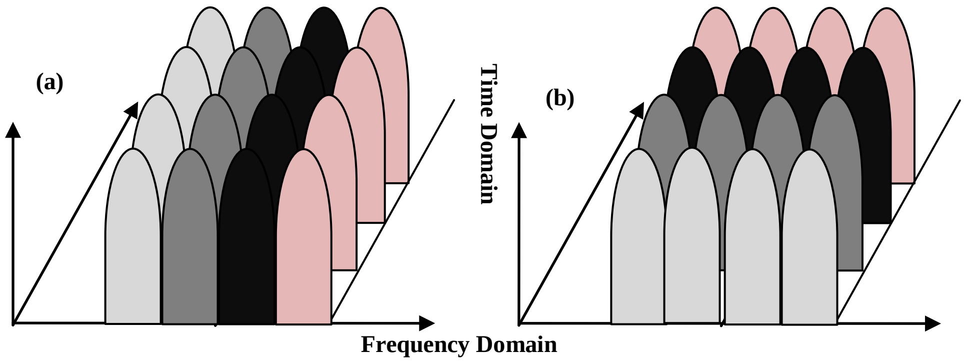

Figure 2.7: Illustration of OFDM (a) and SC–FDMA (b) systems.

The important advantage of implementing SC–FDMA is the lower PAPR of the transmitted signal. Lower PAPR makes SC–FDMA become a preferred technology for LTE uplink and become a preferred favourite for UE terminals.

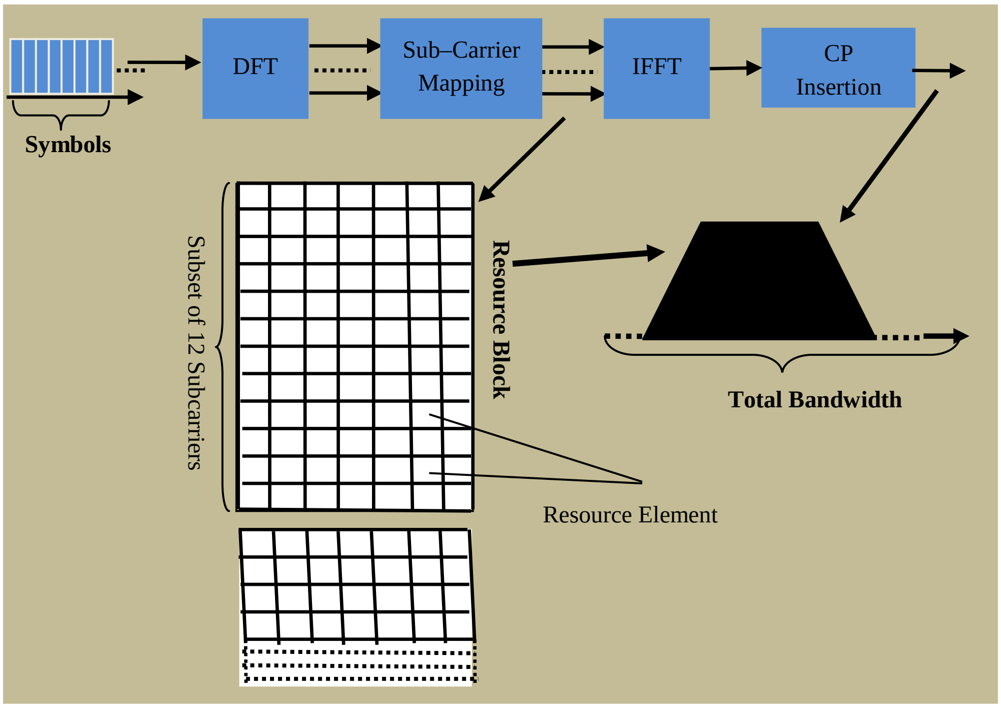

Figure 2.8: SC–FDMA structure and symbol mapping and single carrier generation.

Table 1 summarizes the physical layer parameters and their values employed in LTE SC–FDMA uplink.

Table 1: LTE SC–FMDA uplink physical layer parameters [1].

Parameter	Value	Description
Subframe duration	1 ms	
Slot duration	0.5 ms	
Subcarrier spacing	15 kHz	
SC–FDMA symbol duration	66.67 µs	
CP duration	Normal CP	5.2 µs for first symbol in each slot, 4.69 µs for all other symbols
	Extended CP	16.67 µs for all symbols
Number of symbols per slot	7 (Normal CP) 6 (Extended CP)	
Number of subcarriers per RB	12	

Bandwidth (MHz)	Value	FFT size	No. of Subcarriers	No. Of RBs
	1.25	128	72	6
	3	256	180	15
	5	512	300	25
	10	1024	600	50
	20	2048	1200	100

The same resource structure is employed for uplink as for downlink. A 10 ms radio frame is divided into ten subframes, each lasting for 1 ms consisting two 0.5 ms slots. Subcarrier space in LTE SC–FDMA is also as the same as that in LTE OFDM, meaning that the smallest element is Resource Element (RE), which is equal to one subcarrier in frequency representative and one SC–FDMA symbol in time representative. A Resource Block (RB) contains REs, spreading into 12 subcarriers for duration of one slot as depicted in Figure 2.8. Modes of CP are supported as those in LTE OFDM; normal CP (4.69 μs) and extended CP (16.69 μs).

With multiple user access schemes, different users are shared system resources. An eNodeB schedules the resources and allocates them to users fairly so that the transmissions are not overlapped. Before allocating resources to users, the base station understands well the need of users.

2.3. LTE Packet Scheduling, Link Adaptation and Channel Coding

Packet scheduling, channel coding and link adaptation are key features in LTE Layer–2 Control Plane that ensure high efficiency transmission. In this subchapter, those three features are discussed.

2.3.1. LTE Packet Scheduling

Scheduling plays a very important role in LTE network. It assigns shared resources to requesting users in most efficient manners. An eNodeB Medium Access Control (MAC) scheduler at MAC sublayer is responsible for downlink and uplink scheduling.

The MAC scheduler runs the scheduling algorithms which determine what gets sent, when sent and to whom. Inputs of the MAC scheduler come from various sources that guide the scheduling algorithms. The MAC scheduler' outputs are a series of resource assignments for a downlink and uplink subframe. Resource assignments are defined in term of resource blocks, which occupy 1 slot in time domain and 12 subcarriers in frequency domain – see Figure 2.8.

The resource assignments also indicate the transport blocks' size and what physical layer resources are to be used in sending it to receivers; UE/eNodeB;

2.3.2. LTE Channel Coding

Channel coding, together with link adaptation, plays the most important roles affecting link performance in digital communication systems. Channel coding can be considered as the main difference between analog and digital systems, making error detection and correction possible. Automatic Repeat reQuest (ARQ) and Forward Error Correction (FEC) are two main existing error correction techniques.

ARQ requires retransmission of the packet if errors are detected. The retransmission will be finished, until the received error–free packets or a maximum retransmission time is reached. In LTE, the maximum number of retransmission Hybrid ARQ (HARQ) process is three. In FER, receivers are able to correct the received packet if errors are detected. Some redundancy bits are added to original data bits.

In LTE system, block codes and convolutional codes are used. Besides, an enhancement coding technique from convolutional code so–called Turbo code, which provides a better performance rather than the two ones mentioned above, is used.

In block codes, the input data blocks, which can be seen as vectors are multiplied by a generator matrix, producing a code word vector. Unlike block codes, convolutional codes have a similar structure like Finite Impulse Response (FIR) filters and operator bitwise. The principle of a convolutional encoder is a shift memory register with m stages, which means the coded bits not only depends on the prevailing bit but also some m previous bits. Let take a look at the convolutional encoder $C_{(k,\ n,\ m)}$, where k is the number of input bits, which are fed to the encoder with m–stage shifting register to produce n output bits. The rate code is defined as: $R = {}^{k}/_{n}$. For example, the structure of LTE convolutional encoder with k = 1, n = 3, m = 6 and therefore the code rate R =1/3 can be illustrated in Figure 2.9.

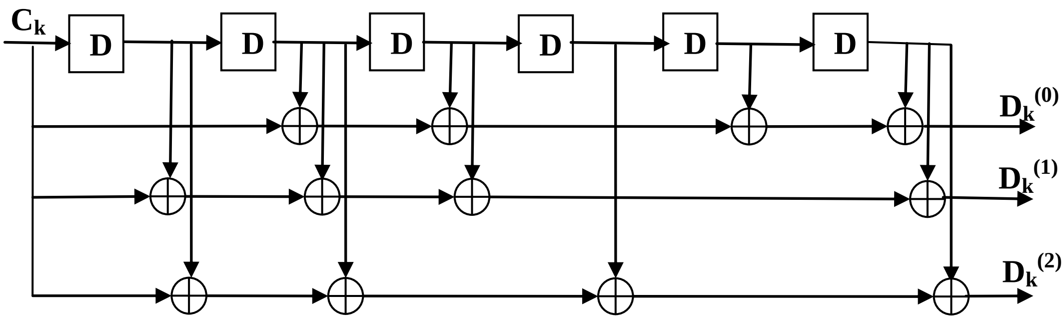

Figure 2.9: LTE convolutional code [9].

In 1993, Turbo codes were first present by Glavieux and Thitimajshima, its performance is close to the Shannon limit. The Turbo encoder in LTE is a systematic Parallel–Concatenated Convolutional Code (PCCC) with two 8–state constituent encoders The following channels use Turbo coding: Uplink Shared Channel (UL–SCH), Downlink Shared Channel (DL–SCH) [9].

Figure 2.10 shows an overall data transmission flow in LTE physical layer where channel coding is involved. Data transferred from transport layer to physical layer is called Transport Block (TB). At physical layer, each TB is added by a 24 Cyclic Redundancy Check (CRC) bit sequence for detection. The TB is then segmented into ‘code blocks. It is followed by attaching 24–CRC bits to each code block. The CRC–inserted code block then inputs to a channel coder with matching rate. Depending on what types of data on which channel, convolutional or turbo coder is used. Then, encoded data will be fed for scramming and modulating before it is mapped to antenna port.

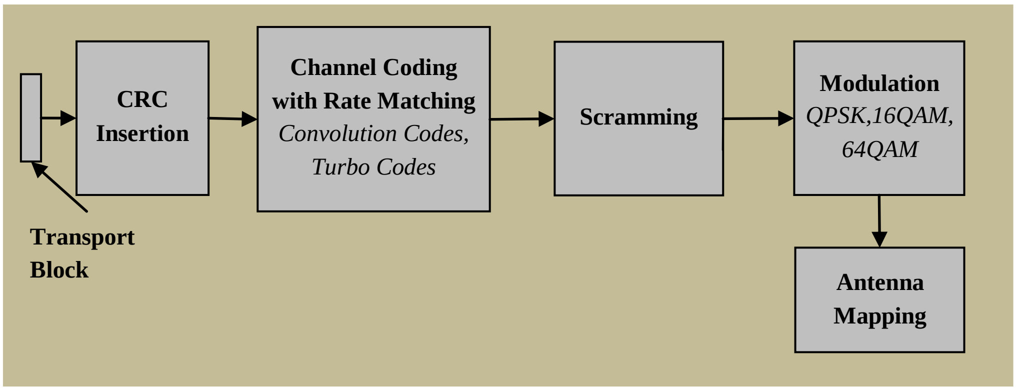

Figure 2.10: Channel coding in physical data transmission flow [1].

2.3.3. LTE Link Adaptation

Link adaptation is the fundamental to the design of a radio interface, which makes efficiency use of the channel capacity possible, matching the transmission parameters, modulation schemes and code rate dynamically to the channel. Link adaptation principle in UMTS is based on fast closed–loop power control to support circuit–switched service, it is done in a way the link rate remains roughly unchanged while the transmitted power is adapted to the changes of the channel. Unlike that preceding principle in UMTS, link adaptation in later advanced UMTS HSPA and in LTE adjusts data rate dynamically to match the instantaneous variations of channel. LTE link adaptation is based on Adaptive Modulation and Coding technique (AMC), which can be illustrated as following [9]:

- Modulation scheme: If SINR is sufficiently high, higher order modulations with higher spectral efficiency like 64 Quadrature Amplitude Modulation (64QAM) are selected to increase data rates. In channels where have poor Signal–to–Interference Plus Noise Ratio (SINR) values, a lower order modulation such as Quadrature Phase Shift Keying (QPSK) is used, this selection is more robust against transmission error but lower bit rate and spectrum efficiency.
- Code rate: Selection of code rate depends on modulation scheme and channel condition, shown in Table 2. The better quality of the channel, the higher coding rate, and then the higher data rate can be achieved.

For transmission in LTE downlink, the Modulation and Coding Scheme (MCS) is selected to ensure Block Error Rate (BLER) is less than 0.1 [9]. UEs estimate current downlink channel by measuring and evaluating reference signals sent in downlink, feedbacks are then transmitted to the eNodeB in uplink. Pilot–assisted channel estimation is a method in which known signals called pilots. Pilots are transmitted with application data to obtain channel knowledge. Algorithms, Least Square (LS), Minimum Mean Square Error (MMSE), are channel estimation methods used in LTE downlink. The detail of those methods can be further dig deeply in [10]. The input for MCS selection process is Channel Quality Indicator (CQI).

CQI is a feedback indication to assist link adaptation process, by measuring and mapping with SINR level. An example of CQI–SINR mapping is shown in Figure 2.11. There is no transmission at all if SINR goes below –10 dB since CQI is equal zero. On the other hand, highest CQI equal to 15 is reported to an eNodeB if SINR is more than 20 dB, highest transmission efficiency is expected. The quality of the measured signal depends on not only channel quality of the serving cell, interference level from other cells, noise but also quality of the receivers.

Dependently on levels of SINR, up to 16 possible levels of 4–bit CQI are defined, the corresponding combination of modulation scheme and coding rate chosen is up to this CQI level as shown in Table 2. As can be seen from the table, the lowest CQI is 1, referring to the simplest transmission manner. QPSK is selected as the modulation mode and the lowest code rate is 0.076, which is selected for the worst channel quality. When the channel quality is getting better, higher modulation orders and faster coding rates can be the choices. The highest modulation and coding rate are 64QAM and 0.93 relatively and correspond to a CQI value of 15. The CQI values are used also to select the optimal resource block, the optimal subcarriers and the optimal time slot.

Table 2: CQI levels and corresponding MCSs and spectral efficiency [9].

CQI index	Modulation scheme	Coding Rate	Efficiency (information bits per symbol)	CQI index	Modulation scheme	Coding rate	Efficiency (information bits per symbol)
0	No transmission	—	—	8	16QAM	0.48	1.9141
1	QPSK	0.076	0.1523	9	16QAM	0.6	2.4063
2	QPSK	0.12	0.2344	10	64QAM	0.45	2.7305
3	QPSK	0.19	0.3770	11	64QAM	0.55	3.3223
4	QPSK	0.3	0.6016	12	64QAM	0.65	3.9023
5	QPSK	0.44	0.8770	13	64QAM	0.75	4.5234
6	16QAM	0.59	1.1758	14	64QAM	0.85	5.1152
7	16QAM	0.37	1.4766	15	64QAM	0.93	5.5547

Two types of CQI reporting; periodic and aperiodic; are introduced in LTE downlink. In periodic reporting manner, CQIs are reported by UEs in a periodic time interval on Physical Uplink Control Channel (PUCCH). In contrast, UEs only report CQIs in aperiodic mode when they are requested by eNodeB to know the channel. Physical Uplink Shared Channel (PUSCH) operates aperiodic CQIs reporting. Normally, periodic CQI report is used. However, in some cases, such as handover situation or loss of synchronization, aperiodic report is used.

There are also three kinds of CQI values: wideband CQI, eNodeB–configured sub–band CQI and UE–configured sub–band CQI. UEs report a wideband CQI to eNodeB, which indicates channel quality for the whole system bandwidth. In addition, UEs are requested to report eNodeB–configured sub–band CQIs, in which the sub–band is configured by the eNodeB. The last type is UE–configured CQI, meaning UE selects a preferred sub–band to report CQI as well as the sub–band position.

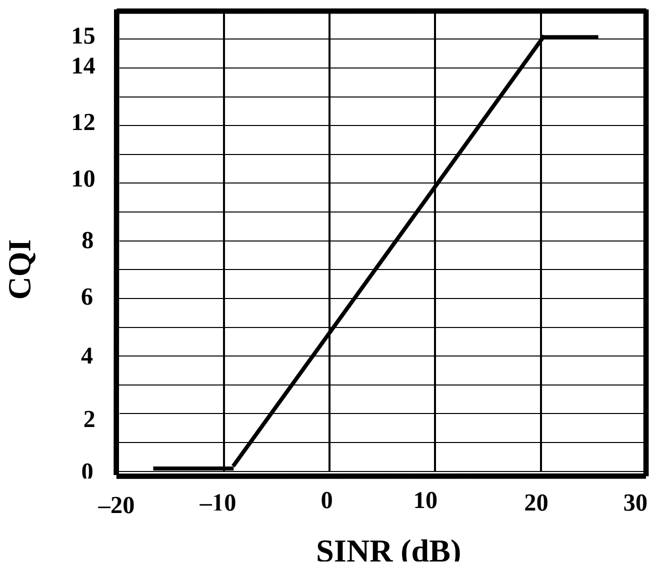

Figure 2.11: CQI–SINR mapping [11].

Additionally, UEs report Ranking Indicator (RI) and Pre–coding Matrix Indicator (PMI). Again, PUCCH carries periodic RI, PMI and CQI reporting which aperiodic RI, PMI and CQI feedbacks are reported by using PUSCH. RI and PMI feedbacks assist the eNodeB for making decision of MIMO multiplexing operation rather than link adaption.

RI indicates the number of layers an eNodeB should operate to obtain performance efficiency. Even the eNodeB is configured in multiplexing but one layer can be used due to UEs experience bad SNR at once, guiding the eNodeB to fallback to transmit diversity in MIMO mode. In Release 8, up to four layers are transmitted simultaneously so the maximum value of RI is four. UEs feedback PMI to indicate eNodeB which optimum pre–coding matrix should be used for downlink transmission. [12] proposes RI calculation in conjunction with PMI computation since they are involved in MIMO operation. The method is based on maximizing mutual information. Another RI calculation method based on Reference Signal (RS) is proposed in [13].

3. LTE MULTIPLE ANTENNA TECHNIQUES

Multiple antenna techniques have earned reputations to be a cutting–edge technology, which can boost significantly wireless communication performances in combination with advanced signal processing. The principle of multi–antenna technique is to produce multiple link transmissions with different properties to come up with diversities of the radio propagations in time domain as well as frequency domain. In LTE network, with present of MIMO, up to seven Transmission Modes (TM) in downlink (Release 8) are defined to make LTE being able to deal with every kind of severe radio propagation, the use of each of TMs depends on particular scenarios. Those LTE TMs are built on the base of three commonly implemented techniques; beamforming, diversity and spatial multiplexing techniques, which are described briefly in this chapter.

3.1. LTE Transmission Modes

MIMO configuration allows a LTE eNodeB make use of transmission mode diversity. An eNodeB is able to dynamically alter between those transmission modes to fully optimize performances due to quickly changes of channels. For instance, when eNodeB is configured to use closed loop mode, but there is a chance to fallback to transmit diversity or single antenna modes if the channel is not good to utilize multiplexing. The transmission scheme of each of these TMs is referred to one of four multiple antennas schemes illustrated in Figure 3.1. Those are: Single Input Single Output (SISO), Single Input Multiple Output (SIMO), Multiple Input Single Output (MISO), Multiple Input Multiple Output (MIMO). SISO refers to one transmitting and one receiving antenna at two ends. SIMO means one antenna being used at transmitters and multiple ones at receivers while if multiple antennas at sending side and one at receiving side, the scheme is called MISO. MIMO operates with multiple antennas at two ends. Nevertheless, usually in literature MIMO also refers to multiplexing operation. Seven TMs are as [14]:

- TM1: Single–antenna port; Port 0: This is similar to most traditional wireless communication systems, which use a single data stream (one codeword) mapped to one antenna for transmitting. At reception, either one (SISO) or more (SIMO; reception diversity) antennas are employed to receive the signal.
- TM2: Transmit Diversity. Multiple antennas at the transmitting side are used. At reception, one antenna is received the transmitting signals. This mode refers to MISO transmission scheme.

- TM3: Open–Loop Spatial Multiplexing (OL–SM). This mode supports multiplexing of two to four layers that are multiplexed to corresponding two for four antennas. The mode requires less UE feedback, no precoding matrix indicator is included. Therefore, this mode is a choice when the channel knowledge is missing or when UE is moving with high velocity.
- TM4: Closed–Loop Spatial Multiplexing (CL–SM). This closed loop mode differs from open loop mode, precoding matrix feedback is required. TM3 and TM4 imply MIMO schemes.
- TM5: Multi–User MIMO. This mode is similar to TM4. It uses codebook–based closed loop multiplexing. The difference from TM4 is that one layer is dedicated for one UE. This mode refers to MIMO scheme.
- TM6: Closed Loop Rank 1 with Pre–Coding. This mode is a special case of TM4 with only one stream is used.
- TM7: Single–antenna port; Beamforming. MISO is the scheme of this transmission mode. The system uses multiple antennas at transmitter to form a desired beam. At the receiver, only one antenna is used for receiving the signal.

Only TM1 is based on conventional transmission scheme in wireless communication SISO. The remaining modes are based on either one of three multiple antenna techniques; beamforming, diversity, spatial multiplexing; presented in the next subchapter.

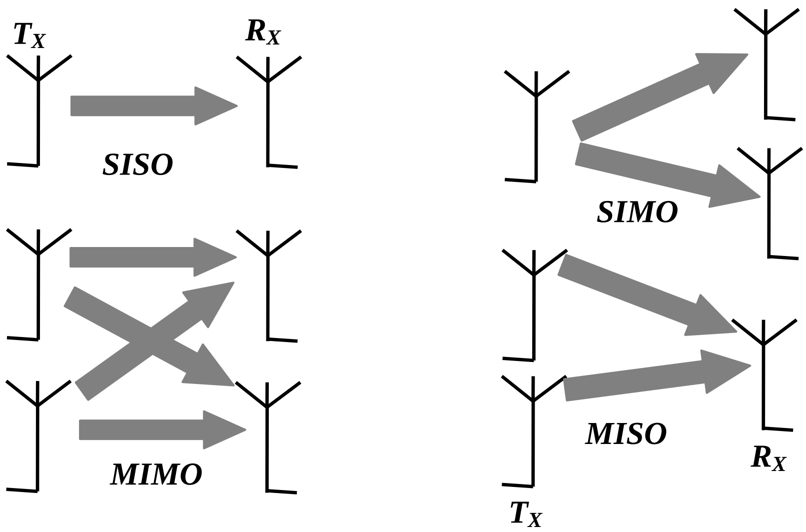

Figure 3.1: Multiple antenna access schemes.

3.2. Beamforming Technique

Beamforming or spatial filtering can be considered as an advanced multiple antenna technique that provides enhanced transmission link between a BTS and UE. In wireless communication, the idea is to construct dynamically directional beams to intended angles but destructing the beams in other angels where the transmission is not needed.

For example, this makes it possible to provide better coverage to specific areas along the edges of cells. Because, each element antenna in the array makes a contribution to the combined steered signal, an array gain, hence, is accomplished. On the other hand, there is a chance to destruct the signals to produce null–forming at some points, and the intra–cell and inter–cell interference are therefore by far improved. An adaptive antenna array consists of a column of radiating element, each of which can create a solid radiation beam. By adjusting the phase and relative amplitude of each generated signal, an adjustable pattern can be formed. The phase and relative amplitude are referred as weight.

Beamforming technique has also been adopted in cellular networks, becoming more advanced through generations to make use of more complex systems to achieve higher cell densities and higher throughput.

LTE downlink TM7 utilises beamforming technique. TM7 is the rank one technique based on beamforming using linear antenna array. This mode is used to extend the cell coverage by concentrating the transmitted signals to the direction of specific users. The increased SINR is achieved by phase adjustments of the signals transmitted on the different antennas with the aim of making the signals add–up constructively on the receiver side. Beamforming gain is composed of two parts:

- Array Gain: $= 10 * \log(\text{Number of antennas})$
- Diversity Gain: The gain depends on modulation and multipath severity.

TM7 is an open loop technique where PMI feedback from UE is not required, therefore it may be used for fast moving subscribers. Description of this beamforming–based transmission mode can be illustrated in Figure 3.2:

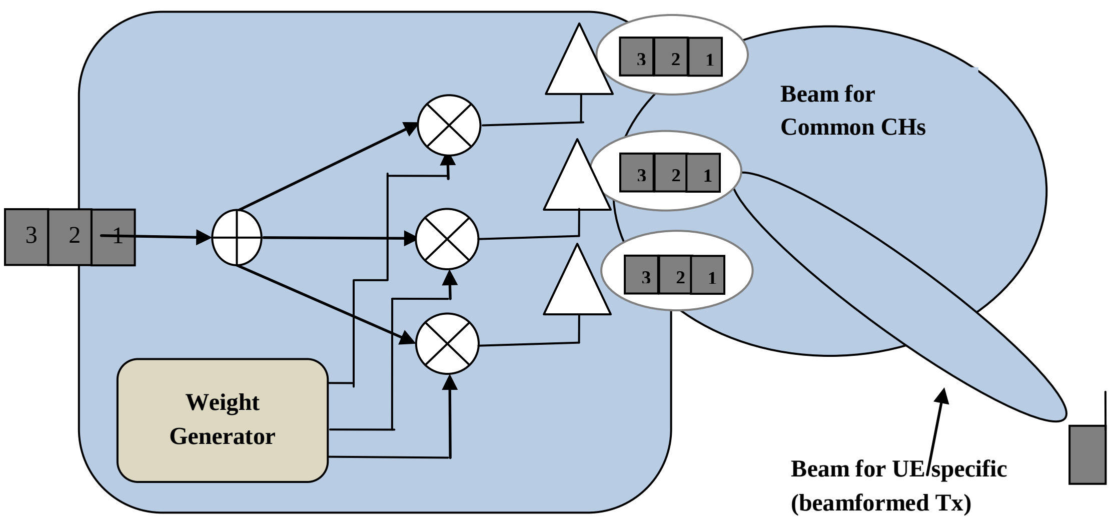

Figure 3.2: Beamforming in TM7; UE–specific beam.

The beamforming specification in LTE continues gets more advanced in Release 9. While TM7 utilise beamforming with only one layer, TM8 in Release 9 specifies two–layer beamforming, this enable the technology which beamforming and multiplexing are combined to serve for one specific UE or multiple specific UEs. The practical implementation is that either two layers can be assigned to one UE or each of them is pointed to each UE. More understandings of this technique can be viewed in [14].

3.3. Diversity Technique

Fast fading caused by multipath radio propagation, which results in large variation of the received signal level and delay distortion, is a very critical issue in wireless communication. Many methods have been developed to approach these impairments. Diversity technique is one of them.

The fundamental idea of the technique is that multiple radio links carrying the same information data are used instead of only one link, which is used in traditional systems. By having multiple transmission streams, the probability for the combined SINR received above an acceptably pre–defined threshold is higher, leading to lessen BER at reception, and then higher performances can be accomplished.

In LTE downlink, TM2 uses transmit diversity scheme, which means by having up to two antennas or four antennas at eNodeB in combination with pre–coding to achieve spatial diversity when transmitting a single data stream. These antennas need to be as much uncorrelated as possible to take full advantage of diversity gain, so they need to be well separated relative to the wavelength (Space Diversity) or have different polarization (Polarization Diversity). Transmit diversity in LTE is implemented by using Space Frequency Block Code (SFBC). SFBC is a frequency adaption of Space Time Block Code (STBC) where encoding is done in antenna frequency domain rather than in antenna time domain. STBC is also known as Alamouti codes [14]. STBC is not used in LTE since it operates on pairs of modulation symbols and in LTE; the number of modulation symbols in one subframe is often odd. While SFBC operates on pairs of adjacent subset of subcarriers, the technique is very feasible with OFDM systems. Hence, each pair of modulation symbols is mapped directly to OFDM subcarriers of the first antenna. Mapping of each pair of symbols to corresponding subcarriers of second antenna are reversely ordered, complex conjugated and signed reversed as shown in Figure 3.3. Equation (3–2) is the mathematical derive of a pair of transmitted symbols in space domain (antenna ports) and frequency domain (adjacent subcarriers):

$$X = \begin{bmatrix} x^{(0)}(1) & x^{(1)}(1) \\ x^{(0)}(2) & x^{(1)}(2) \end{bmatrix} = \begin{array}{c} \xrightarrow{\textit{Space}} \\ \begin{bmatrix} S_o & -S_1{}^* \\ S_1 & S_o{}^* \end{bmatrix} \end{array} \Big\downarrow \textit{Frequency} \qquad (3\text{–}1)$$

Where $x^{(p)}(k)$ denotes the symbols transmitted at antenna port p at k^{th} subcarrier [10].

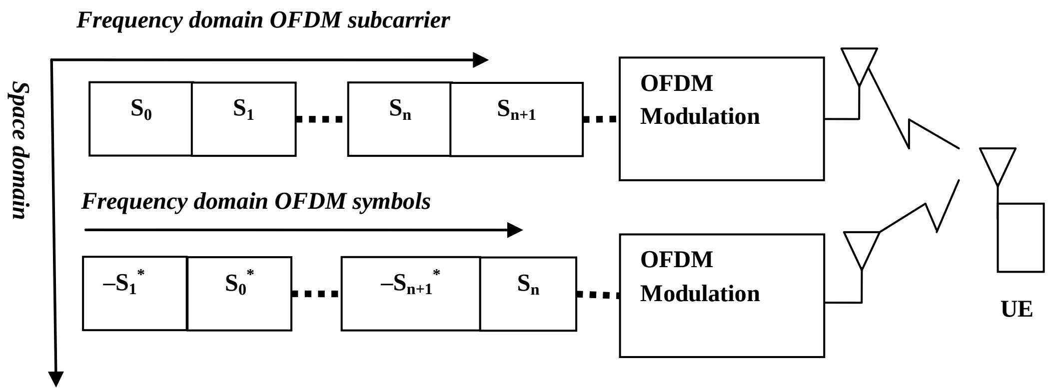

Figure 3.3: Space Frequency Block Code with two antennas transmit diversity [10].

With four–antenna architecture, the implementation is very much the same. A combination of SFBC and Frequency Switched Transmit Diversity (FSTD) is employed. In LTE, transmit diversity is used as a fallback option for multiplexing transmission modes, for example CL–SM and OL–SM, in the scenario where SNR is too low for spatial multiplexing to be utilized. Control channels, such as PBCH and PDCCH, are also transmitted using transmit diversity.

3.4. Spatial Multiplexing Technique

While the present of beamforming and transmit diversity is to extend coverage and overcome fast fading due to multipath propagation, spatial multiplexing pave the way for boosting very much data rate of wireless systems. Hence, multiple antenna operation with spatial multiplexing has become the primary technology and mostly used in LTE. The practical implementation of spatial multiplexing is that multiple separate data streams are parallel transmitted simultaneously over the channel, which is formed by a matrix $N_t \times N_r$ antennas at transceivers, where N_t stands for the number of antennas at the transmitter and N_r is the number of antennas at the receiver. Therefore, up to maximum $N_l = \min(N_t, N_r)$ number of streams is created. Each of those streams can be independently modulated and coded. In theory, it is possible to achieve the data rate proportionally linear with the number of antennas. In practical performance point of view, this is, however, never the case due to mutual correlations between the signals at different antenna pairs.

In LTE, there are two different modes that are operated based on spatial multiplexing principle: TM3 Open–Loop Spatial Multiplexing and TM4 Closed–Loop Spatial Multiplexing. The basic difference between the two modes is that while CL–SM requires PMI feedback from UEs, OL–SM does not. The CQI and RI feedbacks remain needed for both modes.

The basic structure of CL–SM is fully depicted in Figure 3.4. There also describes the layer mapping principle in the figure.

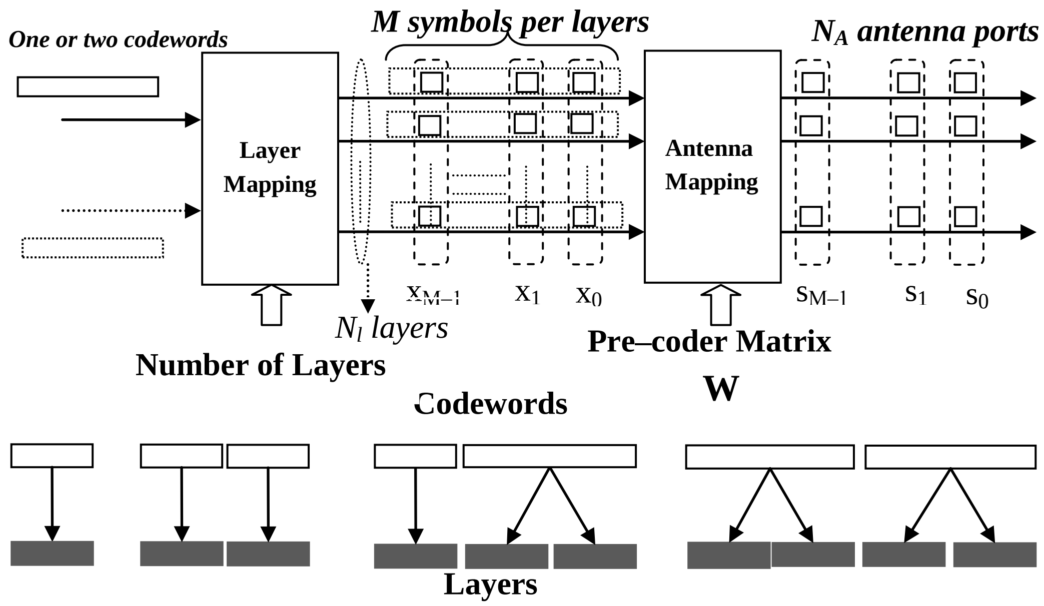

Figure 3.4: The basic structure of Closed–Loop spatial multiplexing and layer mapping [2].

Layer mapping converts one or two codewords, corresponding to one or two transport blocks, into a number of layers as illustrated in Figure 3.4. The layer mapping is done in such a way that the number of modulation symbols for each layer is equal. The number of layers may range from minimum one layer up to a maximum number of four layers that is equal to the number of four antenna ports (currently implemented in Release 8). Thus, there is only one codeword for a single layer. In the case of three layers needed for transmission, the second codeword, which is mapped to the second and the third layer, is doubled in length compared to the first codeword. In case of four layers, the first codeword is mapped to the first and second layer, while the second codeword is mapped to the third and the fourth layer. In this case, the two codewords have the same size.

After codeword–to–layer mapping, a set of N_l modulation symbols at once is linearly combined and mapped to the N_A antenna ports. The combining is considered by means of a pre–coder matrix W of size $N_A \times N_l$. Input of the combiner is a set of modulation symbols denoted as vector X_i size of N_l. Vector S_i with size of N_A, consisting of each symbol for each antenna, is outputted by multiplying input vector X_i with pre–coder matrix W: $S_i = W \times X_i$.

In case of a single layer, the matrix W is the $N_A \times 1$ vector and results in a beamforming for a single symbols spreading to N_A antenna ports. Therefore, beamforming can be considered as a special case of close loop spatial multiplexing if there is only one layer is used. LTE supports two or four antenna ports, making the pre–coder matrix one of the following forms:

- Two antenna ports: $N_A \times N_l = 2 \times 1 \; or \; 2 \times 2$.
- Four antenna ports: $N_A \times N_l = 4 \times 1,\; 4 \times 2,\; 4 \times 3 \; or \; 4 \times 4$.

It is important to note that RI and PMI are the feedback indicators that a UE recommends the serving eNodeB a number of layers and a pre–coder matrix relatively, which should be used with that estimated channel. The eNodeB may or may not follow the terminal's recommendation. If not following, the eNodeB will explicitly inform the UE which pre–coder matrix is used in downlink.

CL–SM outperforms when the knowledge of the channel is known at transmitters but it is not always the case. In some cases, the channel estimation becomes unknown at transmitting side, OL–SM is utilized since it does not require a pre–coder matrix recommendation from terminal. The basic idea of this mode is that a pre–defined codebook of precoder matrix is cycled across the frequency band, along with a layer permutation designed to give each layer similar average channel quality. No precoder feedback is needed, OL–SM is thus by far suitable in scenarios where timely channel dependent feedback cannot be made available, for instance, in high–speed scenarios.

Spatial multiplexing schemes perform best when the signals are uncorrelated. As the correlation between signals increases, the performance of SM declines. Lower correlation is achieved in scenarios where there are rich of scatterings. Dense urban areas are expected to give high scattering signals, and therefore SM schemes at such areas are expected to perform at their best.

Signal correlation is also dependent on antenna design, particularly separations of the antenna elements in an array. The larger distance between antenna elements in an antenna array provide lower correlation between signals received at antennas [15]. Antenna polarization also has impacts on signal correlation. Details of antenna design for diversity scheme will be mentioned in Chapter 5.

4. INDOOR PROPAGATION

There are many aspects making RF propagation in indoor environment being distinguished it from an outdoor environment. The aspects include multipath component issue, which becomes more severe. A Line of Sight (LoS) path may not exist, and characteristics of the environment may vary significantly over a very short time or distance. Walls and floors, doors and ceilings, people, and furniture located all around need to be taken into account when modelling an indoor wireless communication system since they may cause significant loss and make behaviours of the signals becoming more complicated. In order to understand effects of these factors on electromagnetic wave propagation, it is necessary to introduce three basic mechanisms of electromagnetic wave propagation and indoor propagation models. This chapter will describe the fundamental propagation mechanisms and some well–known indoor propagation models.

4.1. Propagation Mechanisms

Basically, there are three propagation mechanisms which are fully describe behaviour of a signal; they are reflection, diffraction and scattering.

The first and most commonly occurred mechanism is reflection. Reflection occurs when an incident wave encounters a smooth object having larger dimensions than signal wavelength. The object separates two mediums. During reflection, a part of the wave may be transmitted into the object medium; the mechanism is so–called refraction, causing a refracted wave. The remaining of the wave may be reflected back into the medium, which the original wave coming, that called reflected wave. Snell's law of reflection, which defines the angle of the reflected wave respecting with the incident wave's angle, may be used to find the point of reflection given by a pair of transmitter and receiver [15]. Snell's law is displayed as Equation (4–1):

$$\text{Ø}_\mathrm{r} = \text{Ø}_\mathrm{i} \text{ and } \sin(\text{Ø}_\mathrm{t}) = \sin(\text{Ø}_\mathrm{i}) * \frac{\mathrm{n}_1}{\mathrm{n}_2} \qquad (4\text{–}1)$$

Where $Ø_r$, which is the angle of the reflected wave, is equal to the incident wave's angle $Ø_i$. While the refracted wave's angle, $Ø_t$, is computed related to the properties of the two mediums. n_1 and n_2 are, correspondingly, the refractive indexes of medium 1 and medium 2. In indoor, there are rich of such objects that can cause reflection and refraction, such as walls and floors, tables, etc.

When the path between a transmitter and a receiver is shadowed with sharp irregularities, diffraction propagation may happen. Diffraction causes bending of the incident waves around obstacle. Various diffraction theories have been given to explain this propagation phenomenon, or used in computer simulation. Calculation of diffraction parameters and losses is based on Huygens' Principle [15]. Objects in an indoor environment, which can cause diffraction, include furniture and large appliances. The third wave propagation mechanism is scattering. Scattering occurs when an incident wave propagates through a rough medium in which there are a large number of objects with dimensions smaller than the wavelength. Hence, the incident wave is reflected to many different directions simultaneously. In indoor environment, objects such as plants and small appliances may cause scattering. Figure 4.1 illustrates three mentioned propagation mechanism

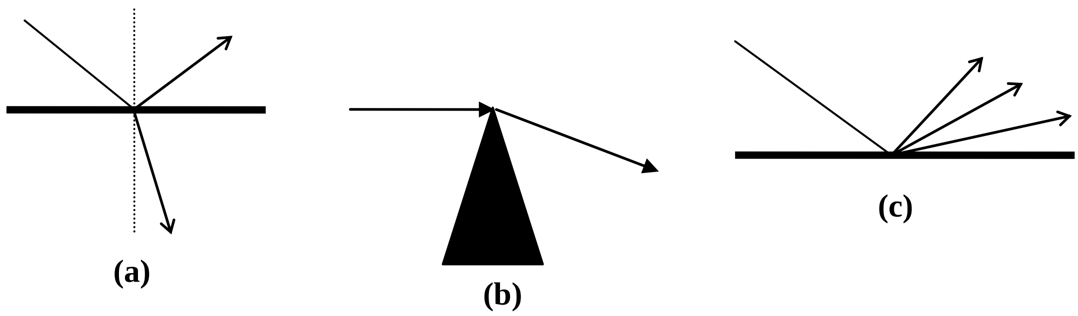

Figure 4.1: Illustration of propagation mechanism.
(a): Reflection and Refraction. (b) Diffraction. (c) Scattering.

4.2. Multipath Propagation

Combined effects of reflection, diffraction and scattering cause multipath propagation. When a signal is propagated between a BTS and mobile, there may have some possibilities to go. The shortest path is when the BTS and mobile are visible each other, a straightforward path is possible (LoS). However, in typical mobile network, it is difficult to achieve LoS path due to many objects in between. Multipath results from when a transmitted signal arrives at receiver by more than one path. Different paths may have different lengths and they, therefore, may arrive at the receiver with phase different. The multipath components results in a distorted version of the original signal at reception.

4.2.1. Delay Spread

Delay spread, denoted as τ, is the amount of time delay at a receiver form a signal travelling from the transmitter along different paths, it represents for time–variant impulse response of a channel in time domain with respect to power profile, shown in

Figure 4.2. Delay spread quantifies the number of multipath delays. Delay spread is also a function of cell size. Delay spreads in typical environments are shown in Table 3.

Table 3: Characteristic of typical environments [3].

Environment	Angular Spread (deg)	Fast fading	Delay spread τ (µs)	Coherent Bandwidth Δf_c [MHz]	Propagation Slope (dB/dec)
Macrocellular					
Urban	5–10	NLOS	0.5	0.32	40
Rural	5–10	N(LOS)	0.1	1.6	25
Hilly	5	N(LOS)	3	0.053	20
Microcellular	40–90	N(LOS)	< 0.1	> 1.6	20
Indoor	90–360	N(LOS)	< 0.01	> 16	20

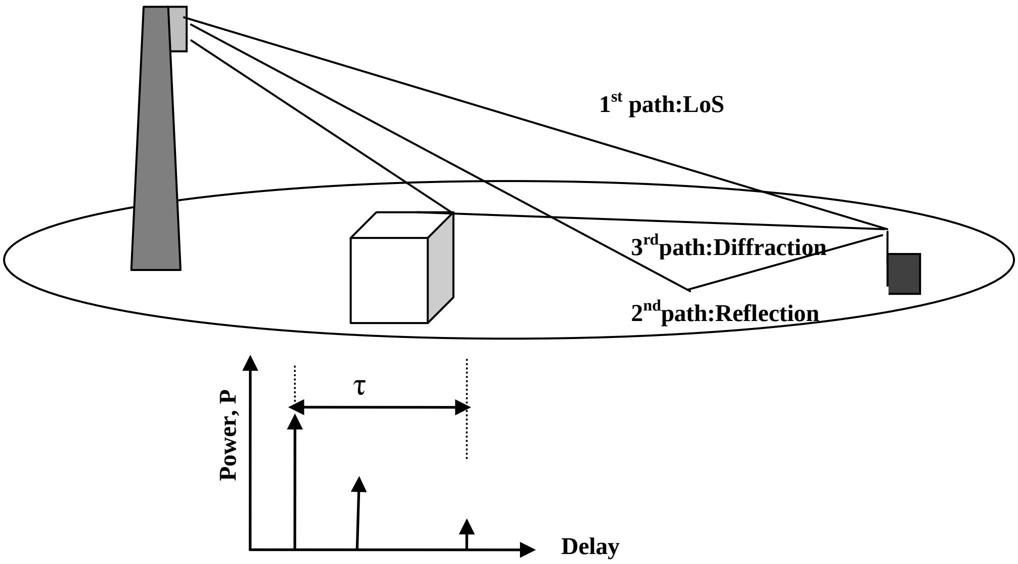

Figure 4.2: Multipath scenario and power profile with delay spread.

4.2.2. Coherent Bandwidth

Delay spread in time domain results in coherence bandwidth in frequency domain, they are inversely related. Coherent bandwidth, indicated by Δf_c, is the maximum transmission bandwidth over which the channel can be assumed to be approximately constant in frequency. That means a signal having frequencies with a coherent bandwidth Δf_c will be roughly similarly influenced or so call ‘flat’ by the channel. The relation between delay spread and 50.0% coherent bandwidth can be illustrated as Equation (4–2) [15]:

$$\Delta f_c \approx \frac{1}{5\tau} \qquad (4–2)$$

In practice, the term 50.0% coherent bandwidth or 90.0% coherent bandwidth are used. It means that the correlation of channel response for two frequencies within Δf_c is 0.5 or 0.9. In Table 3, coherent bandwidth Δf_c, alters along different scenarios, being wider band from macrocellular environment to narrow indoor environment.

In indoor propagation, delay spread is typically less than $0.01\,\mu s$, and therefore resulting in coherent bandwidth larger than approximately 16 MHz. A LTE signal with 10 MHz bandwidth propagating in indoor environment is considered narrowband since its bandwidth is smaller than coherent bandwidth.

Differently, wideband propagation is the term that defines a signal propagating an environment in which its bandwidth is much larger than channel coherent bandwidth.

4.3. Fast Fading and Slow Fading

4.3.1. Fast Fading

Multipath components result in fast fading in frequency domain, which means certain frequencies experience attenuating than others. A dispersive signal is combined at receivers. The combination is done in such a way that, the resulting signal can be constructive or destructive; a rapid fluctuation might take place. An undesirably destructive signal causes a headache issue for reception engineers.

In no LoS environment, where there is no direct signal between a BTS and mobile, its multipath paths are uniformly and randomly distributed. The Rayleigh distribution is used to model no LoS fast fading channel. On the other hand, in LoS environment, the LoS signal is much stronger than other paths. Its propagation profile is similar to Rice distribution, and therefore, Rice distribution is appropriate to model this type of channel. More details about those distributions can be found in [15].

4.3.2. Slow Fading

Slow fading occurs when there are obstacles such as buildings, mountains, hills, etc. in between a BTS and a mobile. Those shadow signals. Slow fading is therefore called shadowing. Variations have changed slowly, depending on visible obstacles. Slow fading variations are smaller than that in fast fading.

To minimize effects of slow fading and ensure a certain coverage probability, certain allowances must be added. This is called the ‘slow fading margin’, or the ‘shadow fading margin’.

The difference found in slow fading is reflected by the standard deviation of slow fading. The standard deviation of slow fading give the knowledge how the radio signals’ strength are distributed at different testing points at similar distance from the transmitter. The standard deviation varies along territories. Standard deviation values range from 5 dB to 12 dB depending on environments [15]. Table 4 shows standard deviations for various scenarios.

The slow fading margin can be calculated based on cell edge coverage probability and standard deviation of slow fading as presented as shown in Equation (4–3):

$$\text{EdgeCoverageProbability} = 1 - Q\left(\frac{\text{SlowFadingMargin}}{\text{StandardDeviation}}\right) \tag{4–3}$$

Table 4: Standard deviations in typical environments [15].

Scenarios	Standard Deviations of Slow Fading (dB)
Densely populated urban area	10
Common urban area	8
Suburban area	6
Rural area	6
Microcell	6–10
Indoor	3–6

4.4. Indoor Propagation Models

The number of picocells has increased over recent years since indoor users tend to exploit more applications like games, entertainment applications, etc. and therefore, demanding strongly traffics. Hence, there is a need to extend coverage in buildings by means of a picocell. There are several approaches, which have been taken for modelling the picocells. Physical model is considered more accurate and practical than empirical model since it provides information that is more practical and it considers many practical aspects when modelling a picocell. However, empirical model also earns its reputation to be less complex and easy–to–use model that is suitable for initial research and first planning.

4.4.1. Indoor Empirical Models

Wall and Floor Factor Models and COST231 Multi–Wall Model are two empirical models described in this part. Both are constructed on the base of path loss law. First model is an extension to simple path loss model introduced by Keenan [15] who characterizes indoor path loss exponent equal to two and introduces additional attenuation parameters including number of floors n_f and walls n_w. The propagation loss is given as on Equation (4–4) [15]:

$$L = L_1 + 20\log_{10}(r) + n_f a_f + n_w a_w \tag{4–4}$$

Where a_f and a_w are attenuation factors of each floor and each wall, in that order. L_1 is the reference path loss at the distance $r = 1\,m$. In this model, the path loss does not depend on the frequency of signals. Therefore, signals operating at different frequencies will experience the same path loss if they operate at the same environment. However, it is not accurate because in sense of penetration loss theory, different frequencies are affected in different ways when signals cross an object.

ITU–R model provides an more advanced approach on path loss computation, frequency effect is included. Path loss exponent n varies depending on properties of buildings. The model is derived as:

$$L = 20 \log f_c + 10 * n * \log(r) + a_f(n_f) - 28 \tag{4–5}$$

Where f_c is the frequency of a signal. n is the path loss exponent, the selection of path loss exponent depends on signal frequency and the environment as provided in [15]. a_f is the penetration loss which happens due to floors.
The second well–known empirical model is COST231 Multi–Wall Model. The path loss exponent of this model is linearly proportional to the number of walls penetrated. In addition, a penetration loss due to signals, which penetrate through floors, is also included. The model is illustrated as following Equation (4–6) [15]:

$$L = L_F + L_C + \sum_{i=1}^{W} a_{wi}\, n_{wi} + a_f n_f^{\left(\frac{n_f+2}{n_f+1} - b_f\right)} \tag{4–6}$$

Where L_F is the free space path loss, which means the loss for the LoS signal passing straight from the transmitter and the receiver. L_C is the empirically derived constant. Each floor will experience a_f penetration loss, and n_f is the number of floors that the signal passes into. Similarly, a_{wi} and n_{wi} are the wall penetration loss and the number of walls crossed by the path, respectively. Some recommended values can be used for estimation are as [16]:

Table 5: Wall attenuations in LTE networks.

Cellular System	Available LTE Bandwidths	Single Concrete Wall Attenuation
LTE 900	5 MHz	12 dB
LTE 1800	10 MHz	14 dB
LTE 2100	15 MHz	17 dB
LTE 2600	20 MHz	20 dB

a_f is equal to 18.3 dB (1800 MHz) and $b_f = 0.46$ [15].

4.4.2. Indoor Physical Models

Physical prediction propagation models apply the ray tracing and the geometrical theory of diffraction, full details of the building geometry and material are needed. Therefore, deterministic models become more complicated. Those knowledge are not going to be presented in this thesis, further details can be referred in [15].

5. LTE INDOOR NETWORK PLANNING

Why is indoor network planning important? Why do we need indoor planning since network operators already deploy macro cells and micro cells? The fact is that around 80% of mobile users are inside buildings and approximately 70% – 80% of mobile traffic is inside buildings as well [17]. Therefore providing high–performance indoor coverage, especially on higher data rates like in LTE, is a challenge. The technical challenges are typical such as lacks of coverage, low quality of service, need more capacity, want higher data rates and to offload the existing macro networks. As a radio network planner, it is important to pay special attention on indoor planning, which will be focused on by this chapter.

5.1. Radio Network Planning

Like outdoor radio network planning (RNP) process, indoor RNP process is divided into three processes as illustrated in Figure 5.1; pre–planning (so–called dimensioning), detailed planning, post–planning and optimization. The main target of indoor planning is to satisfy indoor users in all aspects; coverage, capacity and quality of service. However, indoor planning differs from outdoor planning in the details of each phase since it considers only a small business area, while outdoor planning involves a big region.

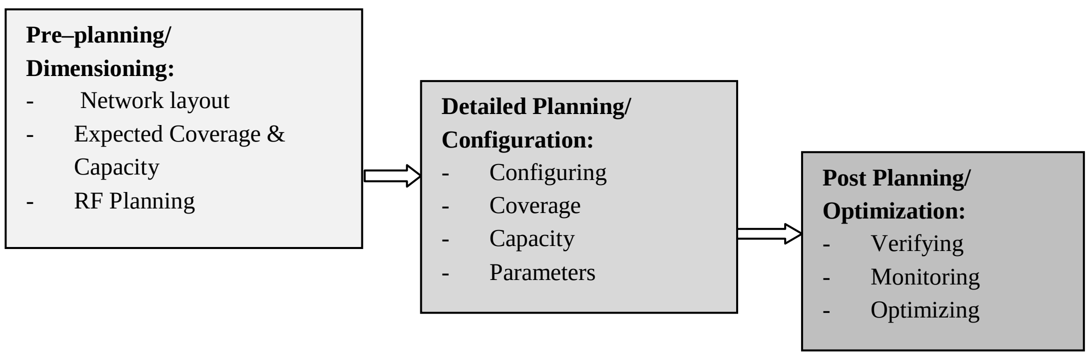

Figure 5.1: Indoor radio network planning.

5.1.1. Dimensioning

The process starts with dimensioning or so–called pre–planning; which contains coverage dimensioning and capacity dimensioning. The dimensioning needs requirements from customers, which are also the inputs for planning. There must be clearly defined goals. The inputs for indoor dimensioning may include:

- Number of users.
- Types of users.
- Types of service requirements, data speeds, etc. needed.
- Expected coverage.
- Expected capacity.

In order to define the required coverage, the documentations of buildings need to be provided for RF planners. A RF indoor planner should think following points when coverage planning [17]:

- Floor plans
- Floor plans showing the coverage needed in the different grades and areas
    - 100% coverage
    - 90% coverage
    - Areas where it is ‘nice to have’ coverage.
- Floor plans showing different environment types:
    - Dense areas with heavy walls
    - Open office areas
    - Storage and Elevators

After taken quite enough data for coverage planning, an initial link budget for each service is calculated. The objective of calculating the link budget is to estimate the path loss between transmitters and receivers in downlink and uplink with taking into account some parameters such as noise, interference, frequency use, etc.

Dimensioning process also involves designing an indoor system after collecting enough data. The RF indoor planner designs an indoor solution system based on those inputs. There are several indoor systems; active Distributed Antenna System (DAS), passive DAS, Repeater, Femtocell solution. Each of these approaches has their pros and cons, all depending on the project at hand. A good solution is to fully satisfy the demands of customers and to minimize cost as well.

RF planning is also a part of dimensioning process, which means a very first version set of RF devices, that are going to use for implementation, is drawn. For example, antenna types antenna locations, cable types, connectors, etc.

The output of the dimensioning step is an initial indoor solution, plus the number of indoor cells and the number of indoor antennas.

5.1.2. Detailed Planning

Coverage Planning

In detailed–planning process, the assumptions made in pre–planning step are further refined with values. A very detail of link budget with some additional parameters such as slow fading margin, indoor penetration, antenna gains, etc. is made to have possibly accurate path loss, and then coverage can be estimated through indoor propagation models presented in Chapter 4.

Radio frequency repeater is also a choice for indoor network planning. A repeater is just like a bridging amplifier that captures a signal from outdoor macro cellular by a donor antenna, amplifies and then guides that amplified signal to indoor DAS by using a service antenna. A repeater operates at physical layer, there is no higher–layer signal processing [18]. There are also layer–3 repeaters. Figure 5.2 gives an illustrational implementation of a repeater in supporting for indoor network. The repeater with two antennas is placed on the top of a building. The repeater also introduces some gains downlink and uplink detailed in [18].

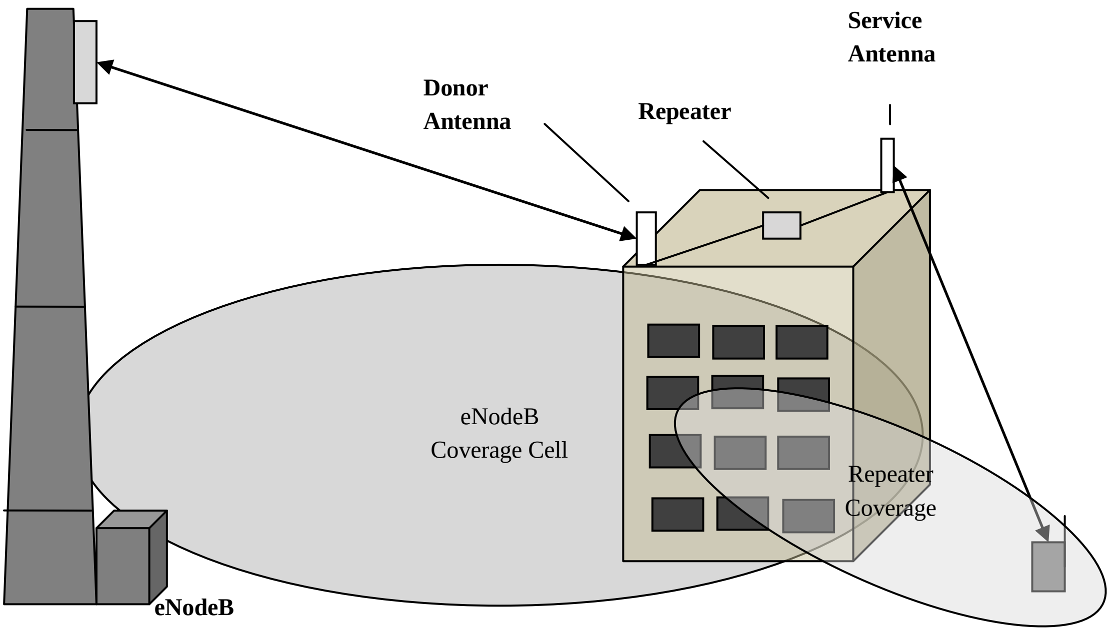

Figure 5.2: Repeater for indoor solution.

If DAS solution is chosen for implementation, a detailed diagram of the system is drawn, consisting of a trunk cable and a set of branches connecting to antennas installed in a building. Splitters' attenuation, losses of cable, length of cables are also presented. The basic idea of DAS is to split a signal from indoor base station to several antennas throughput the inside of the building. Ideally, these antennas points should operate roughly at the same power level, and have the same noise figure on the uplink. The objective of DAS actually is to extend coverage in indoor environment rather than to provide higher capacity [15]. However, the data rate of each link will be improved since

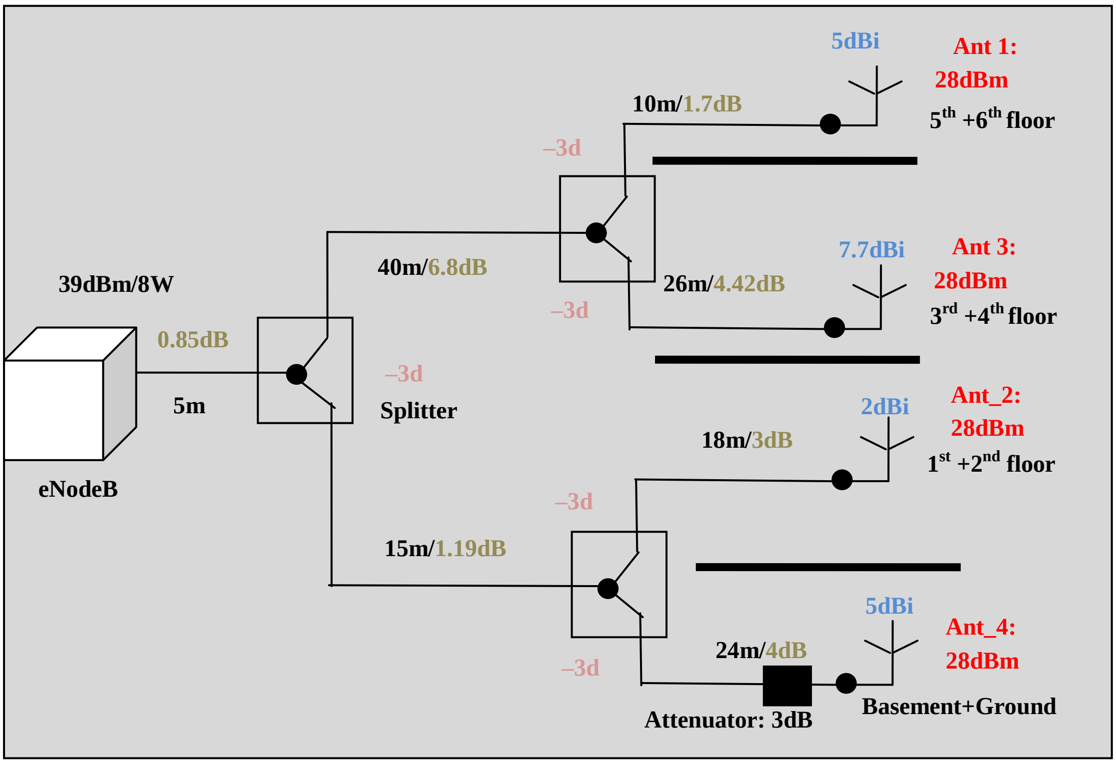

Figure 5.3: Illustration of LTE passive DAS indoor system.

SINR gets improved. Figure 5.3 present an illustration of LTE passive DAS solution in an 8–storey building. An indoor eNodeB generates 39 dBm signals. Cables, splitters, attenuators, connectors, will attenuate a signal generated by an eNodeB before it comes out of distributed antenna system. Powers of signals at all antennas are roughly equal, and equal to approximately 28 dBm Three two–way splitters are used, powers are equally divided at two output ports, introducing 3 dB loss per splitter. Cables cause 0.17 dB loss per meter. Some attenuators are employed at few branches to ensure equal powers at antennas. Loss of all connectors in each branch is assumed equal to 1 dB.
The very first link budgets in down and up links can be illustrated as in Table 6. From the given link budget in downlink and uplink as seen, the downlink with path loss equal to 129.5 dB will limit the transmission. The coverage is calculated by using COST231 Multi–wall Model. The path loss calculation is remained as shown on Equation (4–5):

$$L = L_F + L_C + \sum_{i=1}^{W} a_{wi}\, n_{wi} + a_f n_f^{\left(\frac{n_f+2}{n_f+1} - b_f\right)} \tag{5–1}$$

The free space loss is as:

- $L_F = 32.5 + 20 * log_{10}\left(f_{c_{MHz}}\right) + 20 * log_{10}(r)$
  $= 32.5 + 20 * log_{10}(2100) + 20 * log_{10}(r)$
  $= 99 + 20 * log_{10}(r)$.

Table 6: Indoor LTE downlink and uplink link budget with DAS solution.

	LTE Downlink 10 MHz = 50 RBs	**LTE Uplink 10 MHz = 50 RBs**	
Data rate (kbps)	1024	64	Data Rate (kbps)
Transmitter (eNodeB)			Transmitter –UE
Tx power (dBm)	39.0/ 8 W	23.0	Max Tx Power (dBm)
Tx antenna gain (dBi)		0.0	Tx antenna gain (dBi)
Cable loss, Splitter Loss (3dB),	Figure 5	0.0	Body loss (dB)
Connector Loss (2dB), Attenuators,	11 dB (Loss)	23.0	EIRP (dBm)
EIRP(dBm)per Antenna.	28		
Receiver – UE			Receiver –eNodeB
UE noise figure (dB)	7.0	2.0	eNodeB noise figure (dB)
Thermal noise (dB)	–104.5	–118.4	Thermal Noise (dB)
Receiver noise power (dBm)	–97.5	–116.4	Receiver noise (dBm)
SINR (dB)	–9.0	–7.0	SINR(dB)
Receiver sensitivity (dBm)	–106.5	–123.4	Receiver Sensitivity(dBm)
Interference Margin (dB)	4.0	1.0	Interference margin(dB)
Control Channel Overhead	1 dB (20 %)		Cable loss(dB), Attenuator,
Rx Antenna gain (dBi)	0.0	Figure 5	Spliter Loss,
Body Loss (dB)	0.0	11 dB (Loss)	Rx ant gain (dBi)
Path Loss	**129.5 dB**	**134.4 dB**	**Path Loss**

Assuming that the measurement is carried out in the indoor environment, in where the wall is thick (25 cm) concrete wall type with windows and large incident angles [15]. A LTE signal will be attenuated roughly 10 dB when penetrating each wall. Then if the scenario has around four such walls, the total wall attenuation is as:

- $\sum_{i=1}^{W} a_{wi}\, n_{wi} = 10\ dB * 4 = 40\ dB.$

One antenna serves for two storeys, the signal needs to penetrate one floor. Floor penetration is about 10 dB per floor. Hence, the total floor penetration is as:

- $a_f n_f^{\left(\frac{n_f+2}{n_f+1} - b_f\right)} = 10 * 1^{(1.5-0.46)} = 10.96\ dB$

Therefore, the coverage can be obtained (one floor penetration taken into account):

- $20 * \log_{10} r = L - 99dB - 44dB = 129.5\ dB - 99dB - 40dB - 10.96dB$
  $= -20.46\ dB.$
- $r = 10^{-20.46/20} = 0.0948\ km = 94.84\ m.$

So, with the example indoor system, the coverage is about 94.84 m, it is appropriate for in–building network coverage.

Capacity Planning

Regarding capacity planning, depending on following aspects as surveyed; the estimated number of users, types of services and airtime traffic at a time within a planned building; an overall estimated capacity need is given. In general, the capacity of downlink system depends on the following:

- System Bandwidth
- Hardware Configuration: MIMO, Modulation and Coding Schemes
- Network loading: number of subscribers in a cell that affects the overhead

The following is an example how to calculate the capacity of LTE system based on some typical configurations and then the illustration of how to adjust capacity on LTE through basic parameters. Let's assume the LTE system as:

Table 7: LTE parameters for downlink and uplink capacity [4].

LTE System Parameters	Downlink	Uplink
Bandwidth (RBs)	10 MHz (50 RBs)	10 MHz
Modulation and Coding Schemes	64QAM, Coding rate $R_{downlink} =$ 0.93	16QAM, Coding rate $R_{uplink} =$ 0.93
MIMO usage	2x2	SISO, SIMO.
No. OFDM symbols in a slot (Normal Cyclic Prefix)	7 OFDM symbols in a slot 0.5 ms	7 SC–FDMA symbols per a slot 0.5 ms
Overhead	PDCCCH: 17.86% Reference Symbols: 4.76% CP+Guard band: 11.66% Other: ~ 2.6%	Reference Symbols: 14.3% Random access: 0.625% CP+Guard band: 11.66%

A 10 MHz bandwidth in downlink results in the number of downlink resource blocks $N_{RB}^{DL} = 50\ RBs$. Actually, 50 RBs results in around 9 MHz frequency band, so the rest 1 MHz is used for guard bands and cyclic prefix bands. First, the number of resource elements N_{RE}^{DL} in a subframe 1 ms is computed:

- $N_{RE}^{DL} = 12\ subcarriers\ \times 7\ OFDM\ symbols\ \times 50\ RBs\ \times 2\ slots = 8{,}400\ REs.$

Assuming that 64QAM is chosen as the modulation scheme with a maximum coding rate 0.93 (64QAM and 0.93 are correspondingly the highest modulation and coding rate for downlink). The MAC downlink capacity (MAC downlink included overhead, physical capacity extracts overhead or so–called application capacity) with no MIMO C_{MAC}^{DL} is:

- $C_{MAC}^{DL} = 6bitper64QAMsymbol\ \times 0.93 \times 8{,}400\ REs\ /1msec = 46.872\ Mbps.$

If $2 \times 2\ MIMO\ is$ used, then MAC downlink MIMO data rate ${C_{MAC}}_{2\times2MIMO}^{DL}$ is:

- ${C_{MAC}}_{2\times2MIMO}^{DL} = 46.872\ Mbps\ \times 2 = 93.744\ Mbps.$

Now, overhears related to control signalling such as Physical Downlink Control Channel (PDCCH), Physical Broadcast Channel (PBCH) channels, reference and synchronization signals, and coding have to be subtracted from above capacity:

- PDCCH channel can take 1 to 3 symbols out of 14 in a subframe. Assuming that on average it is 2.5 symbols, the amount of overhead due to PDCCH becomes: ${}^{2.5}/_{14}$ = 17.86 %.
- Downlink RS signal users 2 symbols in every sixth subcarrier in frequency domain to meet requirement forced by coherent bandwidth and 2 symbols in each slot in time domain to deal with Doppler effect, resulting in (2+2)/(12x7) = 4.76%.
- The other channels; Primary Synchronization Signal (PSS), Secondary Synchronization Signal (SSS), PBCH, Physical Control Format Indicator Channel (PCFICH), Physical Hybrid ARQ Indicator Channel (PHICH); added together amount to ~ 2.6% of overhead [4].
- Cyclic Prefix+Guard Band: 6.66% $\left(\sim {}^{1}/_{16}\, OFDM\ symbols\right)$ + 5% = 11%

The total approximate amount of overhead Δ^{DL} for 10 MHz downlink channel is:

- $\Delta^{DL} = 17.86 + 4.76 + 2.6 + 11.66 = 36.88\%$

The downlink physical peak data rate $R_{PEAK}{}^{DL}_{2\times2MIMO}$ is then:

- $R_{PEAK}{}^{DL}_{2\times2MIMO} = (1 - 0.3688) \times 93.744\ Mbps = 59.17\ Mbps.$

Similarly, uplink physical peak data rate $R_{PEAK}{}^{UL}_{2\times2MIMO}$ for 10 MHz bandwidth with parameters provided in Table 5 can be computed:

- $$R_{PEAK}{}^{UL}_{2\times2MIMO} = 4\frac{bps}{Hz} \times 0.93 \times \frac{8{,}400REs}{1ms} \times (1 - 14.29\% - 0.625\% - 11.66\%) \times 2 = 45.888\ Mbps$$

The system bandwidth in LTE can be chosen flexibly ranging from 1.25 MHz to 20 MHz. The overall capacity is increased by widening the system bandwidth, and therefore increasing the amount of total RBs available for users. However, by increasing bandwidth, the noise is also increased, then affecting on lower coverage.

LTE indoor planning differs from UMTS or GSM indoor planning due to the configuration of MIMO, up to 4×4 MIMO is configured in Release 8. Planning and designing MIMO play an important role in capacity indoor planning since the propagation behaviour in indoor environment is more complicated and hard to predict. In order to fully utilize MIMO, a precise calculation MIMO antenna options and distance separations is needed. The combination planning of DAS system and MIMO configuration for indoor is also an option, in which each antenna branch can carrier each

MIMO stream. In practical, it is possible to achieve around 60.0 Mbps downlink MAC throughputs with 2x2MIMO at good channel condition.

5.1.3. Post–Planning and Optimization

The final step of indoor RNP is the post–planning and optimization step. In this phase, after done installation, initial RF measurement is needed to verify the installed system. Measurement test concentrates on coverage satisfaction, data speed, handovers (indoor cells handover, indoor–to–outdoor handover and vice versa), MIMO usage, dominance areas, etc. If something is not qualified enough as required, some modifications on network parameters; such as antenna types, antenna placements, transmit powers, MIMO configurations, system bandwidth, need to be made for optimization.
The operation of the network is also constantly monitored. There are some key statistics, also called key performance indicators (KPI), i.e., loads, connection failures, and transfer rates in the network are being continuously kept track [3]. Moreover, if necessary, there will be then performed of post–planning and optimization tasks.

5.2. Antenna Configuration

The basic principle of an antenna is converting the electrical waves in a waveguide, feeder cable or transmission line into radiating waves travelling in free space, or vice versa. Therefore, antennas have a very critical role in cellular network. To design an antenna for a cellular radio network application, a radio network designer needs to understand these following antenna basic parameters besides system configurations; those are the most important among antenna parameters:

- Radiation Pattern of an antenna is the graphic depiction of the antenna power pattern versus angle in two–dimensional pattern, a function of both azimuth and elevation angles. Radiation pattern also show the main lobe of the antenna and its side lobes. Main lobe is the sector between two nulls, which contains the angle of radiation intensity maximum. On the other hand, side lobes contain the angles between two nulls but not containing main lobe.
- Beamwidth of antenna is defined as the angular width between two points on the antenna mainlobe that are 3–dB drop compared to the maximum gain point. In cellular network, antenna with 33^o, $65\ ^o$ and 90^o beamwidths are chosen for deployment. Beamwidth is also called half–power beamwidth (HPBW).
- Directivity is the amount of radiation intensity in a certain spatial dimension respect to average radiation intensity.
- Isotropic radiator is an ideal antenna that radiates equal amount of power in all directions. The isotropic radiator is also sometimes called an omni–directional antenna. However, an omni–directional antenna also refers to an antenna that radiates equally in all angles in one plane but varies in other plane. For example, an antenna radiates equally over azimuth plane but varies with elevation.

- Antenna Gain refer to the gain of a spatial dimension that an antenna radiates greater than other directions. The antenna gain is usually expressed in dBi to emphasize the use of isotropic radiation as a reference.
- Effective Isotropic Radiated Power (EIRP) of an antenna indicates the amount of power that an equivalent theoretical isotropic antenna would radiate. EFRP takes into account the connection loss, transmit power and involves the gain of the antenna.
- Polarization is defined as the orientation in a plane that contains the electric field of an electromagnetic wave. There are three types of polarizations. An antenna is called linear polarization if the radiated wave it generates or receives is vertical or horizontal or 45–degree slanted polarization. Circular polarization is similar to linear polarization, except that the polarization vector spins either clockwise or counter–clockwise, generating right–hand circular or left–hand circular. Circular polarization is a special case of elliptic polarization, where the vertical and horizontal components of the polarization vector are of equal amplitude.
- Polarization matching refers to the matching of polarizations between incoming waves and receiving antenna. For example, a vertically polarized antenna perfectly matches with an incoming signal with vertical polarization. There appears polarization–mismatching loss if polarizations of the transmitting antenna and receiving antenna are not matching.
- Bandwidth is defined as the frequency band ranging from the lower frequency point f_{lower} to upper point f_{upper} in which the performance of the antenna conforms to a specified standard. An antenna is said narrow band antenna if the criterion $(f_{upper} - f_{lower})/f_{centre} < 5\%$ is satisfied. On the other hand, if $f_{upper} : f_{lower} > 10 : 1$ is satisfied, the antenna is wide band antenna.
- Impedance and Voltage Standing Wave Ratio (VSWR). An antenna produces its impedance. The impedance of an antenna should match with that of transmission line in order for the power delivers to radiation and vice versus completely. The other term that expresses the same thing is return loss. Return loss implies the amount of power returned to transmission line due to impedance mismatch between an antenna and transmission line. When antenna and transmission line's impedance are not matched, this results in a reflected wave. Reflection coefficient refers to the ratio between the reflected wave and incident wave. It also implies how much incident power is transferred into radiation. Additionally, reflected and incident waves produce VSWR on the transmission line. The VSWR reflects the quality of an antenna in term of power loss.

With the present of multiple antenna techniques, it puts more challenges and complexity on antenna design for cellular network to achieve best possible performances when combining single antenna into an array. The biggest challenge is that by transmitting more than one signal simultaneously to channels there causes correlations between signals. High correlation will degrade the performances of MIMO system. By designing an antenna array in proper ways, including space diversity and polarization diversity, the low correlation can be possibly achieved, then leading to maximum achievable performance in wireless communication [19], [20] and [21]. Those methods involve space diversity and diversity with different polarization pairs.

5.2.1. Space Diversity

Space diversity is a fundamental method in multiple antenna systems. The structure consists of two or more horizontally or vertically spatial separated antennas deployed at a base station or mobile. The idea is to either increase link reliability by increase SNR level in diversity technique or increase data rate by having more than cross–correlation data streams transmitted simultaneously in spatial multiplexing technique. The correlation between branches is the function of separations between antenna elements. The objective of space diversity of to find an optimum separation in order to obtain uncorrelated branches, this depends heavily on the environment and the receiving end. As a result, the multiplexing and diversity techniques can be utilised.

The basic model to illustrate the two–antenna space diversity is depicted in Figure 5.4. The two antennas is distanced by d. One antenna receives two signals with length differences, described (r_1–r_3) at antenna 1 and (r_2–r_4) at antenna 2 from an UE. The two signals are scattered via Scatterer 1 and Scatterer 2 before they arrive at BTS antennas. The phase differences of the total received signals at each antenna are proportional to the differences in path lengths from the scatterers to each antenna [15]. The distances of the scatterers, r_s, and antenna distance d, affect the path length differences in a way that if these distances increase, then path length differences also increase, generating a larger phase difference between signals at antennas. This, contrarily, would rise a lower correlation between signals arrived at the antennas. Hence, the expectation is that lower correlation could be achieved with increase either d or r_s [15].

In the environments where the distances from antennas to scatterers are much greater than the antenna separation d, the phase differences can be functioned with the angular spread (Ø) distribution illustrated in Figure 5.4. It is proved that a narrow angular distribution will produce a slow decrease in the correlation with antenna spacing, which will limit the usefulness of space diversity [15]. Contrastingly, in the environment, where there is significant number of scatterers around the antennas, good space diversity can be produced. The rich of scatterers at UEs allow larger angular distribution of signals coming to UE’s antennas, this results in a reasonable antenna space to achieve lower correlation. Opposingly, it seems that not many objects surrounding BTS in macrocells, signals come to BTS with a narrow angular. Therefore, a large separation between antennas at BTS would be needed to generate lower correlation.

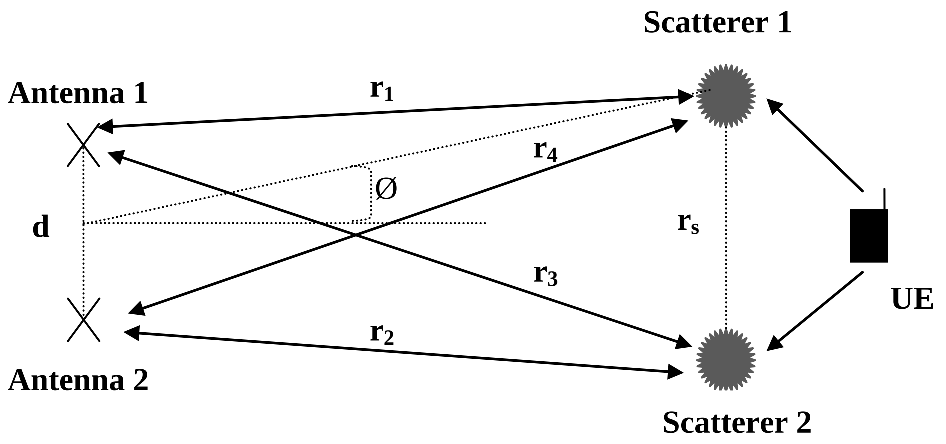

Figure 5.4 : Path length differences in space diversity scenario [15].

Horizontal space diversity would be a preferred choice for space diversity implementation in cellular network. Vertical space is rarely used. The reason is that vertical space diversity would require a very large separation to obtain low cross–correlation and because different heights of antennas would cause significant differences in the path loss for each link, this degrades the diversity effect. Nevertheless, it may be more convenient to separate vertically within a single structure (two antennas are packaged into a single vertical structure) than to have two horizontal separation elements.

The practical implementation for space diversity is considerably different at BTS and UE, the differences are also for environments. At BTS in macrocells, the antennas are expected to be separate up to from 10 to 30 wavelengths for uncorrelated channel achievement and that is around 0.1, 0.5 or 2 wavelength separation in mobile [20]. The richer multipath components, the better MIMO and transmit diversity perform.

In picocells, the angles of arrival will be distributed even more widely due to many objects around BTS side and UE side, particularly when propagating takes place between floors. Space diversity with a reasonable horizontal space will then yield low correlation, even at the base station [15]. Hence, the experiments with space diversity would not expect a remarkable improvement in picocells.

Additionally, mutual coupling between antennas at terminals affect the correlation coefficient in a way that it tends to reduce the correlation coefficient. Hence, the acceptable diversity can be obtained with horizontal spaces as small as a fraction of wavelength.

5.2.2. Polarization Diversity

Space diversity is not always easy to deploy and sometimes having large separation between elements is not feasible due to space limitation. Hence, polarization diversity can be a suitable choice. Polarization diversity is different from space diversity but it is also a technique to achieve higher capacity and link reliability for MIMO and diversity.

It is based on the concept that in high multipath environments, the signal from a portable received at the base station will have varying polarization due to reflections, diffractions, and scattering. It is found experimentally that vertical polarized and horizontal polarized antennas are almost uncorrelated at base station, so a pair of cross–polarized antennas can obtain signal uncorrelation without spacing between them [15]. However, a pair of cross–polarized component would lower considerably power than co–polar components, although this happens in LoS environments. The degradation of received power tends to reduce SNR and therefore reduce diversity gain in diversity technique and possibility of achieving higher data rate in multiplexing technique.
The cross–polar ratio Γ is defined as the ratio between mean powers of the vertically and horizontally polarized electrical fields as in Equation 5–2:

$$\Gamma = \frac{E[|E_v|]^2}{E[|E_h|]^2} \tag{5–2}$$

The mean values of cross–polar ratio are around 6 dB and 7 dB to 8 dB in macro cells and micro cells, respectively [15]. These cross–polar ratio mean values result in remarkable low correlation coefficient around 0.1 in both cases. Polarization diversity has the potential for significant gains, although the mean powers of branches experience large different when Γ is high.
A combined method to obtain higher diversity gain is a combination of polarization diversity and space diversity. In this case, it has been shown that the total correlation coefficients are approximately multiplied as:

$$p \approx p_x(\alpha) \times p(r, h) \tag{5–3}$$

Where $p_x(\alpha)$ is the correlation, which would be obtained with polarization diversity at an angle α, and $p(r, h)$ is the correlation, which would be achieved with a horizontal separation r and a vertical separation h of the collocated polarized antennas. Thus, the total correlation coefficient can be less than that obtained from polarization diversity alone.
The polarization diversity is even more attractive at UE side due to the limited size available. Nevertheless, the effect of polarization diversity at UE becomes complex since the impacts of the large angular spread and mutual relation between antenna elements and human body are put into consideration.
There also appears mutual coupling (MC) between antenna elements since they are placed closely, generating the radiation of intermodulation products at the power amplifier of the transmitter and therefore has greatly affected on spatial correlation and power ratio between branches. Base on theoretical analysis as well as simulation, [22] proves that MC can raise the spatial correlation but decrease the average power different between the two elements, causing a reduction of cross–polar ratio Γ. Thus, MC degrades polarization diversity gain. In order to avoid the significant effect of MC,

a term called Cross–polar Isolation (XPI) is introduced, it is necessary to exceed 30 dB isolation between ports.

Other parameter that is used to qualify polarization diversity of an antenna pair is Cross–Polar Discrimination (XPD). XPD is defined as the ratio of the co–polarized average received power to the cross–polarized received power. XPD quantifies the separation between transmission branches that use different polarization orientations. The larger XPD, the less energy is coupled between the cross–polarized channels. Thus, most dual–polar antenna systems are required to have high degree of XPD. The practically obtained values of XPD at mobile antennas in picocells are roughly from 5 dB to 11 dB [23]. These values are consistent with measurements, and which are typically used in system specification. [23] also provides the effects of some of environments' parameters such as angular spread, LoS and NLoS on XPD. Low XPD can possibly obtained in indoor NLoS environments. In the indoor environment, where LoS is dominant, the measured XPD was higher than 10 dB. Large angle spread degrades XPD, as angle spread increases to more than 30^o, XPD approaches zero. Figure 5.5 illustrates horizontal–vertical polarization pair, cross–polarization pair as well as the co–polarized pairs that are usually the possible choices for BTS antenna deployment for MIMO.

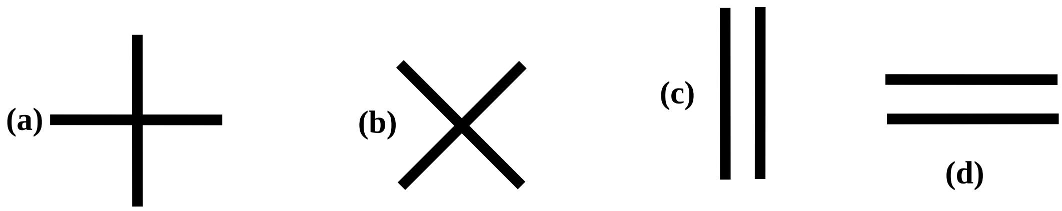

Figure 5.5: Polarization schemes: (a) Horizontal–Vertical polarization pair (b) Cross–polarization pair (c) Vertically co–polarized pair and (d) Horizontally co–polarized pair.

6. MEASUREMENT SETUP

The purpose of this measurement campaign is to study performances of LTE radio network with different antenna configurations supported for MIMO technique at both eNodeB and UE ends. It is important to note that indoor performances depend heavily on types of indoor environments. As mentioned in previous chapter, the floor plan is one of important steps for indoor radio planning. Floor planning includes the layout of planned buildings, descriptions of wall materials, windows, etc. In this chapter, a briefly descriptive document of the environment where the measurement campaign carries out is given. Additionally, the system and tools RF equipments and components for the measurements are shortly listed. The last part of this chapter introduces four test cases prepared for measurements.

6.1. Measurement Tools and Systems

The LTE eNodeB used for the measurement is manufactured by Nokia Siemens Network. The eNodeB offers two MIMO branches connecting to two indoor antennas as illustrated in Figure 6.1. Two–branch MIMO configuration allows 2x2 MIMO operation possible, offering up to approximately 60.0 Mbps MAC capacity. The software version installed to the eNodeB supports 3GPP Release 8 features.

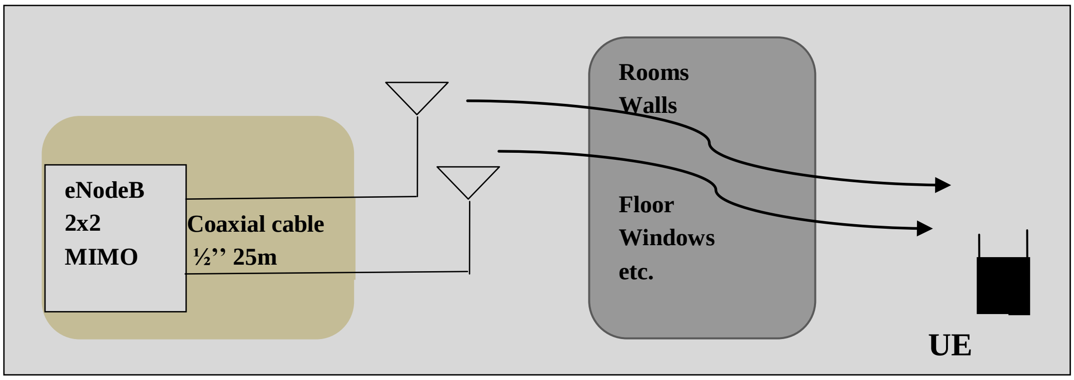

Figure 6.1: Illustration of physical measurement set–up.

The eNodeB location illustrated in Figure 6.1 is along the 2–meter corridor C. Two parallel coaxial feeders, each 25–meter long and $^1/_2$ inches diameter, and N–type connectors are used to connects antenna ports to antennas. Antennas are positioned outside the room and directed along the corridor. Two antennas are hanged on two

1.64–meter posts above the second floor. Flexible antenna type and configuration enable understanding behaviours of the network. Type of antennas and configuration will be presented in the session 6.3. A $^1/_2$"– diameter cable adds around 11 dB attenuation to 2100 MHz signals every 100–meter long.

The multiplexing technique used in the eNodeB is frequency division duplex, which means frequency bands separate downlink and uplink transmissions. The frequency bands for downlink and uplink transmissions in this measurement are 2130 MHz and 1940 MHz in that order. The eNodeB can support flexible bandwidths from 5 MHz up to 20 MHz. In this measurement, 10 MHz bandwidth had been used which leads to approximately 50 RBs. As calculated in Chapter 5, capacity with 10 MHz bandwidth results in roughly 60.0 Mbps MAC throughput. The eNodeB’s transmission power is set at 8 W or equivalent to 39 dBm and is also configured to operate using three transmission modes among seven modes that it can offer. The configured transmission modes are single antenna TM1, transmit diversity TM2, closed loop spatial multiplexing TM4. Three TMs studied in this thesis can be changed using this remote control tool. Table 8 provides eNodeB configuration parameters, together with antenna configuration for the measurement campaign.

Table 8: Parameters of the eNodeB set-up for measurement campaign.

Parameter	Value
DL carrier	2130 MHz
UL carrier	1940 MHz
Transmission Mode	1x2 SIMO TM1, 2x1 Transmit Diversity TM2, 2x2 Closed Loop MIMO TM4
Carrier Power	8 W / 39 dBm
BTS antenna height	1.64 meter
MS antenna height	1.2 meter
BTS antenna types	Directional X–pol 8.7dB Gain Ant_A [24] Directional–Vertical Polarized Ant_B [25] Omni–directional–Vertically Polarized Ant_C [26]
Mobile Type	LTE 4G Cat 3 [27]

Regarding UE, a LTE 4G stick product had been using, this mobile can operate at 800 MHz, 900 MHz, 2100 MHZ and 2600 MHz frequencies with different network systems like GSM, WCDMA and LTE. The mobile stick has two internal antennas; therefore, 2x2MIMO in downlink can be operated. Addition to that, the stick also has two ports which can support two external antennas. The UE is category–3 mobile and according to 3GPP specification, maximum throughputs the mobile can receive in downlink and transmit in uplink are approximately 50.0 Mbps and 25.0 Mbps due to its buffer limitation with 10 MHz bandwidth [4] [27]. A cat–3 hand–held product also can support 2x2MIMO, 64QAM and 16QAM in downlink and uplink modulations, correspondingly. The used UE uses Qualcomm MDM9200TM chipset. At the time of measurements, the UE and eNodeB are set to operate at LTE 2100 MHz frequency band and operate FDD. The stick connects to laptop via USB 2.0 standard and supports Window XP, which is the current operating system of the measurement laptop.

6. MEASUREMENT SETUP

There are three sorts of indoor antennas used for this measurement denoted as Ant_A, Ant_B and Ant_C in Table 8. The first antenna, Ant_A, is multi–band directional X–pol (Cross–Polarization) antennas. The Ant_A consists of two 45–slanted polarization antennas operating at multi–band ranging from 1710 MHz to 2170 MHz. The half–power beamwidths of horizontal and vertical patterns in frequency band 1920 MHz to 2170 MHz are 65^o and 63^o relatively. Gains are 2x8.7 dBi. Maximum power input is 150 W. Cross–polar Isolation between two ports is more than 30 dB guaranteeing that the mutual coupling effect is not critical. VSWR of this antenna type is below 1.4. More detail of this indoor antenna can be viewed in [24].

The second antenna model, Ant_B, is directionally vertically polarized and the third model, Ant_C, is omni–directionally vertically polarized. The specifications of these antennas are briefly summarized in Table 9 below:

Table 9: Antennas Specifications.

Parameters	**Ant_A [24]**	**Ant_B [25].**	**Ant_C [26].**
Frequency Range	1710 MHz–2170 MHz	1710 MHz–2700 MHz	1710 MHz–2200 MHz
Gain	2x8.7 dBi	7 dBi	1 dBi at 2100 MHz
VSWR	<1.4	<2.0:1	<3:1
Polarization	Cross–Polarized	Vertical	Vertical
HPBW	65^o horizontal plane	90^o	Omni–directional
Horizontal Plane	63^o vertical plane		
Cross–polar Isolation	>30 dB	>25 dB	

Ant_A was used for LTE transmission modes measurements while Ant_B and Ant_C were used for antenna configuration measurements at both ends eNodeB and UE. Figure 6.2 shows the radiation pattern of X–pol indoor Ant_A in horizontal and vertical planes. Ant_B, its radiation pattern and Ant_C, its gain range are provided in Figure 6.3 and Figure 6.4, correspondingly. All those antennas have 50 Ω impedance.

Table 10: Hardware devices and software for measurements.

Measurement devices	**Types/ Features**
Measurement laptop	IBM T61, Win XP
Measurement software	Nemo Outdoor V6.3 [28] Nemo Analyzer V6.3 [29]
Mobile	LTE Cat–3 Chipset: Qualcomm MDM9200TM Operate: 800 MHz, 900 MHz, 2100 MHZ and 2600 MHz. 2x2MIMO

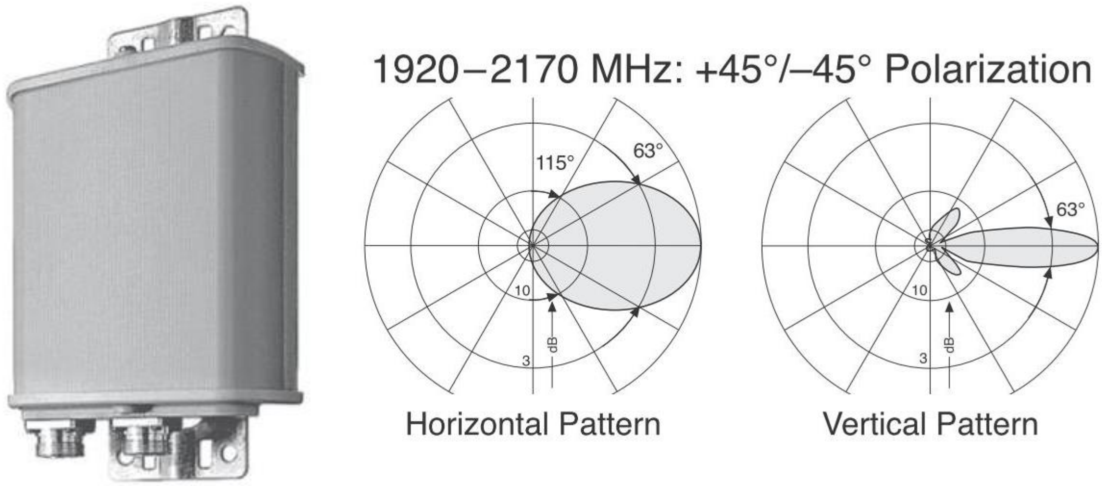

Figure 6.2: Indoor X–pol Ant_A, H–Plane and V–Plane HPBWs [24].

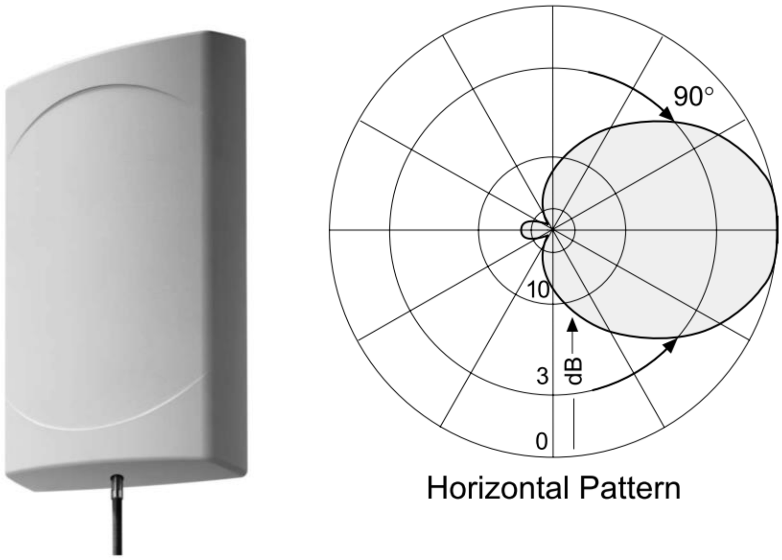

Figure 6.3: Indoor vertical polarized Ant_B and H–Plane HPBW [25]

Gain dBi
1 dBi at 2.1 GHz

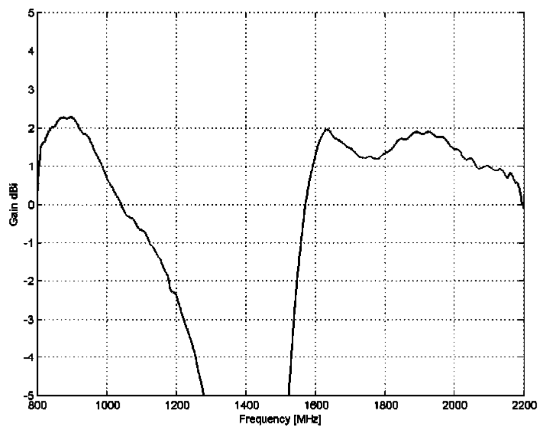

Figure 6.4: Indoor omni–directional Ant_C and gain ranges [26].

Commercial field measurement software V.6.3 [28] was used for recording the measurements, allowing not only to record but decode view all transmission parameters, signalling, data traffic, interactions between an UE and eNodeB. It also enables easy–to–look presentation of some needed values and parameters in real–time in different types of charts and graphs. Measured files were saved and used for post–processing later on. Scripts were also utilised for controlling and monitoring the UE behaviours and to perform requested operations such as, voice calls, FTP file transfers, HTTP. Script is written based HTTP protocol. Additionally, analysis software [29] was also used. It allows measurement records to be replayed, and to be able to transfer to Excel format for post–processing. Table 10 lists hardware devices and software supported for measurement.

The primarily interesting parameter is downlink throughput. The measured throughputs allow comparative performances possible between defined channel conditions. Degree of SNR and Reference Signal Received Power (RSRP) classifies channel conditions. For analysing throughputs, some parameters are linked. Link adaptation has influence on throughput, therefore CQI parameter is measured and then for analysing. UE reports RI and PMI levels to the eNodeB based on the strength of SNR and RSRP it estimated. Upon the reporting knowledge, the eNodeB decides how to transmit data optimally. The term, MIMO Utilization, implies to how much percentage MIMO utilised within one 1 ms Transmission Time Interval (TTI). MIMO, in literature, sometimes also implies spatial multiplexing, or different data streams are transmitted concurrently. MCS values, resulting in the modulation schemes and coding rate for data transmission, is also essential for understanding network behaviours. The choice of MCS depends mainly on the reported CQI. MCS ranges from zero, which means no transmission at all, to highest degree at 28, which implies system is operating at the highest degree, highest modulation order, maximum number of data streams, highest coding rate, etc.

6.2. Measurement Environment

The measurements were carried out at the second floor of Tietotalo building Tampere University of Technology, Finland. Figure 6.5 shows the layout of the measurement environment, and locations where the eNodeB and antennas were placed, together with detailed static locations and routes where measurement was taken place. All doors around routes and static locations are kept closed during the measurements.

There are nine static locations and five routes for measurements. The purpose of having both locations and routes for the trial is to ensure that precise study covers in all kinds of channel conditions from very bad to excellent channel condition as well as static and moving condition. The stationary measurements are taken in rooms or at corridors with different distance from the transmit antenna. When measurement occurred at locations, UE was kept at one place and slowly spun it around in order to diminish the effect of radio propagation on throughput. The UE was placed on a trolley pictured in Figure 6.5, which is moved slowly at walking speed approximately 3 km/h following the defined routes depicted on the layout (Figure 6.6).

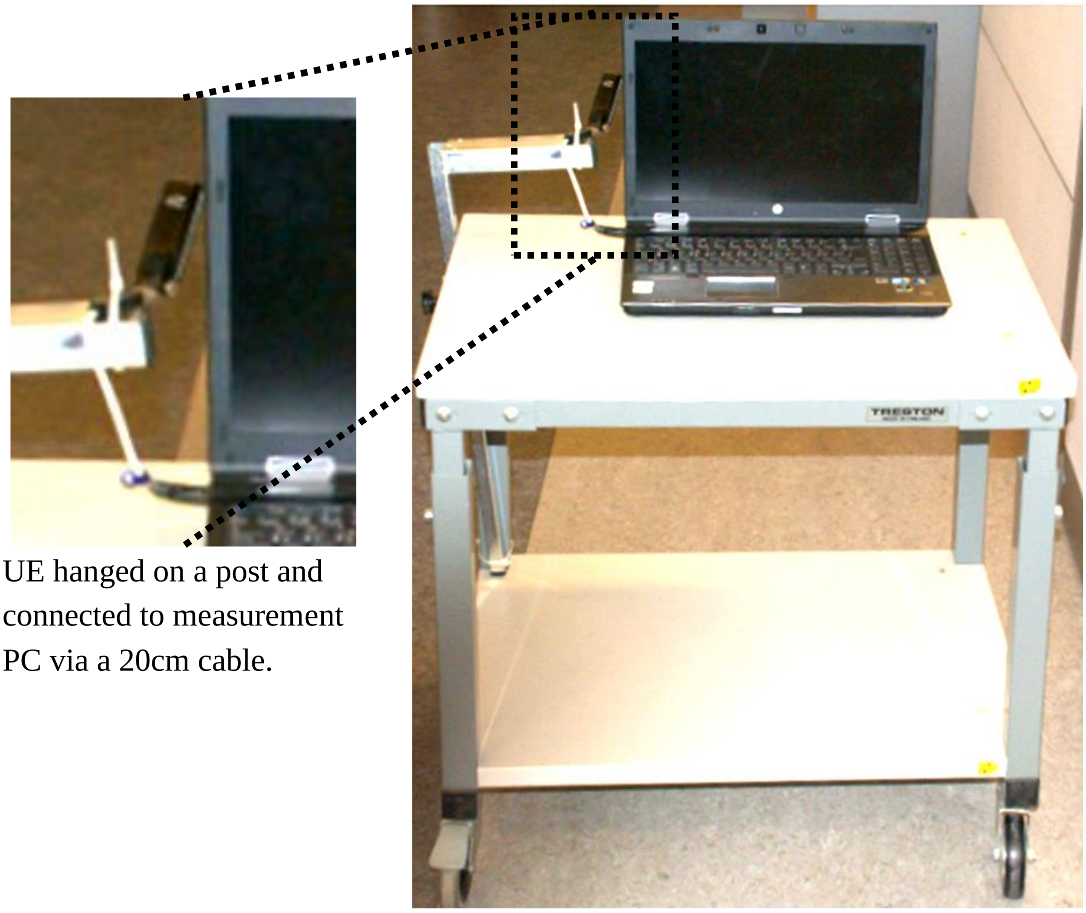

Figure 6.5: Mobile equipment set–up for measurement campaign.

All measuring locations and routes are classified into four different channel classifiers based on channel condition, particularly based on measured SNR and RSRP parameters. Four different colours help distinguish easily four channel classifiers. The aim of dividing classification is to study performance comparison at various channel conditions and some thresholds can be recognized. In order to avoid unexpected behaviours happened and significantly affecting on the results, 5 and 95 percentiles (5%–tile and 95%–tile)are applied to the measured results. 5 and 95 percentiles mean 5 percent of the result that is above minimum level and 5 percent of the result that is below maximum level are taken away. Table 11 describes the characteristic of the channel classifiers in detailed.

The first ‘LoS–Excellent Classifier’ channel propagation is represented by red colour. Location1, Location7 and Route1 are grouped into this condition. At those locations and route, UE is able to receive LoS signals from the eNodeB. 5%–tile and 95%–tile of RSRP and SNR at this channel condition are approximately from –60 dBm to –35 dBm for the former and from 23 dB to 28 dB for the later, relatively.

‘NLoS–Good Classifier’ is the second channel condition marked by blue colour. At these measurements, the UE and eNodeB antennas are not visible each other, signals, so only no LoS signals are received. However, because these measured places are quite near to the eNodeB antennas, the UE still obtained quite good signals. Location2, Location6, Route2 belong to ‘NLoS–Good Classifier’. RSRP at those measurement places are roughly between –75 dBm and –65 dBm. 95%–tile SNR is 26 dB and 5%–tile SNR is around 20 dB.

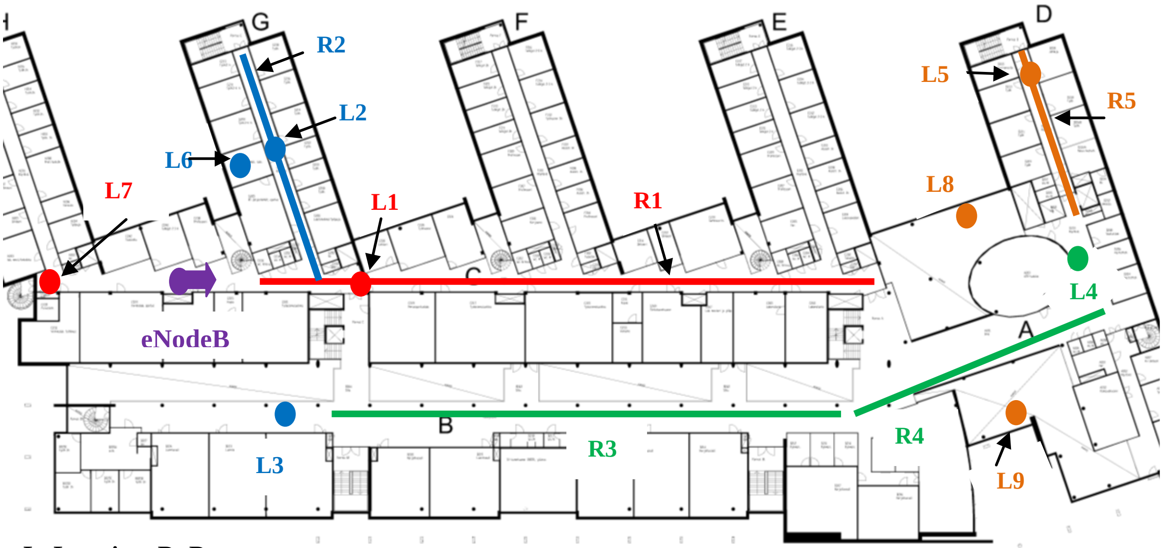

Figure 6.6: Layout of measurement environment.

Table 11: Channel condition classifications.

Classifier	Locations (L) and Route (R)	Channel	Signal Strength	RSRP (dBm) [5%–tile 95%–tile]	SNR (dB) [5%–tile 95%–tile]
1	L1, L7, R1	LoS	Excellent	[–60 –35] dBm	[23 28] dB
2	L2, L6, L3, R2	NLoS	Good	[–75 –65] dBm	[20 26] dB
3	L4, R3, R4	NLoS	Weak	[–100 –75] dBm	[10 20] dB
4	L5, L8, L9, R5	NLoS	Cell edge	[–125 –100] dBm	[–7 15] dB

The third channel condition, ‘NLoS–Bad’, consists of Location4, Route3 and Routes4, those were measured at corridor B. Those measurements are near cell–edge area, so the received signals are quite weak. RSRP for this channel propagation rarely goes above –100 dBm but seldom below –75 dBm. 5%–tile and 95%–tile SNR is in the range of 10 dB and 20 dB.

The last channel condition comprises locations and routes at cell–edge region specified by yellow colour. Location8, Location5, Location9 and Route5 are at the cell–edge, therefore belong to ‘NLoS–Celledge Classifier’ channel condition.

To ensure that effects of external interferences are minimum, an empty cell and free frequency band are used. However, due to unexpected motions and phenomenon caused by people, furniture inside the building, called time–variant channel, there generates small variations on measurement results. Furthermore, the 4G LTE operating frequency of the measurement campaign is around 2100 MHz, this frequency band may coincide with the frequency bands that some commercial 3G network are serving. Hence, interference may happen. These effects are minimised by taking a measurement over a longer period, repeating it by multiple times and then averaging the results.

6.3. Test Cases

Four test cases are defined in order to study the behavioural performance of LTE MIMO and effects of antenna configuration on indoor LTE MIMO. The test cases are described in Table 12 below:

Table 12: Descriptions of four measurement test cases.

Test case	Test name	Variables and configurations	Environment
1	LTE MIMO in indoor environment	TM4 (CL–SM). Ant_A (X–pol).	Overall indoor environment and indoor channel conditions.
2	MIMO gain over transmit diversity and single antenna	TM1, TM2, TM4. Ant_A (X–pol).	Overall indoor environment and indoor channel conditions.
3	Space diversity configurations	TM4 (CL–SM). Ant_B, Ant_C. Separation: 0.5λ, 7λ.	Overall indoor environment.
4	Different polarization pair configurations	TM4 (CL–SM). Ant_C.	Overall indoor environment.

Different test cases are taken place using same measurement routes, locations and system set–ups in order to ensure valid comparison of results. Moreover, in each test case, multiple measurements up two or three times are conducted for averaging results and getting a precise result.

6.3.1. LTE MIMO in Indoor Environment

The test case is built to study effects of different channel conditions on system performance. RSRP and SNR affect CQI, RI and PMI reports, and as a result influencing MIMO Utilization, MCS and MAC link throughput. Furthermore, different channel condition classifiers provide different indoor propagation manners and that all affect system performance.

LoS and NLoS cases were also studied as well as the distance–dependent performance. Theoretically, LoS signal limits MIMO Utilization because the first main component dominates the multipath components. The delay spread is shorter. Hence, coherent bandwidth might become larger. As a result, the channel becomes frequency flat channel. Therefore, all subchannels will behave in the same way, they are very much becoming correlated channels. In LoS case, MIMO Utilization is low but SNR is quite high since UE is able to get LoS signals, high values of CQI, RI are reports, resulting higher modulation order, coding rate and number of ranks.

On the other hand, in the NLoS environment, where multipath components are rich, channels become frequency selectivity; MIMO branches are estimated to be uncorrelated. The use of MIMO is more efficient in this case. However, low SNR diminish throughput.

Indoor X–pol 8.7dBi–gain antennas are used. eNodeB is configured to operate closed loop spatial multiplexing, TM4. It is important to note that although the eNodeB is forced to closed loop spatial multiplexing, it is not always transmitting using two independent data streams. Sometimes, the eNodeB fallbacks to single antenna mode or transmit diversity due to bad channels.

This test case gives analysis base for MIMO setup performance in different indoor channels. The test case is also used as a performance reference for other test cases

6.3.2. LTE MIMO gain over Transmit Diversity and Single Antenna

Spatial multiplexing is expected to give better capacity over transmit diversity (TxDiv) and traditional communication (single antenna). This test case evaluates performances of three transmission techniques (TM1, TM2, TM4) in the given channel to compare how well MIMO outperforms over TxDiv and single antenna in LTE indoor network. The comparison evaluation is done for each channel condition and an overall comparison is made afterward. The diversity gain of TxDiv over single antenna mode is also studied.

Figure 6.7 provides an illustration measurement set–up for this test case. At eNodeB side, each of three following TMs is configured in turn. They are:

- TM1: Single antenna (so–called SIMO). The eNodeB uses port 0 to transmit one data stream to free space.
- TM2: Transmit diversity. Two antennas spread one data stream simultaneously. SNR is improved at reception, thus rising data rate.
- TM4: Closed–Loop SM. Two separate data streams are modulated, coded and then spread independently.

Indoor X–pol 8.7dBi–gain antennas typed Ant_A are used in this test case.

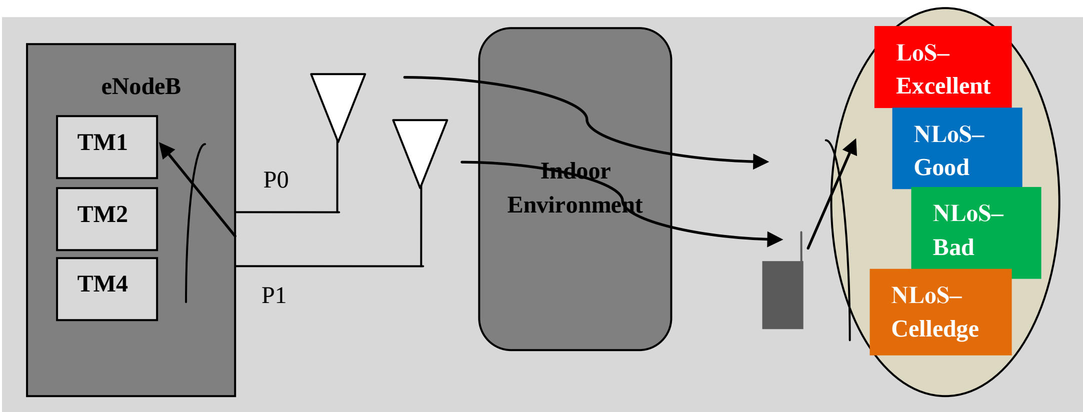

Figure 6.7: MIMO gain over transmit diversity and single antenna measurement set–up.

6.3.3. Space Diversity Configurations

Diversity gain and spatial multiplexing can be achieved using space diversity. The idea is to construct two or more horizontally spatial separated antennas deployed at a base station or mobile. The correlation between branches is the function of separations between antenna elements.

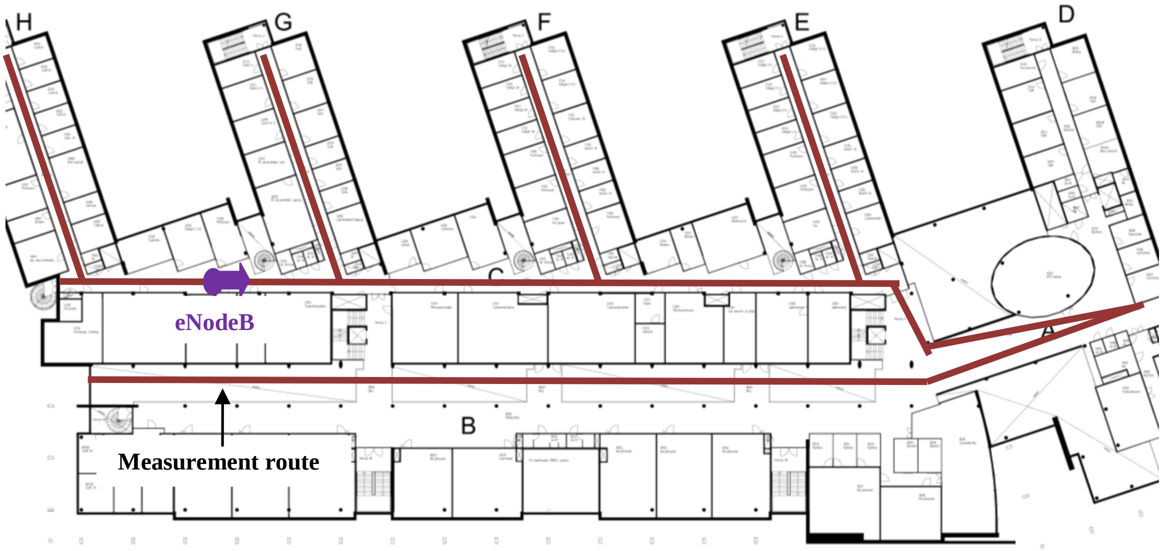

Figure 6.8: Measurement route for space diversity and polarization diversity test cases.

Table 13: Space diversity configuration at eNodeB.

Antenna Types	Separation measurements	
Omni–directionally	Half–wavelength	Seven–wavelength
Vertically–Polarized antennas	Separation ‖	Separation		
Directionally	Half–wavelength	Seven–wavelength
Vertically–Polarized antennas	Separation ‖	Separation		

In this test case, space diversity at BTS is employed. 2x2 MIMO branches are connected to two antennas. The eNodeB is forced to operate closed loop spatial multiplexing. However, as analysed, sometimes transmit diversity can be used as a fallback of multiplexing due to bad channels reported. The measurements of horizontal 0.5λ and 7λ separations between the two antennas at BTS are conducted.

Two types of antennas are used. Either the same two directionally vertically polarized typed Ant_B or omni–directionally vertically polarized antennas typed Ant_C employed at the eNodeB are tested, as presented in Table 13. The measurements are also to compare which antenna type, Ant_B or Ant_C, provides better performance and how these pairs different. The seven–wavelength separation is expected to provide better performance since channels theoretically become more uncorrelated in contrast with half–wavelength separation. However, the improvements are expected not to be significantly due to indoor propagation with wide angular spread.

In space diversity and polarization measurement test cases, all measurements are done on a same route. The route, represented by red line in Figure 6.8, covers second floor of the building. All kinds of channel conditions, from LoS excellent to NLoS cell–edge channel condition are involved.

6.3.4. Different Polarization Pair Configurations

Other way to achieve diversity gain and spatial multiplexing is on the base of signal polarization theory. The concept is that in high multipath environments, the signal from a transmitter received at a receiver will have varying polarization. The mechanism of decorrelation for the different polarizations is the multipath reflections encountered by a signal travelling between a mobile and base station. The reflection efficient encountered by each polarization is different. The performance can be improved by using two receive or transmit antennas with orthogonal polarizations and combining these signals. The polarization diversity can be implemented at both ends of a mobile system.

The first purpose in this test case is to compare performances of polarization pairs at the eNodeB while UE antennas are kept the same. An omni–directional antenna pair, Ant_C, is used, but they are configured to have different polarizations as shown in Table 14. For each polarization pair measurement, the system set–up, indoor environment remain the same to have valid comparisons. Three following polarization pairs are measured.

Table 14: Polarization pairs configuration at eNodeB.

<table>
<tr><th>Polarization Pair at eNodeB</th><th>UE Polarization</th></tr>
<tr><td>Vertical–Horizontal Pair (|–).</td><td rowspan="3">UE keeps using two internal antennas. Those are supposed to be vertical polarizations.</td></tr>
<tr><td>Vertical–Vertical Pair (||). 0.5λ separation.</td></tr>
<tr><td>X–pol Pair</td></tr>
</table>

The second purpose is to compare performances of polarization pairs at the UE. For doing so, antennas' polarizations at the eNodeB remain unchanged, different polarization pairs are applied to the UE. X–pol antenna typed Ant_A is used at BTS and it is kept using in all three cases changed in turn at the UE. Vertical–Horizontal (|–) polarization pair, antenna type Ant_B, is used afterward and it remains the same in all three UE–polarization cases. Now, UE starts using external antennas instead of internal ones. The UE supports two antenna ports, where external antennas can be attached. The two omni–directional antennas type Ant_C is used for this purpose. Table 15 provides measurement set–up for this test case.

Table 15: Polarization pairs configuration at UE.

<table>
<tr><th>UE Polarization</th><th>Polarization Pairs at eNodeB</th></tr>
<tr><td>UE internal antennas
Vertical–Vertical pair (| |), Ant_C, 0.5λ separation.
X–pol pair, Ant_C.</td><td>X–pol pair,
Ant_A antenna type.</td></tr>
<tr><td>UE internal antennas
Vertical–Horizontal pair(|–), Ant_C.
X–pol pair, Ant_C.</td><td>Vertical–Horizontal (|–) pair.
Ant_B antenna type.</td></tr>
</table>

7. MEASUREMENT RESULTS AND ANALYSIS

Results of measurement test cases explained in previous chapter are analyzed in this chapter. Each test case is studied separately by figures which show the measurement performances and comparison results. Furthermore, there will be some tables which provide statistic mean values of each measurement. In these measurements, some of different categories parameters will be studied, those parameters provide deeper understanding on the results and support analysis. RSRP and SNR depict channel condition and are reflected to channel classifiers. Indicators such as Rank Indicator, Channel quality Indicator and Modulation and Coding Schemes give deeper cognizance on how performances are obtained. In addition, MAC throughput is analyzed, providing the most practical indicator.

7.1. LTE MIMO Performance in Indoor Environment.

In this section, the performances of indoor LTE system with 2x2MIMO at different channel conditions will be studied. Furthermore, through these performances, some thresholds are able to be detected and recognized for planning.

SNR and RSRP divide indoor environment into four channel classifiers as explained in Section 6.2. The 'LoS–Excellent Classifier' has very high SNR and RSRP and there is possibility for LoS signal to reach its desired destination. RSRP and SNR that UE experience are 90–percentile more than –60 dBm and 23 dB. At those signal strength, UE is expected to give the best operation, highest CQI values and highest order of modulation can be achieved.

For the rest channel conditions, the eNodeB and UE are not visible each other, no LoS signals can be achieved, leading RSRP and SNR dropped. However, there are possibilities to provide high MIMO Utilization because of rich of multipath components, the theory to explained why high MIMO Utilization can be achieved at NLoS channels is provided in Chapter 5 and Chapter 6. At 'NLoS–Celledge Classifier' region, SNR and RSRP are very weak. Table 12 in Chapter 6 summarizes channel classifiers and their distribution SNR, RSRP. It is important to note that the 5%–tile and 95%–tile are used for all summarizing values to remove instantaneously unexpected behaviour.

The performance presentation of each channel classifier is on one figure, there are four sub–figures that describe parameter elements. The interesting parameters for understanding its performance are MAC throughput, MIMO Utilization, CQI reports and MCS.

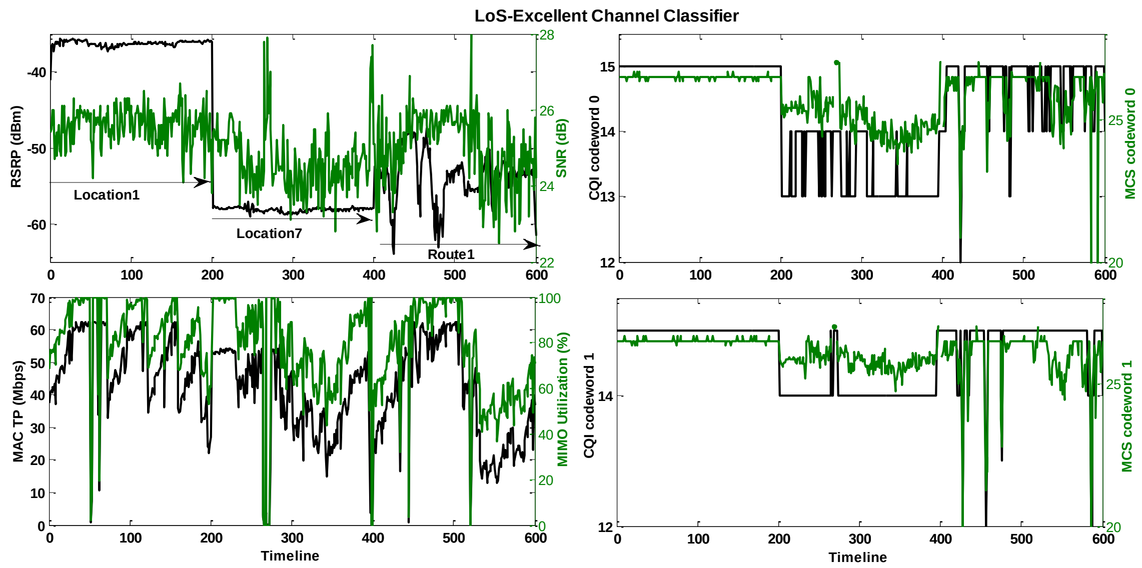

Figure 7.1: Indoor performance at ’LoS–Excellent Classifier’.

Analysing starts with ‘LoS–Excellent Classifier’. Figure 7.1 describes fully behavioural performance at LoS–Excellent classifier in timeline. When measurement is performed stationary at Location1 and Location7, RSRP remains roughly unchanged, usually above –60 dBm. However, there is a small variation in SNR. The reason for the variation is that there may be instantaneous interference affecting the operating signal or sometimes the UE stops functioning. The biggest SNR value is 28 dB, but UE rarely reaches the value even it gets very close to the eNodeB antennas. The most common SNR (around 90 percentage of the measurement) are from 23 dB to 26.5 dB. CQI and MCS variations is small. It is clear that because the channel is excellent, CQIs for codeword0 and codeword1 reported are from 13 to 15, allowing eNodeB to utilize high MCS schemes. MCS levels above 23 can be obtained. High CQI reported leads eNodeB to transmit with high MCSs, allowing 64QAM modulation and high coding rate are the most common used.

Clearly observed that, MAC throughput does not stay stable, its variation is quite large. TCP protocol with congestion control algorithms reset the window buffer to zero when it reaches maximum, causing throughput immediately drop to zero Mbps just after it got the peak. Interestingly, MAC throughput and MIMO Utilization are behavioural in the same way. The highest MAC throughput UE experiences is around 62.0 Mbps. MIMO Utilization is quite high, distributing from 60.0% to 100.0%. The throughput varies with the varying of MIMO Utilization, modulation and coding schemes, etc. However, because the channel is so very good, so always highest order of modulation and coding rate are used. Therefore, in this case, MIMO Utilization varying seems to be the only aspect that affects on the throughput variation. When 100.0% rank2 is used within one TTI 1 ms (MIMO Utilization is equal to 100.0%), MAC throughput reaches 62.0 Mbps.

At ‘NLoS–Good Classifier’ channel, the UE obtains a bit lower RSRP and SNR strengths than that at previous channel condition due to lack of LoS signals, but those are still good because the distances are close to eNodeB's antennas. RSRP and SNR are roughly 90–percentage distributed from –75 dBm to –65 dBm and from 20 dB to 26 dB, correspondingly. Values of CQI, MCS for codeword0 and codeword1, therefore, affected, and are getting lower. Degrees of variations are also bigger. The UE reports CQI mostly from 10 to 14, guiding to use MCS in the range between 20 and 26.

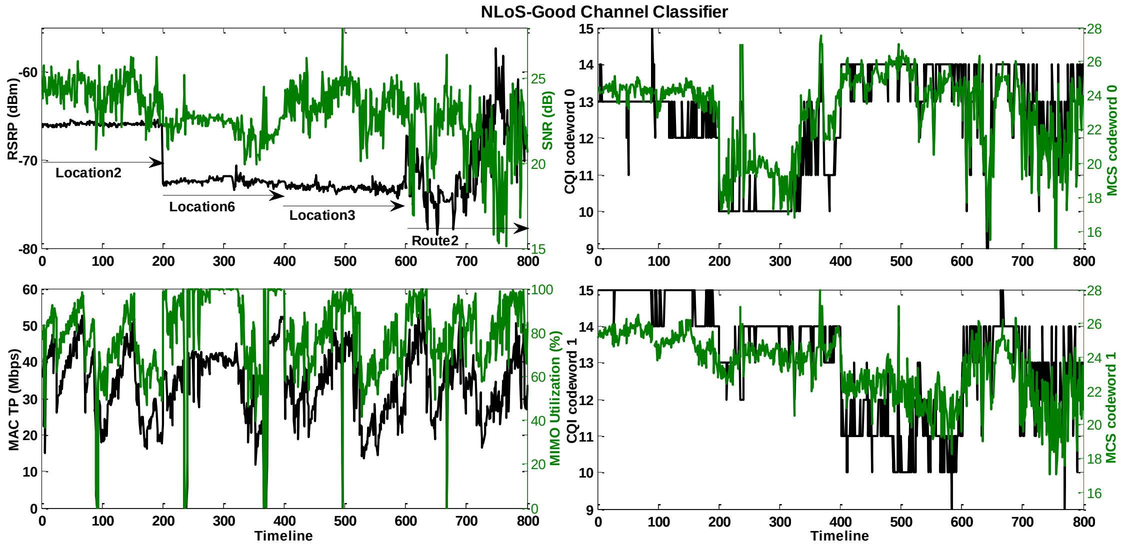

Figure 7.2: Indoor performance at 'NLoS–Good Classifier'.

However, MIMO Utilization is improved as expected. The reason is that NLoS environment provides rich of multipath components, signals becomes more uncorrelated. Hence, the eNodeB optimizes the network by using multiplexing for sending data. In this measurement, the UE experiences obviously higher MIMO Utilization but lower CQI, and MCS in compared with previous measurement. That influence a lower throughput, the peak throughput in this case is around 50.0 Mbps. The behavioural statistic performance is presented in Figure 7.2.

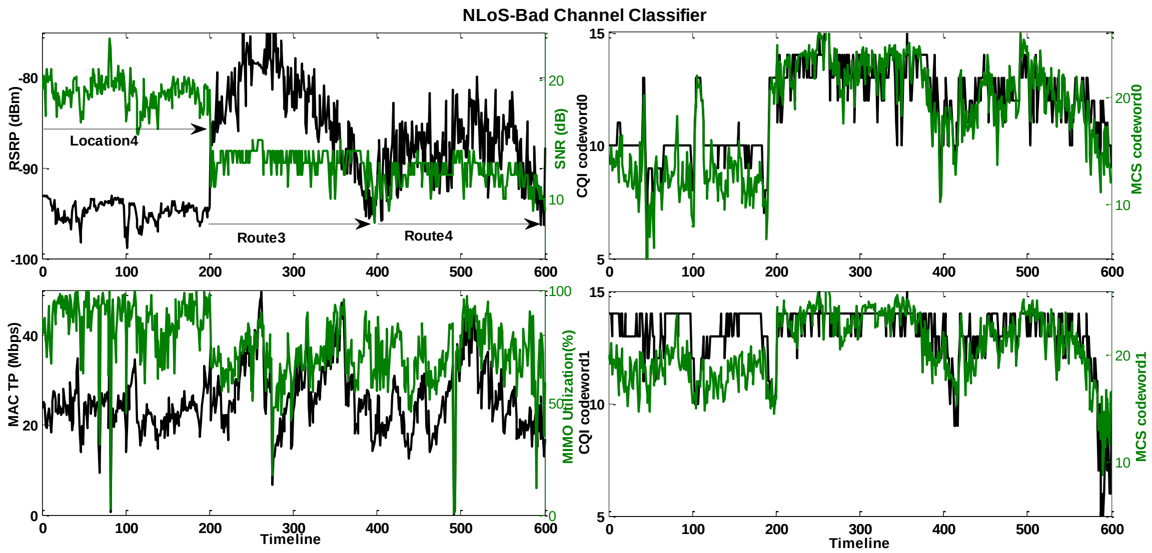

Figure 7.3: Indoor performance at 'NLoS–Bad Classifier'.

At ‘NLoS–Bad Classifier’, the UE is about to move further the eNodeB, the estimated distance between them is about 50 m–80 m. RSRP is mostly below –75 dBm, the lowest value was –100 dBm when UE is at Location4. SNR levels are, 90-percentage distribution, in between 10 dB and 20 dB. CQIs reported are lower, in the range between 8 and 13. MCSs vary quite large from 10 to 25, correspond many modulation schemes, such 64QAM, 16QAM and QPSK, are used. Furthermore, 16QAM is the most used. Due to rich of multipath components, MIMO Utilization is quite high, about 90 percent of the measurement is above 50.0%. However, the number of moments, when BTS uses 100.0%–MIMO Utilization, is low. Although the system utilized MIMO, MAC throughput was low due to bad channel condition and lower order of modulation schemes. MAC TP (MAC throughput) was from 20.0 Mbps to rarely 40.0 Mbps. Performance details and can be viewed in Figure 7.3.

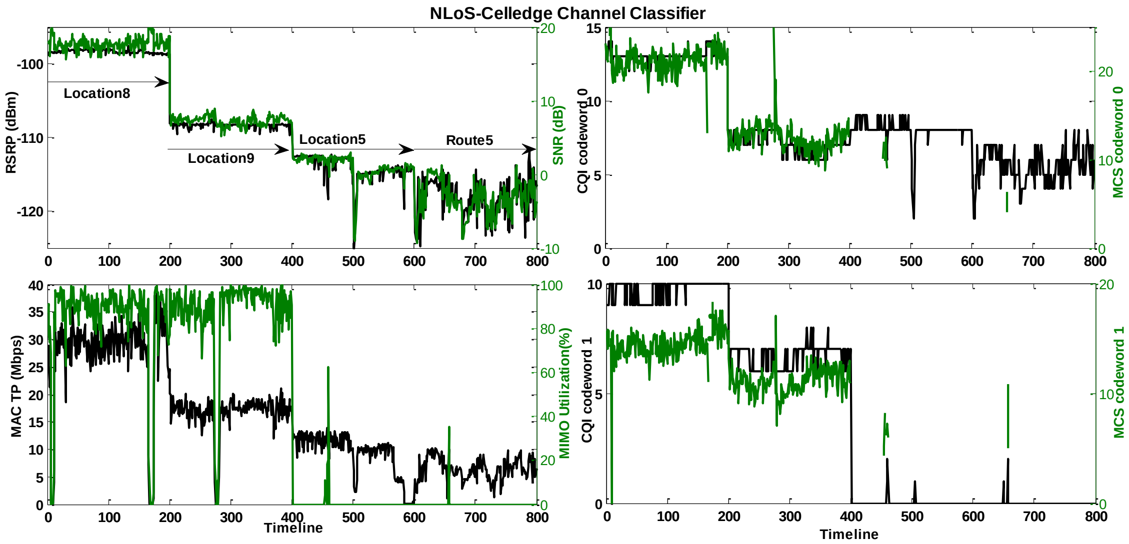

Figure 7.4: Indoor performance at ’NLoS–Celledge Classifier’.

The last measurement of this test case is at cell–edge region, ‘NLoS–Celledge Classifier’. The UE is at corridor D. Signals, which are from eNodeB, have to pass several walls before they reach the UE. Signal attenuation, therefore, is high; causing very low values of RSRP, approximately 90–percentage of RSRP values are in the range [–125 –100] dBm. CQI values are very low; therefore, 64QAM and 16QAM are rarely used. Instead, QPSK and BPSK are the most used. The eNodeB starts transmitting only one branch, multiplexing is not very utilized. If RSRP that UE received goes below roughly –110 dBm, MIMO Utilization would drops to zero. As can be seen in Figure 7.4, CQI and MCS for codeword1, the second branch usually does not appear; CQI and MCS for codeword1 were not recorded when RSRP goes below –110 dBm. Due to lower modulation order and MIMO Utilization, MAC TP at ‘NLoS–Celledge Classifier’ is low. It is about a few Mbps, lower than 12.0 Mbps.

One point needs to be highlighted in ‘NLoS–Celledge Classifier’, which can be obvious seen at Table 17. At this channel condition, two evident performances are distinguished. When RSRP is above –110 dBm, SNR is still very good from 7 dB to 15 dB. That leads to a very good performance MIMO Utilization, 90 percent of its values range from 80.0% to 100.0%. It means that two stream are utilized well. However, there appears a big drop when RSRP goes below –110 dBm, despite of using MIMO, eNodeB switches to use TxDiv, causing zero percent of MIMO Utilization. This observation leads to a conclusion that in indoor environment it is hard to achieve performance as a function of distance.

In Chapter 2, Figure 2.11 shows the mapping mechanism how CQI level is chosen to report to eNodeB regarding the SNR values. Table 17 below shows the relations between some system parameters such as CQI, MCS and MIMO Utilization and the measured RSRP, SNR in indoor environments. It also gives the further understanding on how LTE works.

Indoor performance comparison can be seen in Table 18. The measurement at 'LoS–Excellent Classifier' is used as a reference to compare other indoor performances. (–) or (+) imply a reduction or an increase compared with the reference. Additionally, cumulative distributions of all channel condition performances are shown in Appendix A Figure A.1, and Figure A.2, respectively.

Table 16: Mapping of LTE parameters in connection with measured SNR and RSRP.

Channel Classifier	RSRP (dBm) [5^{th} – 95^{th}] percentile	SNR (dB) [5^{th} – 95^{th}] percentile	CQI [5^{th} – 95^{th}] percentile	MCS [5^{th} – 95^{th}] percentile	MIMO Utilization [5^{th} – 95^{th}] percentile	MAC TP (Mbps) [5^{th} – 95^{th}] percentile
LoS–	≥ –40	[24.5 26.5]	15	[26 27]	[80 100]	[40 62]
Excellent	[–55 –40]	[24.5 26.5]	[13 15]	[25 27]	[60 100]	[30 62]
	[–60 –55]	[23 25]	[13 14]	[25 26]	[60 100]	[20 53]
NLoS–	[–70 –65]	[22 25]	[12 14]	[24 26]	[80 100]	[30 50]
Good	[–78 –70]	[20 24]	[10 13]	[18 24]	[60 100]	[20 50]
NLoS–	[–90 –75]	[12 14]	[11 14]	[18 23]	[60 90]	[25 40]
Bad	[–100 –90]	[11 18]	[8 12]	[10 16]	[50 90]	[20 30]
NLoS–	[–110 –95]	[7 15]	[6 13]	[10 20]	[80 100]	[15 30]
Celledge	[–125 –110]	[–7 5]	[3 8]	[10 16]	[0 0]	[5 10]

Table 17: Indoor performance with mean value comparisons.

Channel Classifier / Parameters	LoS–Excellent (reference)	NLoS–Good	NLoS–Bad	NLoS–Celledge
RSRP (dBm)	– 48.0	– 70.0 (– 45.8%)	– 90.0 (– 87.5%)	– 115.0(– 139.5%)
SNR (dB)	25.0	23.0 (– 8.0%)	20.0 (– 20.0%)	0.7 (– 96.9%)
MAC TP (Mbps)	38.0	33.0 (– 13.2%)	28.0 (– 26.3%)	8.3 (– 78.1%)
MIMO Utilization	72.0	77.0 (+ 6.9%)	80.0 (+ 11.1%)	14.0 (– 80.5%)
CQI codeword0	14.6	12.5 (– 13.7%)	11.7 (– 19.8%)	6.8 (– 53.4%)
CQI codeword1	14.7	13.0 (– 11.6%)	13.0 (– 11.5%)	1.6 (– 89.1%)
MCS0	26.0	23.0 (– 11.5%)	18.0 (– 30.7%)	16.0 (– 38.4%)
MCS1	26.0	23.0 (– 11.5%)	20.0 (– 23.1%)	12.0 (– 53.8%)

Based on the parameter mapping summarized after measurements in Table 17 and the comparisons in Table 18, some conclusions can be made:

- The relations of some LTE system parameters such as CQI, MCS and measured parameters like RSRP and SNR of this measurement are close to what have been studied in literature [1] [4]. Moreover, this test case shows a study of MIMO Utilization in the connection with channel conditions, which has not been mentioned in those literature references.
- The 2x2MIMO maximum TP in this indoor measurement with such configurations, 62.0 Mbps, is a bit lower than that declared in literature [4] and outdoor measurement provided in [30] (70.0 Mbps).
- UE reports CQI based on the measured SNR rather than RSRP. For example, some measurement, RSRP fluctuates in a large range. However, SNR variation is in a small range, corresponding CQI distributes in a small range. Moreover, When RSRP is very low, but SNR still gets quite high, resulting in quite high CQI.
- If SNR is above 24 dB, CQI is most probably higher than 13. Hence, MCS is usually above 25, leading the system using 64QAM and maximum MAC TP equal 62.0 Mbps.
- MIMO is not utilized if RSRP goes below –110 dBm or SNR goes below 2–3 dB
- CQI goes down below five, only one stream (codeword0) is transmitted, transmit diversity is used instead of multiplexing even the transmission mode is forced to be multiplexing.
- The MAC TP is very much dependent on MIMO Utilization.
- LoS environment limits MIMO Utilization. NLoS environments benefit MIMO due to rich multipath. For instance, MIMO in ‘NLoS–Good Classifier’ and ‘NLoS–Bad Classifier’ channels outperform than that ‘LoS–Excellent Classifier’ channel, the former benefits roughly 6.9% increase and the later gets around 11.1% improvement.
- Codeword1 outperforms than codeword0. The eNodeB uses higher modulation order for codeword1 rather than that for codeword0.

7.2. MIMO Performance over Transmit Diversity and Single Antenna.

In this section, MIMO gains over transmit diversity (TxDiv) and single antenna (SIMO) TMs are studied. Performances of MIMO, transmit diversity and SIMO at each channel condition are compared, and indoor overall comparison can be made afterward. Transmission by means of MIMO means there are more than one data streams are modulated, coded independently each other and spread over antennas. However, there is a possibility to fallback to transmit diversity if channel condition gets worse. TxDiv in LTE means only one stream is transmitted over multiple antennas. At reception, there is only one antenna for receiving the signals. There are techniques to combine the signals. Hence, the combined SNR gets improved. TxDiv is expected to provide data rate

improvement in such bad channel. In LoS environment, TxDiv is estimated to diminish throughput since LoS signals are correlated at receivers. There, therefore, increase possibilities to detect errors, requiring retransmissions the error–detected packets. SIMO uses only stream and one antenna for transmitting and multiple antennas at reception are for receiving the signal and its multipath. SIMO is expected to provide good performance in LoS channel. However, low SNR at cell–edge channel will limit system performance. In this measurement, 2x2MIMO, 2x1 TxDiv and 1x2 SIMO are used. SIMO performance is taken as a reference for making comparisons. (given in Table 19).
Table 19 shows MAC throughput results and gains of 2x2MIMO and TxDiv over SIMO. Overall comparison and channel–by–channel comparisons are presented in turn. In general, with such indoor channel conditions spreading from 'LoS–Excellent' to 'NLoS–Celledge', MIMO performs better about 38.0% over SIMO. The improvement is impressive. Moreover, TxDiv improves roughly 16.0% over SIMO in such indoor environment.

Table 18: MIMO gain over TxDiv and SIMO comparisons.

MAC TP (Mbps) (gain in percentage)	**Overall Performance**	**LoS–Excellent Classifier**	**NLoS–Good Classifier**	**NLoS–Bad Classifier**	**NLoS–Celledge Classifier**
MIMO	23.9 (+38.2 %)	39.3 (+34.0%)	33.6 (+17.4%)	28.6(+21.7%)	8.5 (+93.0%)
TxDiv	20.2 (+16.7 %)	28.9 (–2.0%)	29.4 (+3.0%)	26.6(+13.2%)	6.5 (+47.7%)
SIMO (reference)	17.3	29.4	28.6	23.5	4.4
MAX MAC TP (Mbps)	**Overall Performance**	**LoS–Excellent Classifier**	**NLoS–Good Classifier**	**NLoS–Bad Classifier**	**NLoS–Celledge Classifier**
MIMO	62.3 (+99.0%)	62.3 (+99.0%)	60.3 (+92.6%)	59.9(+91.3%)	39.6 (+100.0%)
TxDiv	31.3 (+0.0%)	31.3 (+0.0%)	31.2 (+0.0%)	31.3(+0.0%)	26.6 (+34.3%)
SIMO (reference)	31.3	31.3	31.3	31.3	19.8

Now enhancements in each channel condition are considered. At LoS channel, MIMO provides 34.0% MAC throughput improvement over SIMO. In Ricean scenario, though, where MIMO Utilization is not worked well due to the dominance of very strong LoS signal, MAC TP gain is bigger than other measurement places because of high values of SNR. In addition, from 60.0% – 100.0% of measurement period, multiplexing is functioned as discussed in previous test case.
Obvious MIMO gain over SIMO can be clear seen at 'NLoS–Celledge Classifier', up to 93.0% improvement. There is no doubt that SIMO performs worse at cell–edge region since SNR gets low. MIMO performs well because the system switches flexibly between MIMO and TxDiv. Although eNodeB is told to transmit MIMO, there is, as analyzed, a chance to fallback TxDiv if SNRs get low. Thus, in this channel MIMO provides a 45.3% improvement over TxDiv mode. Besides, 2x2 MIMO at Rayleigh environment (NLoS environment) at good and bad channels gain approximately 17.0% and 21.0% performance, respectively, over SIMO.
Now, turn eyes to TxDiv performance over SIMO. Generally, in such indoor channel TxDiv introduces around 16.0% performance gain over SIMO. However, at 'LoS –Excellent Classifier', where SNR gets highest values, TxDiv does not make any better

in throughput but a degradation of 2.0%. Statistic for Table 19 shows that, as UE is entering to worse channel condition, throughput gain by use of TxDiv is increased. Maximum gain 47.0% is experienced at ‘NLoS–Celledge Classifier’. Theory said that, if SNR becomes very low, and the system takes advantages of using TxDiv in gaining SNR. Similarly, gains in ‘NLoS–Bad Classifier’ and ‘NLoS–Good Classifier’ channel conditions are 13.0% and 3.0%, correspondingly.

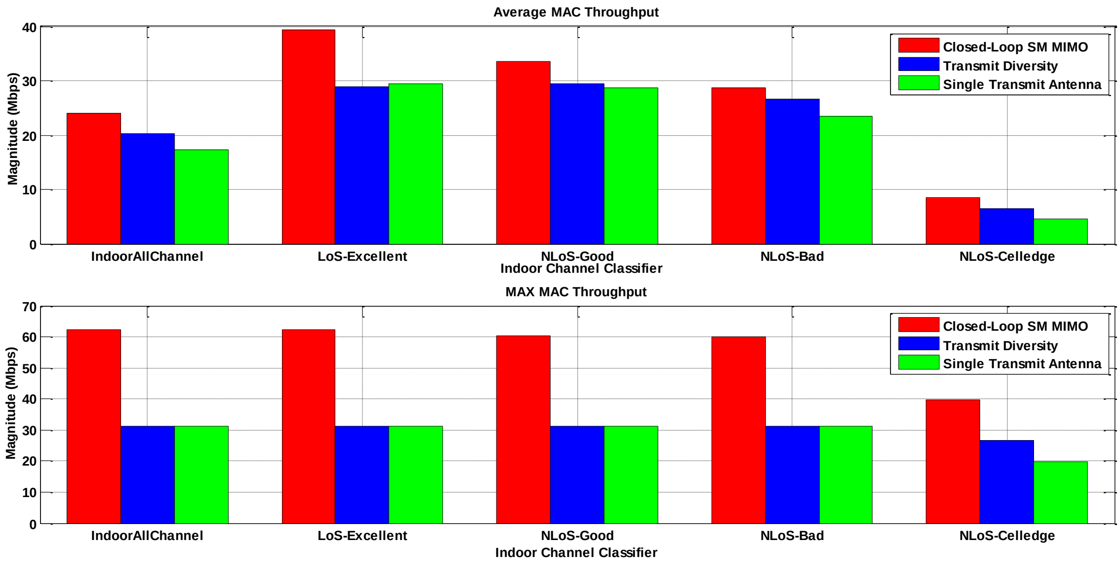

Figure 7.5: MIMO, TxDiv and SIMO performance comparison in indoor environment.

On the other hand, it is worth to note that MIMO outperforms than TxDiv in every kind of channel propagation and in overall. The gains are getting smaller as UE is moving to worse channel condition, the numbers are 36.0%, 14.0% and 8.0% in ‘LoS–Excellent’, ’NLoS–Good’ and ‘NLoS–Bad’ channels, corresponding. Exceptionally at ‘NLoS–Celledge Classifier’, gain of MIMO performance over TxDiv is 45.0%. The gain of MIMO over TxDiv can be computed by subtracting MIMO gain by TxDiv gain shown in Table 19. Those gains at ‘LoS–Excellent Classifier’, ‘NLoS–Good Classifier’ and ‘NLoS–Bad Classifier’ channel conditions are 36.0%, 14.4% and 8.5%, relatively.
In addition, by using two data streams, the maximum MIMO throughput is double to maximum throughput when TxDiv and SIMO, which use single stream, are used as transmission modes, as shown in Figure 7.5. Cumulative distributions of further comparisons at different channels are shown in Appendix A Figure A.3.

7.3. Performance of Space Diversity Configuration

This section provides the results and analysis performances of half–wavelength and seven–wavelength horizontal separations between antenna elements at BTS. In addition, measurements with two types of antennas, omni–directional vertically polarized antennas and directional vertically polarized antennas, are conducted. The objective is to study effects of space diversity and effects of antenna types, omni–directional and directional antennas, on indoor 2x2MIMO. Performance evaluations involve SNR, MIMO Utilization, and MAC TP.

Cumulative distribution function (CDF) presentations are shown for comparison and analysis. Comparison is done parameter–by–parameter. For each measuring parameter, a CDF presentation is shown. CDF for a discrete random variable X at a value x, denoted by $P(x)$, describes the probability that the random variable X, which has density function for instant p_X , is less than or equal x.

$$P(x) = p(X \leq x) \tag{7–1}$$

For continuous random variable with its probability density function, CDF gives the area that is formed by integral of p_X from minus infinity to that value x.

$$P(x) = \int_{-\infty}^{x} p_X(t)dt \tag{7–2}$$

The following three figures show CDF presentation of SNR, MIMO Utilization and MAC TP parameters. From those figures, the details performances of space diversity with two different antennas types are studied and comparisons can be made. There are four curls in each figure, where the two reds represent for measurement with directional Ant_B, and the two blues show measurements with omni–directional Ant_C. Measurements with half–wavelength separation are provided in dot lines while solid lines show seven–wavelength distance between antenna elements performance. Different scenarios are denoted as:

- Omni–ant ||: Measurement with omni–directional antenna, half–wavelength separation (0.5λ, Ant_C).
- Omni–ant | |: Measurement with omni–directional antenna, seven–wavelength separation (7λ, Ant_C).
- Direct–ant ||: Measurement with directional antenna, half–wavelength separation (0.5λ, Ant_B).
- Direct–ant | |: Measurement with directional antenna, seven–wavelength separation (7λ, Ant_B).

Figure 7.5 presents CDF presentation of SNRs. As can be seen from the figure, seven–wavelength separation provides better SNR values than a half wavelength does for all antenna types. SNR ranges from around lowest –7 dB to highest 28, 29 dB. Additionally, directional antennas give a bit better signal strengths compared to unidirectional antennas.

The performance of Omni–ant || (0.5λ, Ant_C) is used as a reference for comparison. The SNR mean value of Omni–ant || measurement is around 17.02 dB. With same omni–directional antennas but well–spaced separation, Omni–ant | |, would give an increase of approximately 10.0% in SNR. By using directional antennas, well–spaced, Direct–ant | |, and small–spaced, Direct–ant ||, separation gains around 12.5% and 7.9%, respectively, over the reference. Those differences in SNR will have impacts on network throughput.

Space diversity introduces some gains in SNRs as imagined in Figure 7.6. Bad channel is when SNR goes below 10 dB. UE gets SNRs above 20 dB; it enters to a good channel. SNRs in between 10 dB and 20 dB define an average channel. At bad channel, the well–spaced separation obtains around 2 dB – 3 dB gains for both types of antennas. At good channel condition, the gains are varied depending on types of antennas. Directional antennas do not give much gain, only 1 dB – 1.5 dB gains would be added to the signal if the eNodeB employs seven–wavelength space between antenna elements while omni–directional antennas introduce up to 3 dB – 4 dB gains with same space diversity. In average channel condition, if omni–directional antennas is used, well–spaced separation gets 4 dB – 5 dB. Otherwise, only 2 dB – 3 dB gain is added if directional antennas are used for space diversity. Those are summarized in details in Table 20. The SNR improvements will contribute to the improvements of network performance.

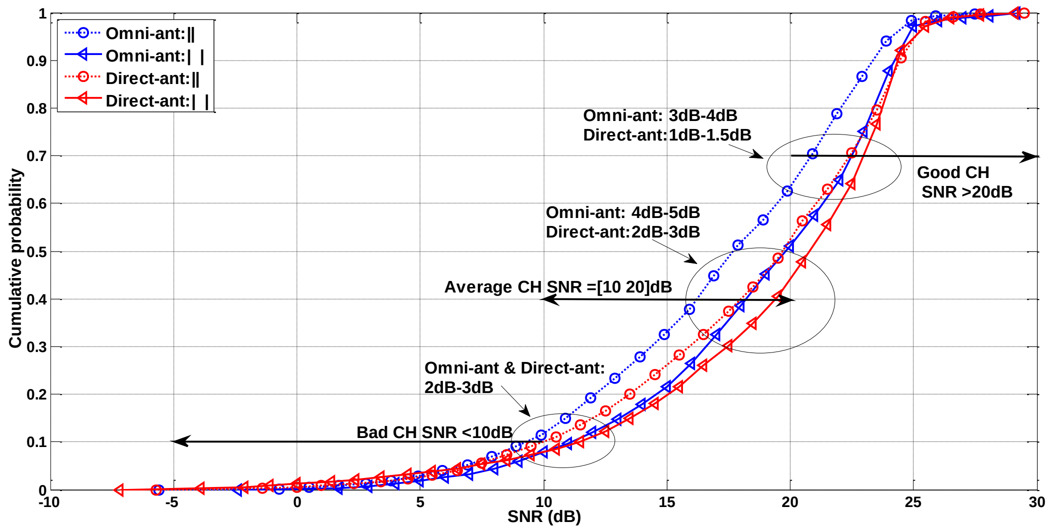

Figure 7.6: CDF plots of SNRs with space diversity.

Table 19: Relative gains in SNR with different scenarios.

Space Diversity Gain	Omni–ant || (reference)	Omni–ant | |	Direct–ant ||	Direct–ant | |
Bad CH	2 dB – 3 dB		2 dB – 3 dB	
Average CH	4 dB – 5 dB		2 dB – 3 dB	
Good CH	3 dB – 4 dB		1 dB – 1.5 dB	
SNR mean (dB)	**17.0**	**18.7(+10.0%)**	**18.3(+7.9%)**	**19.1(+12.5%)**

The primary objective of space diversity implementation is to generate uncorrelated channel. Uncorrelation channel results in high transmission efficiency, higher MIMO Utilization since the system tends to transmit with more than one data streams. Rank1(means single stream) and Rank0 (means no transmission) Utilizations, therefore, are reduced. MIMO Utilization improvements of large separation over small–space antenna elements can be illustrated via Figure 7.7.

As can be seen, a well–spaced antenna elements grants better MIMO Utilization in multi–antenna system rather than a close separation, the true conclusion are made for both types of antennas, omni–directional antennas seems to give higher MIMO Utilization space diversity improvements rather than directional antennas. In this indoor, MIMO tents to work well because just a few moments no MIMO is used. Rank1 or

Rank0 are the choices, instead. This proves what has said in the literature that there is a fallback to transmit diversity in MIMO modes, resulting Rank1 utilization. In this test case, closed–loop SM is forced to be used. However, Rank1 and Rank0 utilization are also quite often the choices within 1 TTI.

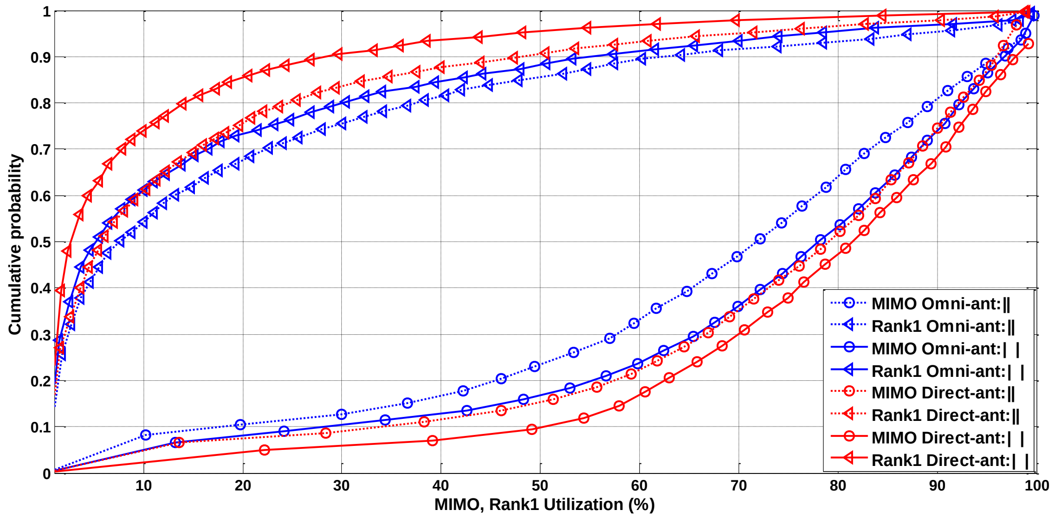

Figure 7.7: CDF plots of MIMO and Rank1 Utilization with space diversity.

Table 21 shows measurement summarizing results. In average, more than about 64.0% of the measurement periods, MIMO is used as a transmit scheme. The table also shows that seven–wavelength separation (in comparison with half–wavelength separation measurement with same antennas used) provides a 10.0% improvement in MIMO Utilization with the use of omni–directional antennas and 5.7% MIMO utilization increase if directional antennas are used. The improvements are over the reference of half–wavelength measurement results with same type of antennas.

In contrast, space diversity degrades Rank1 Utilization as shown in Figure 7.7. Observantly, the measurements, which provide higher MIMO Utilization, give the lower Rank1 Utilization. The lowest Rank1 utilization (in average, 9.7%) UE experiences is when it measures in well–spaced antenna elements with directional antennas. Moreover, in this measurement, MIMO utilization is the highest, 75.8%. Small–space between directional antennas elements improves 36.7% gain in Rank1 Utilization. The improvement by measuring with omni–directional antenna is 15.9% in general.

Table 21 also shows the average of MCS for first stream and second stream, MCS0 and MCS1, correspondingly when MIMO is utilized. For the first stream, there are no much different in MCS for both types of antennas when space diversity is deployed. Particularly, omni–directional antenna pair with well–spaced separation provides, in average, 18.5 MCS0 and 18.6 MCS0 is used with small–space separation. The results for directional antenna pair are 20.6 for MCS0 with well–spaced separation and 19.4 for MCS0 with small–spaced separation.

This statistic means the there is no modulation and coding gains for the first stream if multiplexing is used. However, seven–wavelength separations provide significant improvements for modulation and coding schemes over half–wavelength for the second stream. Those gains are roughly 13.1% for omni–directional antennas and 22.9% for directional antennas.

Table 20: Space diversity measurement summary.

Parameters	Omni–ant | | (reference)	Omni–ant | |	Direct–ant | | (reference)	Direct–ant | |
RSRP (dBm)	–80.6	– 76.9	– 78.4	– 76.5
SNR (dB)	17.0	18.7	18.3	19.1
MIMO Utilization (%)	64.3	70.9 (+ 10.2%)	71.7	75.8 (+5.7%)
Rank1 Utilization (%)	20.3	17.1 (– 15.9%)	15.4	9.7 (–36.7%)
Rank0 Utilization (%)	14.5	12.1	13.0	14.5
MCS0	18.6	18.5	20.6	19.4
MCS1	17.3	19.6(+13.1%)	15.7	19.3(+22.9%)
MAC TP (Mbps)	24.2	27.6(+14.0%)	25.9	27.1(+4.6%)

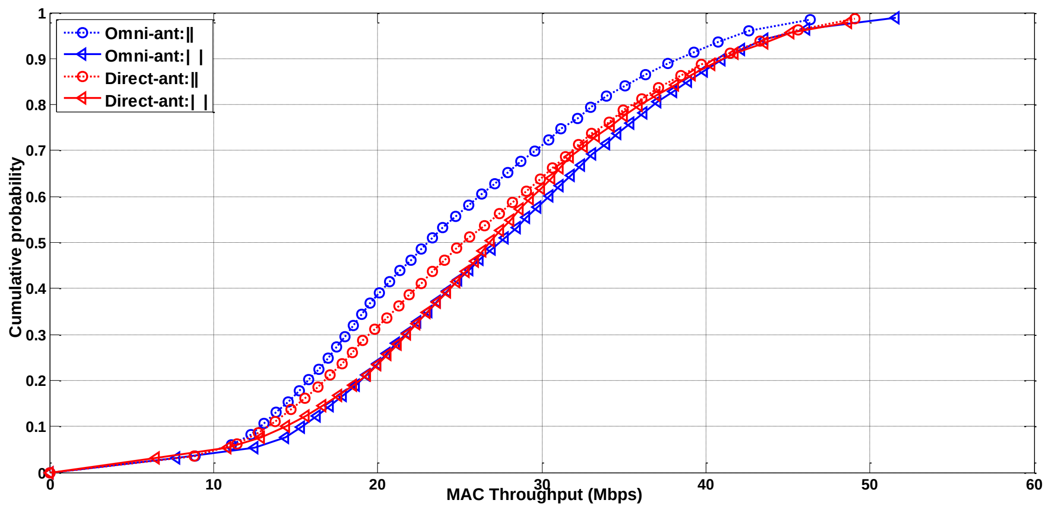

Figure 7.8: CDF plots of MAC TP with space diversity.

Space diversity provides SNR gain and MIMO Utilization gain, leading to improvements in MAC throughput as provided in Figure 7.8. Obviously, there are some gains yielded if seven–wavelength separation is deployed. However, the degrees of gains are varied with different antenna types. Directional antennas yields only 4.6% gains while omni–directional antenna pair benefits roughly 14.0% gain. The reason that can be explained for the low gain in directional antenna measurement is that Rank0 is used so often when large antenna separation (seven–wavelength) is used. Rank0 Utilization means no transmission, which degrades link throughput.

A conclusion can be made for this test case indoor space diversity. Although omni–directional antennas provide lower SNR values, MAC throughput UE achieved is similar to that when directional antennas pair is used. Therefore, in terms of investment, omni–directional antenna pair with seven–wavelength separation is a good choice because it provide as high performance as directional antennas do but lower cost. An indoor radio network planner may consider to this point to reduce the planning cost but still maintain good quality of service.

7.4. Performance of Polarization Diversity Configurations

As previously discussed, the employment of such a large separation at BTS would be very beneficial for network operators since it increase data throughput by having SNR gain and MIMO Utilization gain; Omni–directional antenna with 7λ separation is a good choice in term of cost due to providing high performance but lowering the cost. However, in some cases, larger separation of antenna elements is not feasible. Polarization is, therefore, taken into account for indoor planning.
Different polarization pair measurements are conducted. In this test case, not only polarization configurations at the eNodeB but also those at the UE are also studied.

7.4.1. Antenna Polarization Performance at eNodeB

Figure 7.9, Figure 7.10 and Figure 7.11 show the performances of different antenna polarization pairs at eNodeB. SNR and MIMO Utilization linked with MAC TP are shown and analyzed.

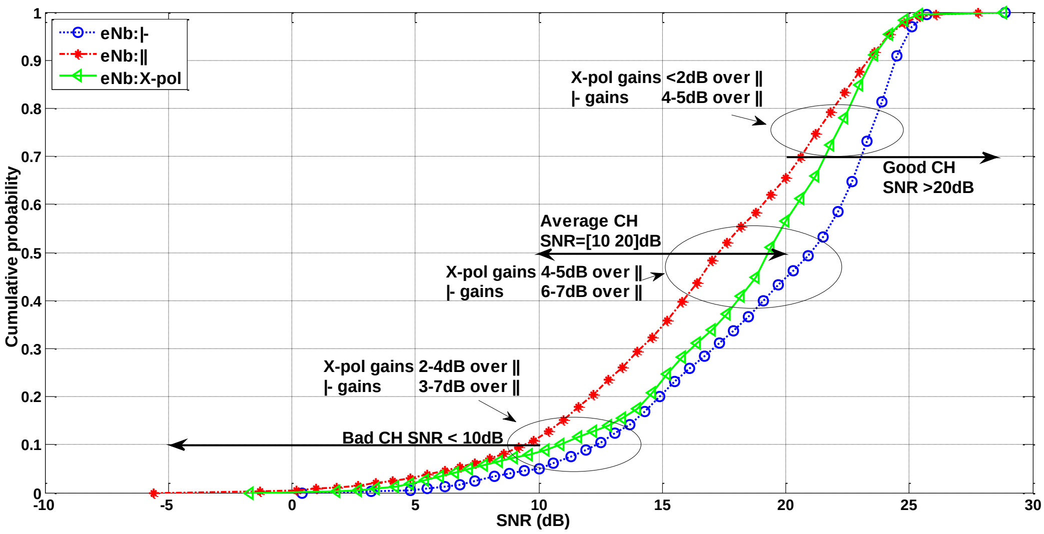

Figure 7.9: Comparison of SNRs with different polarization pairs at eNodeB.

Different measurement scenarios are denoted as follows:

- |–: Vertical horizontal polarization pair.
- ||: Vertical–vertical polarization pair with 0.5λ separation.
- X–pol: Dual polarization.

As can be seen, in general, the vertical–horizontal polarization pair (|–) deployed at the eNodeB provides the best performance among various polarization pairs, vertical–vertical (||) and X–pol pairs.

Regarding the measurement of SNR, it is very important to improve SNR since SNR gained would improve the network performance. Therefore, in evolved wireless systems, there are always evolved techniques designed for SNR improvements.

Polarization matching also affects the strength of combined signals. Polarization matching means the polarization of incoming wave should match polarization of receiving antennas so that polarization loss would not be occurred. However, in indoor environments, where BTS and UE are rarely visible, so the polarization of incoming wave is not possible to be known. UE' antennas are also not stable to have a certain polarization. In indoor environment where has rich of reflectors and scatters, it is better to have different kinds of polarizations at BTS such as horizontal and vertical pair or X–pol pair, so the transmitted waves will be polarized diversely. It will raise possibilities of having matching polarizations at reception. Hence, SNR would obtain high. In that case, |– pair or X–pol would provides better SNR than ||.

Table 21: Summary of antenna polarization performance at eNodeB.

Polarization Pair / **Parameter**	**|| polarization pair (reference measurement)**	**X–pol polarization pair**	**|– polarization pair**
SNR (dB)	16.8	18.2 (+8.1%)	19.4 (+15.5%)
MIMO Utilization (%)	66.5	74.5 (+12.0%)	78.9 (+18.6%)
Rank1 Utilization (%)	21.0	7.1	7.4
Rank0 Utilization (%)	12.4	18.3	13.7
MAC Throughput (Mbps)	23.7	27.1 (+14.4%)	31.3 (+31.7%)

In Figure 7.9, the blue, green and red lines show CDF presentations of SNRs for |–, X–pol and || polarization pair deployed at eNodeB. Clearly seen, |– pair provides the best SNR on the same measurement route. The lowest performance, || pair, can be considered as a reference. In overall, |– and X–pol pairs gain up to 2.45 dB and 1.38 dB over || pair, or corresponding to 15.5% and 8.1% increases, respectively, as shown in Table 22. X–pol pair provides very good SNR gain at low and average channels, the gains are around 2 dB – 4 dB at low channel and 4 dB – 5 dB average channel condition. However, at good channel condition, where having LoS signals is possible and hence SNR is above around 20 dB, gain is reduced, only less than 2 dB gain is achieved. The explanation for this reduce may be that when the UE is able to have LoS signals, X–pol polarization may lose polarization matching between incoming waves and reception antennas. On the other hand, |– pair provides good gain over || pair in the whole measurement route, gain is around 3 dB to 7 dB as illustrated in Figure 7.9.

Figure 7.10 shows MIMO and Rank1 Utilizations measurements of three antenna polarization pairs at the eNodeB. |– provides the best MIMO Utilization with 78.9%, meaning that the use of |– polarization pair help to uncorrelated the channels. It gains up to 18.6% increase in compared to the reference || pair, which provides only 66.5%

MIMO Utilization. In addition, X–pol pair improves 12.0% over the reference measurement as provide in Table 22.

Instead, || utilizes Rank1, up to 21.0 percentage of measurement period, BTS uses only one stream for transmission. The numbers for X–pol and |– pairs are 7.1% and 7.4%.

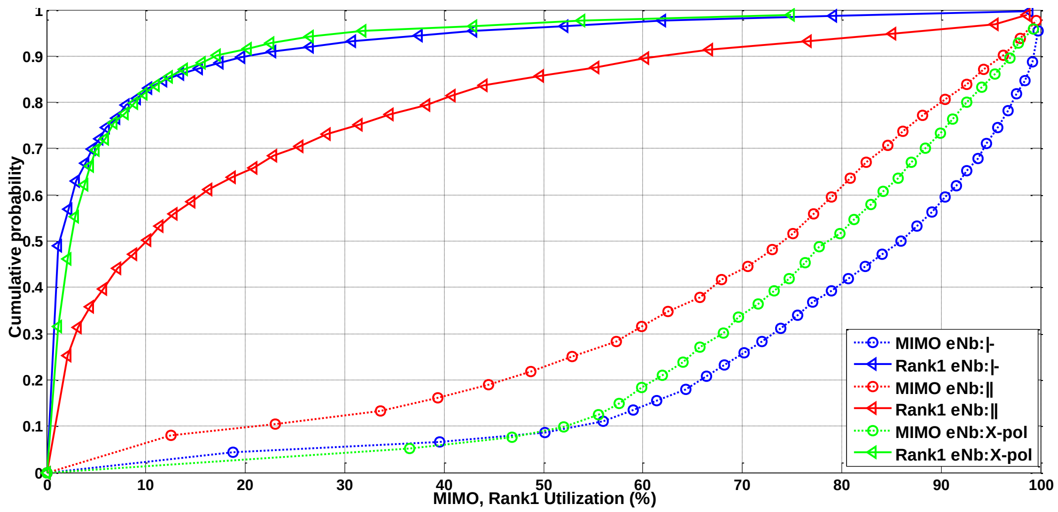

Figure 7.10: Comparison of MIMO and Rank1 Utilizations with different polarization pairs at eNodeB.

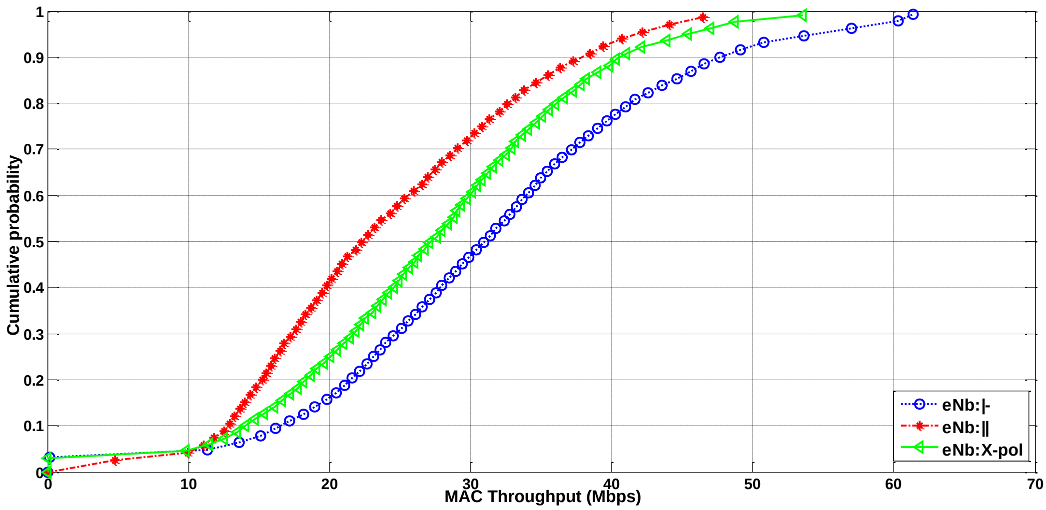

Figure 7.11: Comparison of MAC throughputs with different polarization pairs at eNodeB.

Figure 7.11 gives the CDF plots of MAC throughput performances of three polarization pair cases deployed at the eNodeB. Obviously, the best throughput in average UE obtains is when |– is employed, throughput is 31.3 Mbps in average while || and X–pol pairs provide 23.7 Mbps and 27.1 Mbps, correspondingly. Up to 31.7% improvement is experienced if |– antenna polarization pair is configured instead of || pair.

|– polarization pair also provides very good maximum throughput; around a maximum throughput 62.0 Mbps can be achieved. However, || and X–pol pairs provide only 47.0 Mbps and 55.0 Mbps maximum MAC throughputs. The maximum throughput of 2x2 MIMO in [30] through measurements in macrocell is about 50.0 Mbps with X–pol at eNodeB and || at UE.

In such indoor environment, |– should be the polarization pair deployed at the eNodeB to provide the best performances among X–pol and || pairs. |– also provides the highest MIMO Utilization as expected since dissimilar patter and orthogonal polarizations lead to uncorrelated channels.

7.4.2. Polarization Matching

It is proven that antenna polarization at BTS has affected on the performance of LTE MIMO systems. |– polarization pair deployed at eNodeB provide the highest MIMO and MAC throughput. However, the gains are obtained previously when UE's antennas are internal antennas. In this section, the polarization performances are extended with the present of UE's external antennas. The extensions are that two external antennas will form some polarization pairs at UE.

At BTS, two kinds of polarization pair are deployed, either |– pair or X–pol pair. At UE and, three polarization pair configurations are used for measurements for each pair deployed to eNodeB. Table 15 in Chapter 6 gives the configuration details. The purpose of this measurement test case is to figure out whether the different polarizations at UE affect the overall performance. In this measurement test, the performances when using UE internal antenna are used as references for comparison.

Table 23 provides the summary of polarization matching performances for this test case. Once again, it proves what has been analyzed on previous measurement that |– polarization pair at BTS outperforms than X–pol polarization pairs no matter what is used to UE. The average MAC TP if |– pair is deployed at the eNodeB is around more than 31.0 Mbps while X–pol pair provides only around 28.0 Mbps. However, on each case of polarization pair at eNodeB, the different polarization pairs at UE do not make any significant different on MAC throughput.

The deployment of X–pol polarization at UE provides a little benefit of SNR gain in compared to using UE's internal antennas, particularly the gains are 3.9% and 7% if |– and X–pol pairs are employed at the eNodeB, respectively.

Table 22: Summary of antenna polarization matching performance at eNodeB and UE.

Pol matching / Parameters	eNodeB: |– UE:internal	eNodeB: |– UE: |–	eNodeB:|– UE: X–pol	eNodeB:X–pol UE: internal	eNodeB:X–pol UE: ||	eNodeB:X–pol UE: X–pol
SNR (dB)	19.4	19.6	20.2 (+3.9%)	18.2	18.5	19.5 (+7%)
MIMO Utilization (%)	78.9	77.5	77.0	74.5	75.7	77.7
Rank1 Utilization (%)	7.4	7.1	8.4	7.1	10.4	5.9
Rank0 Utilization (%)	13.6	15.3	14.5	18.3	13.8	16.2
Max MAC TP (Mbps)	31.3	31.8	31.2	28.8	27.4	29.4

Regarding MIMO Utilization, external antennas at UE seem not to provide any differences as can be seen in Table 23. For example, when |– is chosen as eNodeB antenna pair, MIMO Utilizations are 78.9%, 77.5% and 77.0% with the corresponding configurations at UE are internal, |– and X–pol polarization pairs. A little gain is recorded when X–pol polarization pairs are used at eNodeB and UE sides. This result is very different with the polarization matching results obtained in [30] in macrocell since the TP is very significantly varied with different polarization pairs deployed at UE. The measurement in [30] also shows that |– pair at UE would give much improvement in average TP and maximum TP compared to performance of || pair at UE. Cumulative distributions of SNR, MIMO utilization and MAC TP of polarization matching are shown in Appendix A Figure A.4, Figure A.5 and Figure A.6, respectively.

7.5. Error Analysis

Many sources could cause errors to the measurements and, therefore, affect the accuracy and generalization possibility of the thesis. It should be taken into consideration that all measurements presented in this thesis are highly dependable on the chosen antennas, network systems, devices and indoor environment where the measurements are carried out. Hence, the results may be affected if other factors mentioned above are used.

Due to unexpected motions and phenomenon caused by people, furniture inside the building, called time–variant channel, there generates small errors on measurement results. Furthermore, the 4G LTE operating frequency of the measurement campaign is around 2100 MHz, this frequency band may coincide with the frequency bands that some commercial 3G networks are serving. Hence, unexpected interference may occur.

As to polarization test case, the same omni-directional antennas are used to create different polarizations by rotating it around. This configuration, however, change also the radiation beams of the antennas. Dissimilar radiation patterns due to rotating antenna geometry clearly affect on transmitting and receiving signal strength and therefore may influence on the results. The target was to have antennas with similar properties but different polarization, but it seems to be hard to find them in the market.

Additionally, when configuring antennas prior measurements, the down tilting of antennas may have slightly changed, this aspect may have made errors on the results.

7.6. Comparison with Literature

Some results obtained in this thesis follow the expectations what have been studied in literature and previous practical studies but some point out differences.

The relations of some LTE system parameters such as CQI, MCS and measured parameters like RSRP and SNR of this measurement are close to what have been shown in literature [1] [4]. Moreover, this test case shows a study of MIMO utilization in connection with channel conditions, which has not been mentioned in those literature.

The 2x2MIMO maximum TP in this indoor measurement with such configurations, 62.0 Mbps, is a bit lower than that declared in literature [4] (85.7 Mbps) and outdoor measurement provided in [30] (70.0 Mbps) and indoor measurement provided in [31]

(65.0 Mbps). The throughput provided in [4] is obtained in optimum way, highest order of modulation, 64QAM, and theoretical coding rate, 1, are used and MIMO utilization is 100.0% in 1 TTI . However, in practical measurement, this is never achieved since sometimes eNodeB utilizes Rank1 or Rank0. Furthermore, theoretically, LoS environments restrict MIMO utilization and TxDiv; this is proved through the obtained results. MIMO utilization at LoS channel is experienced lower than that at NLoS environments. Similarly, TP of TxDiv at LoS channel is a 2.0% reduction compared to TP received when single stream is used.

In theory, 2x2MIMO double performance over TxDiv and single antenna. In this measurement, this is achieved for maximum TP in every channel. Maximum TP when TxDiv is used is roughly equal to that when single stream is used in every kind of channel. However, this result contrasts with what have been achieved in [31] since maximum TP TxDiv is better only at bad channels, at good channels it lowers than maximum TP achieved if single stream is transmitted.

As to space diversity, theories in [15] [20] and the measurements in [30] with commercial LTE network show a significant TP improvement of large antenna separation over small separation, and this is also further proved in this measurement with two types of antennas, omni-directional and directional antennas. An extensive study in this thesis is to show that omni-directional antennas give better TP improvement rather than improvement obtained with directional antennas, clearly 18.0% TP gain over 4.5%.

Measurements in [30] also indicates that |- polarization deployed at UE provides a very significant gain over other pairs such as || and X-pol pairs in macrocell but in this measurement, the results obtained reflects dissimilarity, different polarization pairs at UE in indoor network do not show clear gains.

This thesis gives the guidelines for network operators when thinking of optimum LTE solutions for indoor planning. The guidelines can be applied to antenna selection, antenna line selection and dimensioning, capacity planning and TM configuration planning tasks for network operators.

8. DISCUSSION AND CONCLUSION

This thesis focuses on aspects of LTE indoor planning. First, the thesis provides a deep understanding on LTE practical performance in indoor propagations, the performances at different indoor channels are then analyzed and compared. The comparison performances of MIMO over transmit diversity (TxDiv) and single antenna are a part of the study. The second aspect of the thesis is to emphasize to the impacts of antenna configurations on MIMO. From the results obtained, optimum ways to boost LTE capacity in indoor are proposed and guidelines for LTE indoor planning can be given.

MAC throughput (MAC TP) and some system parameters in LTE network that are linked with TP are analyzed; those parameters are CQI, MCS as well as MIMO utilization. Effects of indoor propagation, such as LoS, NLoS, good and bad signal levels on SNR strength and MIMO utilization are clarified. The limitation of this measurement is that it is not possible to have a smooth range with equally distributed SNR values from 0 to 28 in such indoor channel so that the relation of CQI, MCS and MIMO utilization with a precise range of SNR can be drawn and then the comparison with theory in literature are be made.

In overall, MIMO outperforms TxDiv (MISO) and single antenna in LTE indoor because of multiple data stream transmitted simultaneously. The overall MAC TP gains are about nearly 40.0% over TxDiv and more than 20.0% over single stream. However, the gains vary with different kinds of channels. LoS environment boost SNR strength. Hence, up to 35.0% MIMO TP gain over single antenna is achieved. LoS signals make the channel becomes correlated due to lack of multipaths, causing that MIMO is not fully utilized. The gain of MIMO over single antenna is reduced at no LoS environments, particularly only around 17.0% and 21.0% MAC TP gains are recorded at NLoS good signal levels and NLoS bad signal levels, relatively. In theory, 2x2MIMO provides double maximum capacity over two latter ones and this thesis' results support the theory by showing that maximum MAC TP of MIMO mode double that in TxDiv and single antenna modes in each channel condition.

The overall TP gain the UE experiences by using TxDiv over single antenna in such indoor environment is roughly more than 20.0%, but LoS environment limits TxDiv performance. Hence, at LoS channel, TxDiv performance is reduced by around 2.0% compared to single stream. The worse the channel, the better TxDiv performs. The highest gain is at cell edge environment when TxDiv improves TP more than 40.0% over single antenna.

As to space diversity, large horizontal separation (7λ) between antenna elements outperforms small separation (0.5λ) in terms of SNR, MIMO utilization and MAC TP.

8. DISCUSSION AND CONCLUSION

The MAC TPs of 7λ separation by using omni-directional and directional antennas are almost similar, around 27.0 Mbps. However, improvements are varied between antennas. In overall, space diversity with omni-directional antennas provide roughly 14.0% TP improvement while around only 4.5% TP gain can be achieved with directional antennas. Because of obtaining uncorrelated channels by using space diversity, MIMO utilization is remarkably improved, the MIMO utilization improvements that UE experiences are roughly 10.0% with omni-directional antennas and 6.0% with directional antennas. Therefore, space diversity with omni-directional antennas seems to be a good choice for 2x2MIMO deployment at LTE BTS in such indoor environment since they provide as similar TP as directional antennas do but they are smaller and might be cheaper. In this thesis, only 7λ and 0.5λ horizontal separations are tested, but the extension can be with other separations to figure out fully effects of space diversity on LTE indoor performance. Space diversity at UE is also an interesting topic even the size of UE is too small to make many choices for antennas' separation.

Vertical–horizontal polarization pair deployed at eNodeB is found to provide better performance over vertical–vertical polarization and X–pol pairs. Signals also appear to be more correlated with vertical-horizontal polarization pair since MIMO utilization gets better values, MIMO utilization gains by having vertical-horizontal pair at eNodeB are around 18.0% over vertical-vertical polarization pair and 6.0% over X-pol pair, resulting in around 31.7% and 17.0% MAC TP gains over the two latter, relatively. Moreover, the deployment of external antennas at UE is to evaluate polarization matching. The results point out that changing polarizations at UE do not give clear MAC TP and MIMO utilization improvements. Furthermore, this result points out differences with the results provided in [30], which is about polarization matching in LTE macrocell, showing that the vertical-horizontal polarization pair employed at UE gives very significant TP improvement in comparison with vertical-vertical pair.

Extensive topics toward the field researched in this thesis can be done in the future. The same studies but with different kinds of measurement set-up; such as using other types of antennas, different indoor environments or using other UEs as well as different LTE BTS of other vendors; can be considered as the next steps in order to be able to generalize the results independent of a particular measurement set-up. Regarding space diversity, more several horizontal separation as well as vertical separations can be studied. Regarding antenna's polarization measurement, directional antenna with different polarization pairs can be the choices for extension and the combination with space diversity is also an interesting topic as proposed in literature.

From the radio network planning point of view, the results obtained in this thesis can be considered as guidelines for indoor network planning and optimization for network operators. The guidelines can be applied to antenna selection, antenna line selection and dimensioning, capacity planning and TM configuration planning tasks for network operators. It is important to conclude that based on the measurements made in this thesis, space diversity (7λ) with omni-directional antennas and vertical-horizontal polarization pairs appear to give optimal indoor solutions.

BIBLIOGRAPHY

[1] S. Sesia, I. Toufik, M. Baker, LTE - The UMTS Long Term Evolution - From Theory to Practical, John Wiley & Sons, 2009.

[2] E. Dahlman, S. Parkvall, J. Sköld, P. Beming, 3G Evolution HSPA and LTE for Mobile Broadband, 2008.

[3] J. Lempiäinen, M. Manninen, UMTS Radio Network Planning, Optimization and QoS Management, Kluwer Acedemic, 2003.

[4] H. Holma, A. Toskala, LTE for UMTS: OFDMA and SC-FDMA Based Radio Access, John Wiley & Sons, 2009.

[5] L. J. Cimini, ”Analysis and Simulation of Digital Mobile Channel using Orthogonal Frequency,” *IEEE Trans. on Communications*, pp. 665-675, July 1985.

[6] J. Rinne, ”Multicarrier Techniques,” Tampere University of Technology, 2011.

[7] V. Selvakumar, S. S. Nemalladinne, P. Arumugam, ”Analysis of LTE Radio Frame by eliminating Cyclic Prefix in OFDM and comparison of QAM and Offset-QAM,” Linneeus University, 2012.

[8] P. Payaswini, D.H. Manjaiah, ”Analysis Of Effect Of Cyclic Prefix On Data Rates In OFDM Modulation Techniques,” *International Journal of Advanced Computer and Mathematical Science*, 2012.

[9] S. Zarie, ”LTE: Channel Coding and Link Adaptation,” December 2009.

[10] A. Mehmood, W. A. Cheema, ”Channel Estimation For LTE Downlink,” Blekinge Institute of Technology, Sep 2009.

[11] J. C. Ikuno, M. Wrulich, M. Rupp, ”System Level Simulation of LTE Networks,” *IEEE Technology Conference*, May 2010.

[12] S. Schwarz, C. Mehlfuhrer, M Rupp, ”Calculation of the Spatial Preprocessing and Link Adaption Feedback for UMTS/LTE,” Vienna, Austria, 2010.

[13] S. Lei, Y. Xiong, X. Yang, ”Novel Rank Indicator Calculation Method in LTE Systems,” Shanghai, China.

[14] S. Bemhard, ”LTE Transmission Modes and Beamforming,” Rohde & Schwarz, October 2011.

[15] S. R. Saunders, A. A. Zavala, Antennas and Propagation for Wireless Communication Systems, John Wiley & Sons, 2007.

[16] A. Khan Afridi, ”Macro and Femto Network Aspects for Realistic LTE Usage

Scenarios,” KTH Electrical Engineering, 2011.

[17] M. Tolstrup, Indoor Radio Planing - A Practical Guide for GSM, DCM, UMTS and HSPA., John Wiley & Sons, 2008.

[18] P. Lahdekorpi, T. Isotalo, A. Mazhar, J. Lempiainen, ”Improving HSDPA Indoor Performance Using Outdoor Repeater,” *Intenational Symposium on Wireless Personal Multimedia Communication.*

[19] L. Jiangang, L. Yinghua, Y. Wang, H. Zhao, C. Han, ”Antenna Spacing Effect on Indoor MIMO Channel Capacity,” *IEEE Conference Publishing*, 2005.

[20] C. Wiliam, Y. Lee, ”Antenna Spacing Requirement for a Mobile Radio Base Station Diversity,” *Bell System Technical Journal*, pp. 1859-1876, 1971.

[21] C. William, Y. Lee, Y. S. Yeh, ”Polarization Diversity System for Mobile Radio,” *IEEE Transactions on Communication*, pp. 912-923, 1972.

[22] J. Zhao, Y. Li and G. Sun, ”Analysis of Antenna Mutual Coupling in the X-type Polarization Diversity System,” *IEEE*, 2009.

[23] H. Xiao, S. Ouyang, Z. Nie, ”The Cross Polarization Discrimination of MIMO Antennas at Mobile Station,” *IEEE*, 2008.

[24] Kathrein-Ltd, ”Multi-Band Panel Dual Polarization Half-power Beam Width Fixed Electrical Downtilt-742210V01”.

[25] Kathrein-Ltd, ”Directional Indoor Antenna with Integrated Combiner”.

[26] Poynting-Ltd, ”Panel Mount Cellular Quad-Band Antenna-OMNI-A0085.”.

[27] Huawei, ”Huawei E398 4G LTE TDD FDD USB Surfstick”.

[28] Anite, ”Nemo Outdoor V6.30-Air Interface Measurement Tool- User Manual,” Anite Finland, 2012.

[29] Anite, ”Nemo Analyze-User Manual,” Anite Finland, 2012.

[30] K. Werner, J.Furuskog, M.Riback, B. Hagerman, ”Antenna Configuration for 4x4 MIMO in LTE-Field Measurement,” *IEEE*, 2010.

[31] J. Kopsala, ”Indoor MIMO Performance with HSPA+ and LTE,” Tampere University of Technology, 2011.

APPENDIX A

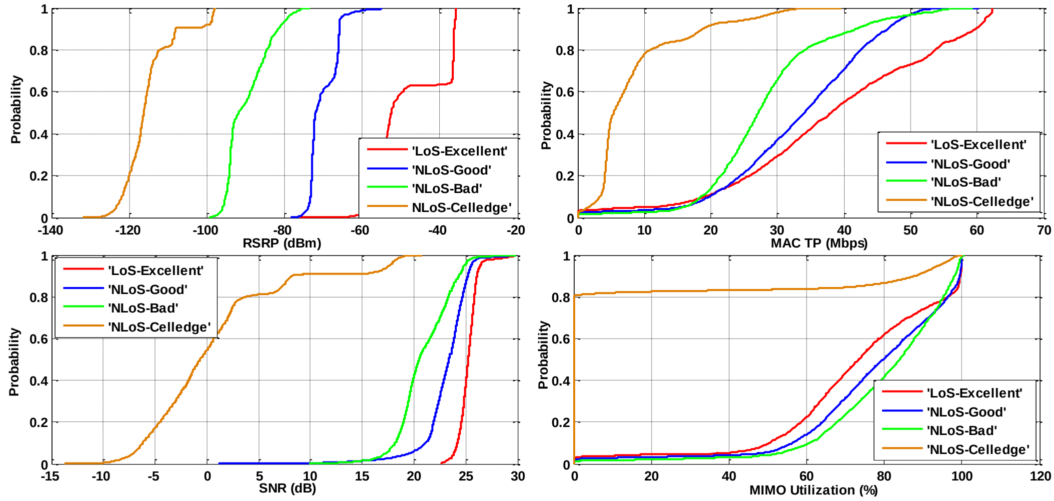

Figure A. 1: CDF plots of MIMO performances at all channel conditions.

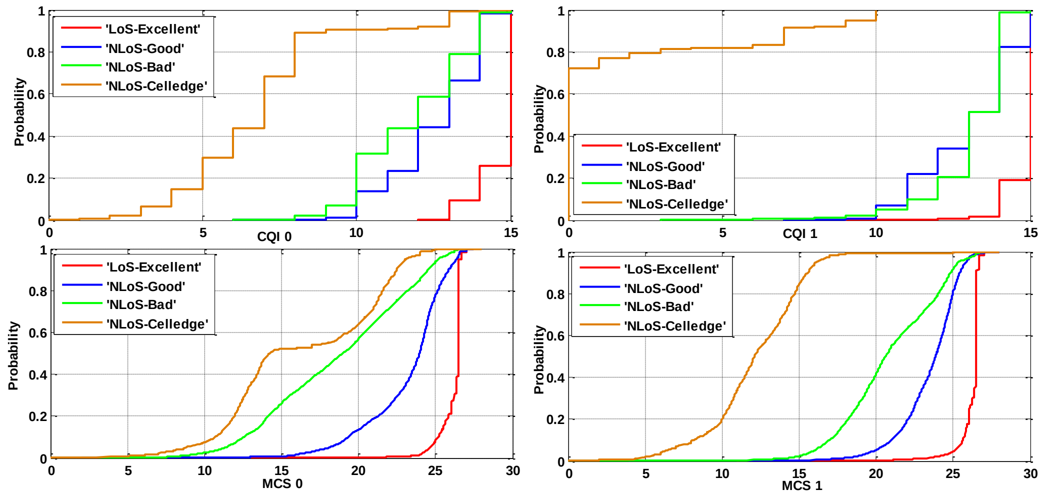

Figure A. 2: CDF plots of MIMO performances at all channel conditions.

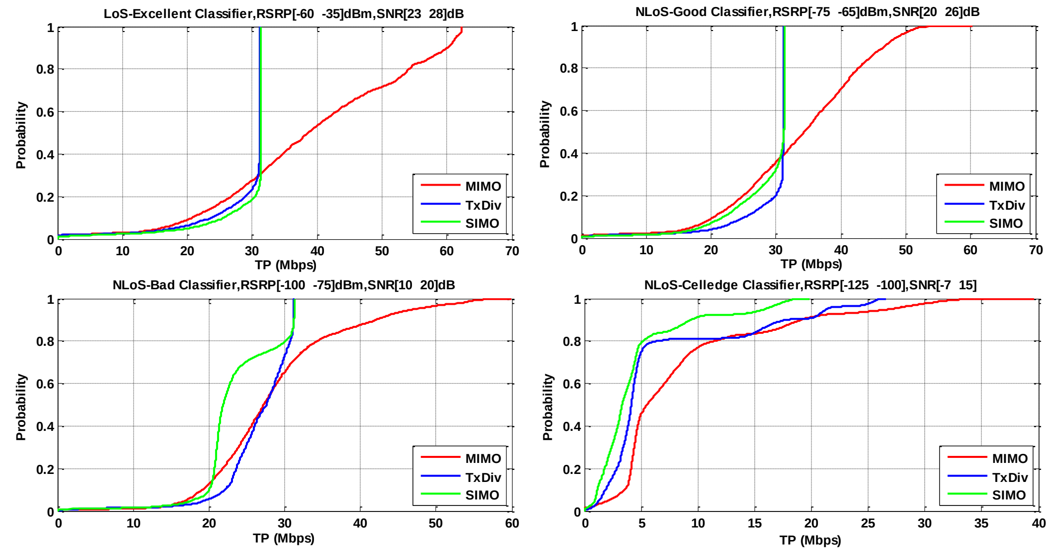

Figure A. 3: CDF plots of MIMO, TxDiv, single antenna performances at all channel conditions.

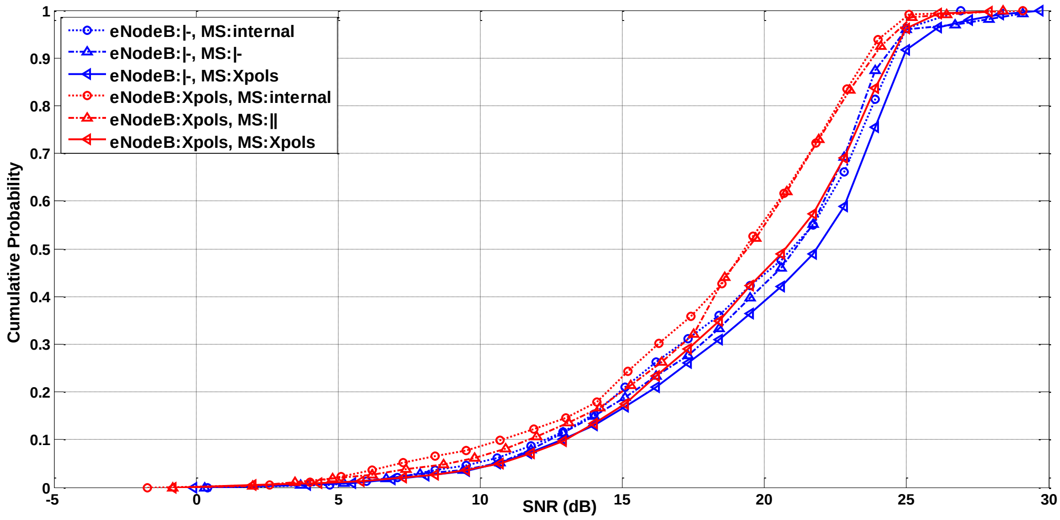

Figure A. 4: CDF plots of SNRs of polarization matching measurements.

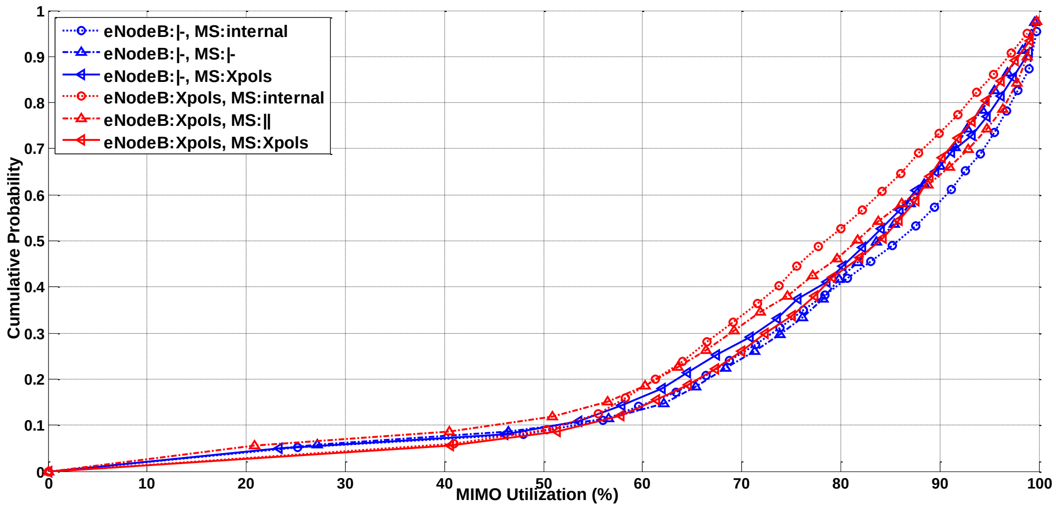

Figure A. 5: CDF plots of MIMO Utilizations of polarization matching measurements.

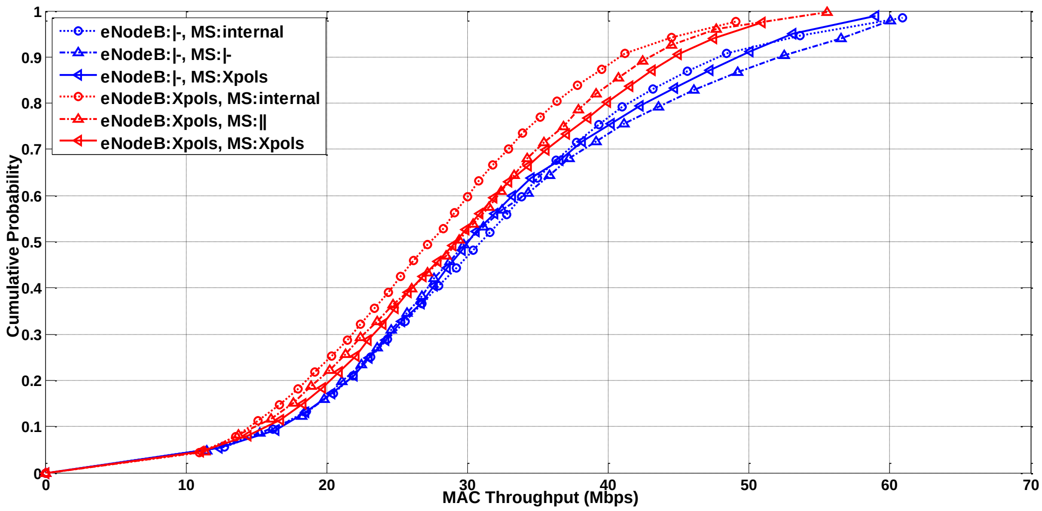

Figure A. 6: CDF plots of MAC TP of polarization matching measurements.